Role of tyrosyl-DNA-phosphodiesterase I in mitochondrial DNA repair

Martin Meagher

Thesis submitted to Newcastle University in candidature for the degree of Doctor of Philosophy

Wellcome Trust Centre for Mitochondrial Research
Institute for Ageing and Health

April 2013

Abstract

The mechanisms for DNA repair in mitochondria is an area in which there is limited knowledge in comparison to the DNA repair mechanisms that have been defined in the nucleus. Although it is understood that mitochondria have less DNA repair mechanisms than in the nucleus there is still a lot more scope for identifying new proteins involved in the repair of mitochondrial DNA (mtDNA).

The main focus of this thesis was to attempt to determine whether there was presence and activity of a DNA repair enzyme in mitochondria, namely tyrosyl-DNA-phosphodiesterase 1 (TDP1), and if so what is the exact role of this enzyme in mtDNA repair. This enzyme has already been characterised as an single strand break repair (SSBR) enzyme in the nucleus, and a mutation in this gene can cause the autosomal recessive disorder spinocerebellar ataxia with axonal neuropathy 1 (SCAN1).

The data in this thesis provides evidence for the presence and activity of TDP1 in mitochondria and that the function of this enzyme on mtDNA is most likely limited to the removal of mitochondrial topoisomerase 1 (TOP1mt). It has also been shown that phosphorylation of amino acid 81 of TDP1 does not facilitate its interaction with DNA ligase 3α in mitochondria and that there most probably no direct link between these enzymes in this organelle, unlike that found in the nucleus.

This data indicates that there is still potential for identification of more enzymes that are involved in mtDNA repair.

Acknowledgements

To begin I would like to thank my supervisors Professors R.N. Lightowlers and D.M. Turnbull for giving me the opportunity to take part in this MRes/PhD programme, and for all their support and advice throughout my time in the group. Gratitude is also shown to our collaborator Dr. Sherif El-Khamisy for all the help in making this project possible and providing much needed knowledge on the intricacies of DNA repair. I would also like to thank Professor Z.M. Chrzanowska-Lightowlers for the influence and any input she has made with respect to my project in lab meetings etc.

I would also like to show appreciation to Dr K. Krishnan for her supervision of my project while still in the lab. Thanks are made to Dr H. Tuppen and Mrs C. Alston for all their help with any sequencing that I required.

Others to mention are the likes of Dr P. Smith and Mr. William 'Willy' Wilson for helping to provide a very pleasant atmosphere to work in, and also as friends outside the lab. This also includes all the people I have worked with in my time within the group, which is something I will look back on fondly!

Lastly I would like to thank my parents, other family members, and friends for their support while carrying out my studies and in helping to remind me that there are things in the world other than mitochondria and Newcastle United!

Table of contents

List of figures

List of Tables

Abbreviations

2D-AGE	Two-dimensional agarose gel electrophoresis
A	Adenine
AD	Alzheimer's disease
$AgNO_3$	Silver nitrate
AOA1	Ataxia with oculomotor apraxia type 1
APS	Ammonium persulphate
ATP	Adenosine triphosphate
BER	Base excision repair
bp	Base pairs
BSA	Bovine serum albumin
C	Cytosine
Co-IP	Protein complex immunoprecipitation
CPEO	Chronic progressive external ophthalmoplegia
CPT	Camptothecin
D-loop	Displacement loop
DAB	3,3'-Diaminobenzidine
DMEM	Dulbecco's modified Eagle's medium
DMSO	Dimethylsulphoxide
DNA	Deoxyribonucleic acid
DNase	Deoxyribonuclease
dNTP	Deoxynucleotide triphosphate
DR	Direct repair
DSB	Double strand break
DSBR	Double strand break repair
DTT	Dithiothreitol
EDTA	Ethylenediaminetetraacetic acid
EGTA	Ethyleneglycoltetraacetic acid

EtBr	Ethidium bromide
EthBr/CsCl	Ethidium bromide/caesium chloride
EtOH	Ethanol
FCS	Foetal calf serum
g	Relative centrifugal force
G	Guanine
Gy	Gray
H_2O	Water
HEK293	Human embryonic kidney 293 cells
HeLa	Henrietta Lacks cells
HR	Homologous recombination
HSP	Heavy strand promoter
IP	Immunoprecipitation
kb	Kilobases
KCl	Potassium chloride
kDa	KiloDalton
KSS	Kearns-Sayre syndrome
LB	Luria-Bertani bacterial medium
LCL	Lymphoblastoid cell line
LHON	Leber's hereditary optic neuropathy
LR-PCR	Long range PCR
LSP	Light strand promoter
$MgCl_2$	Magnesium chloride
MMR	Mismatch repair
MMS	Methyl methane sulfonate
mRNA	Messenger RNA
mtBER	Mitochondrial BER
mtDNA	Mitochondrial DNA

MTS	Mitochondrial targeting sequence
NaCl	Sodium chloride
NaOAc	Sodium acetate
NaOH	Sodium hydroxide
NARP	Neurogenic ataxia with retinitis pigmentosa
NBT	Nitro blue tetrazolium
nDNA	Nuclear DNA
NER	Nucleotide excision repair
NH_4OH	Ammonium hydroxide
NHEJ	Non-homologous end joining
NP-40	NonidetP-40
NTS	Nuclear targeting sequence
Ori H	Origin of heavy strand replication
Ori L	Origin of light strand replication
OXPHOS	Oxidative phosphorylation
PAGE	Polyacrylamide gel electrophoresis
PBS	Phosphate buffered saline
PCR	Polymerase chain reaction
PD	Parkinson's disease
PMS	Phenazine methosulfate
PMSF	Phenylmethylsulfonyl fluoride
qRT-PCR	Quantitative real time PCR
RITOLS	Ribonucleotide incorporation throughout the lagging strand
RNA	Ribonucleic acid
rRNA	Ribosomal RNA
ROS	Reactive oxygen species
SCAN1	Spinocerebellar ataxia with axonal neuropathy type 1
SDS	Sodium dodecyl sulphate

siRNA	Small interfering RNA
SOC	Super Optimal Broth with Catabolite repression
SSB	Single strand break
SSBR	Single strand break repair
T	Thymine
TAE	Tris-acetate-EDTA buffer
TEMED	N,N,N',N'- Tetramethylethylendiamine
Tris	Trishydroxyaminomethane
tRNA	Transfer RNA
TTBS	Tween-tris buffered saline
Tween-20	Polyoxyethylene sorbitanmonolaurate
Triton X-100	Polyethylene glycol octylphenyl ether
U	Unit
UV	Ultraviolet light

Chapter 1. Introduction

1.1 General aspects of mitochondria

Mitochondria are organelles present in almost all eukaryotes that have a vital role in normal cellular functioning (Attardi and Schatz, 1988). One of the main responsibilities of mitochondria is producing the vast majority of cellular energy in the form of adenosine-triphosphate (ATP) through oxidative phosphorylation, although mitochondria have a number of other roles in cells (Bonawitz and Shadel, 2007). Examples of these include biosynthesis of amino acids, phospholipids, and nucleotides, which are produced as a result of a close interplay with the nucleus (Attardi and Schatz, 1988).

Aberrant mitochondrial function can cause a wide variety of severe incurable diseases and is also implicated in the ageing process (Bonawitz and Shadel, 2007). In recent years the profile of mitochondrial research has been increased significantly due to its importance in cells and the potential consequences that can occur as a result of dysfunction in this organelle (Martin, 2012). Mitochondria require precise regulation to prevent negative effects arising from abnormalities in these highly organised organelles. Such organisation includes a double membrane structure, a distinct genome from that in the nucleus (mitochondrial DNA (mtDNA)), as well as a vast proteome that controls an extensive network of processes occurring in mitochondria (Bonawitz and Shadel, 2007).

Encompassed in this thesis are the findings from a project focussed on the molecular mechanisms of mtDNA damage and repair, however, it is important to first review general aspects of mitochondria to provide an understanding of the activities within this fascinating entity.

1.1.1 *Mitochondrial evolution*

For many years it has been proposed that mitochondria originated in eukaryotes as a result of endosymbiosis; a theory termed the serial endosymbiosis theory (Gray et al., 1999). This theory attests that almost all modern day eukaryotic cells were formed when archaeal and eubacterial cells were unified in anaerobic symbiosis before the incorporation of mitochondria (Margulis, 1996). An exception to this is *Giardia intestina* that does not contain mitochondria, and instead incorporates a less developed form of mitochondria known as mitosomes (Henze and Martin, 2003, Tovar et al., 2003). In contrast to mitochondria, mitosomes are not involved in producing ATP, and instead are relied upon for producing iron-sulfur FeS clusters used in ATP production in this organism (Henze and Martin, 2003, Tovar et al., 2003). Hydrogenosomes are another form of mitochondria related organelle (found in *Trichomonas vaginalis, Giardia lamblia, Nyctotherus ovalis, Neocallimastix frontalis*, and *Psalteriomonas lantern*), which contrast to mitosomes in that they produce ATP through substrate-level phosphorylation, but they are also similar to mitosomes as they produce FeS clusters and are less developed than mitochondria (Shiflett and Johnson, 2010). The relevance of FeS clusters in mitochondria is discussed later when reviewing the process of oxidative phosphorylation. Returning to the subject of mitochondrial evolution, much support for the serial endosymbiosis theory has come from the fact that mitochondria contain their own genome (mtDNA), which is suggestive that this organelle has its own evolutionary history (Gray et al., 1999). Sequencing the 16s ribosomal RNA (rRNA) gene within the mitochondrial genome suggested that mitochondria were derived from an ancestor of the alpha (α) subdivision of proteobacteria (Yang et al., 1985, Gray et al., 1999). The human mitochondrial genome is relatively small in comparison to its nuclear counterpart; encoding thirteen proteins involved in oxidative phosphorylation (Anderson et al., 1981). This suggests that, as part of the evolution of eukaryotic cells,

mtDNA has lost the vast majority of its protein encoding regions to the nuclear DNA (nDNA), as the mitochondrial proteome is far greater than that encoded by mtDNA (Gray et al., 1999, Henze and Martin, 2003). Despite this loss mitochondria are capable of performing a wide variety of activities as a result of the close relationship with the nucleus that ultimately provides a myriad of proteins to give mitochondria the required factors for these activities.

1.1.2 *Mitochondrial structure*

Electron microscopy has played a pivotal role in ascertaining the structure of mitochondria with seminal studies in the 1950s that identified mitochondria as being enclosed by a membrane, and containing protrusions that were named as cristae (Palade, 1952, Sjostrand, 1953). Soon after these findings a model was developed for mitochondrial structure that is widely accepted today as being the true basic structure of mitochondria, which is illustrated in figure 1.2 (Palade, 1953).

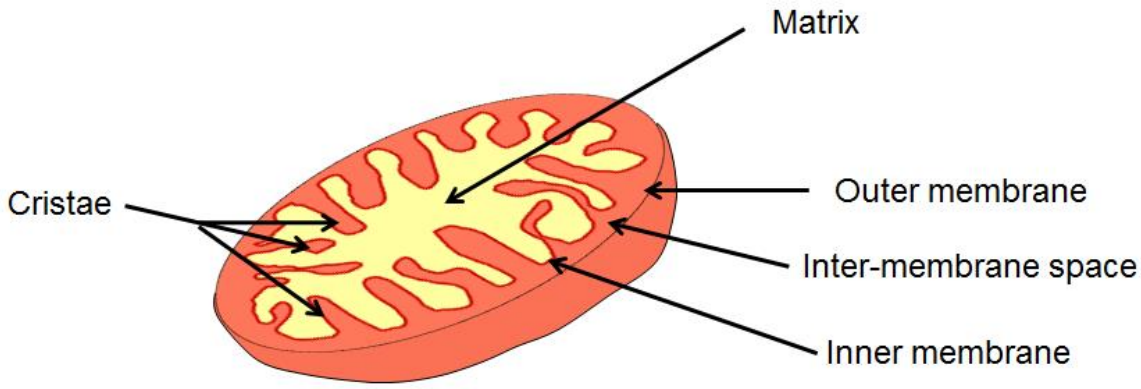

Figure 1.1. *Basic structure of mitochondria* (adapted from Palade, 1953).

From the work carried out by Palade it has since been established that the structure of mitochondria can impact on metabolism depending on the condensation/swelling of this organelle that can affect diffusion of metabolites and subsequently production of ATP from oxidative phosphorylation (Hackenbrock, 1966, Scalettar et al., 1991). It has also

been found that mitochondria undergo fusion and fission processes to allow the transport of energy and metabolites throughout the cell and to ensure that mitochondria remain functional throughout environmental stresses (Palmer et al., 2011, Youle and van der Bliek, 2012). The maintenance of this network of mitochondria is vital for cellular homeostasis as any disruptions to this network can create a variety of complications to the many important processes within mitochondria, including that of oxidative phosphorylation (Palmer et al., 2011, Youle and van der Bliek, 2012). The processes of fission and fusion of mitochondria are mediated by guanosine triphosphatases (GTPases) that involve proteins such as dynamin related protein1 (DRP1) that functions in fission, whereas the mitofusin's 1 (Mfn1) and 2 (Mfn2) play a major role of fusion of mitochondria (Hoppins et al., 2007, Chen and Chan, 2005, Smirnova et al., 2001). Not surprisingly the structure of cristae in fusion and fission processes can be highly variable and therefore correct regulation and performance of these processes is vital in maintaining ATP production through oxidative phosphorylation (Mannella et al., 2001, Germain et al., 2005).

1.1.3 *Oxidative phosphorylation*

Oxidative phosphorylation (OXPHOS) is the process by which ATP is produced as a result of a number of reduction/oxidation (redox) reactions along the electron transport chain that are vital for cell survival (Papa et al., 2012). In mammalian cells more than 80% of ATP is produced through OXPHOS that is then utilised to drive numerous processes in cells (Papa et al., 2012). During OXPHOS electrons are passed along the electron transport chain coupled with transfer of protons from the matrix to the inter-membrane space that creates an electrochemical gradient that is then used in ATP production (Lemarie and Grimm, 2011). Figure 1.3 is a schematic of OXPHOS where movement of electrons and protons ultimately leads to the production of ATP.

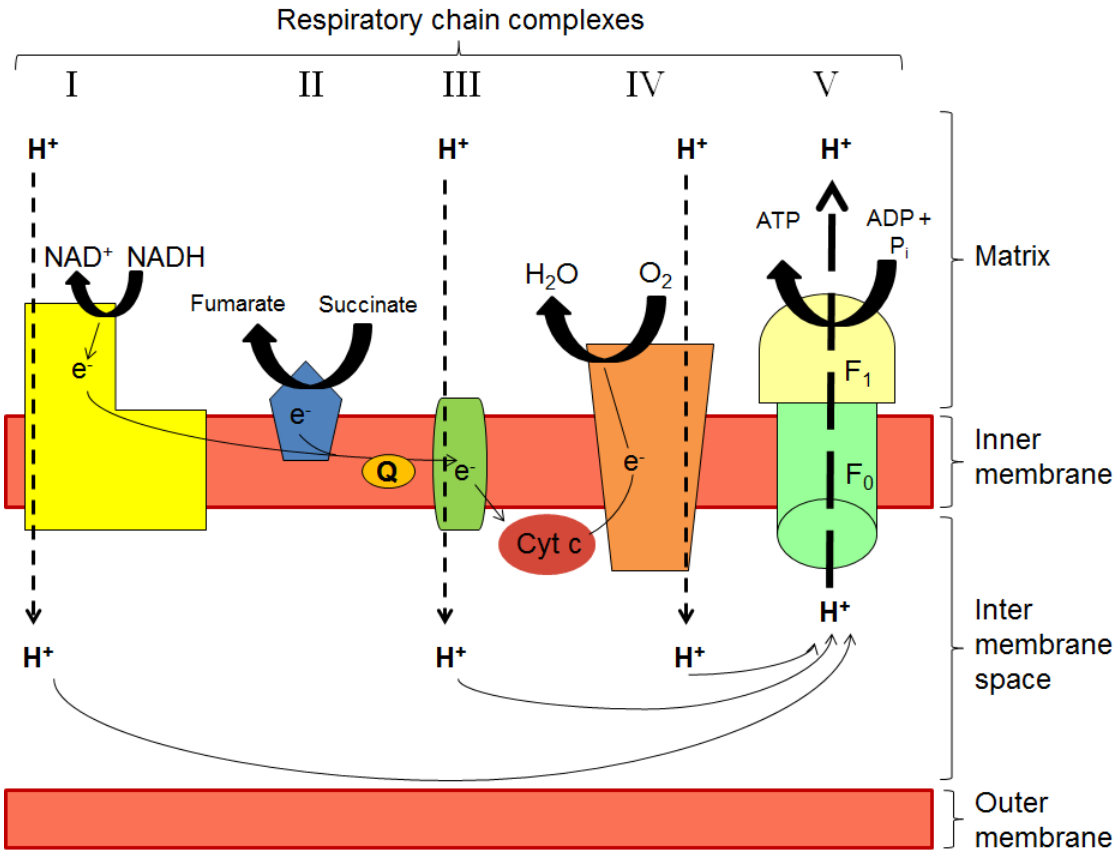

Figure 1.2. *A schematic of OXPHOS*, which simply illustrates that electrons are passed along respiratory chain complexes I to IV whilst protons are moved across the inner mitochondrial membrane and subsequently used to produce ATP (adapted from Lemarie and Grimm, 2011).

Figure 1.3 simply demonstrates that the electron transport chain is located on the inner mitochondrial membrane, however, the processes of electron transport and movement of protons across the membrane is far more complex than is illustrated in this figure (Papa et al., 2012, Lemarie and Grimm, 2011).

The process of OXPHOS often begins with the oxidation of NADH to NAD^+ with electrons being donated to flavin mononucleotide (FMN) in complex I (NADH dehydrogenase) (Hirst, 2005, Sled et al., 1994). Complex I has been established as a multi-subunit complex that has 14 core subunits that are present in all varieties of this enzyme, seven of which are encoded in the nucleus and the other seven in the

mitochondrial genome (Efremov and Sazanov, 2012, Heide et al., 2012). The subunits of this complex are assembled by multiple assembly factors (e.g. Acad9 and Ecsit) to enable adequate function of the complex within the membrane (Heide et al., 2012). Electron microscopy analysis outlined this complex in eukaryotes as being L-shaped and within the inner membrane with the protruding arm extending out to the mitochondrial matrix (Hofhaus et al., 1991). When NADH is oxidised by complex I at this protruding arm the electrons are passed to FMN that is then reoxidised by an FeS cluster and passed along eight FeS clusters before being used to reduce ubiquinone to ubiquinol (Hirst, 2005, Sheftel et al., 2010). These FeS clusters are relevant in many biochemical processes in the cell most probably due to the ability of the iron component to accept electrons, which makes these clusters particularly valuable to OXPHOS (Sheftel et al., 2010). When ubiquinone is reduced protons are translocated across the inner membrane, thus beginning the accumulation of the electrochemical gradient required for ATP production (Hirst, 2005). The reduced ubiquinol can then move through the inner membrane for further redox reactions later in OXPHOS (Hirst, 2005).

In complex II (succinate dehydrogenase (SDH)) succinate from the citric acid cycle is oxidised to fumarate and the electrons generated from this are passed to flavin adenine dinucleotide (FAD) to form $FADH_2$ which then passes the electrons through three FeS clusters (Rutter et al., 2010). The electrons are then used to reduce ubiquinone, but unlike the other complexes of the electron transport chain there is no transfer of protons across the inner membrane as a result of activities in SDH (Rutter et al., 2010). This complex consists of two main domains, one of which extends out into the matrix and the other bound in the inner membrane (Hagerhall, 1997). The domain extending to the matrix contains a dicarboxylate binding site for succinate as well as FAD and FeS clusters for electron transport in this complex (Hagerhall, 1997). These electrons are

then used by the membrane bound domain in oxidation and reduction of ubiquinone in the Quinone pool (Q pool) also present in the membrane (Hagerhall, 1997).

Several redox reactions in complex III (cytochrome bc_1 complex) make the process of electron transfer in this complex arguably the most complicated in the whole electron transport chain (Cramer et al., 2011). Complex III consists of intertwined dimers with a catalytic core made up of three subunits; cytochrome *b*, the FeS Rieske protein, and cytochrome c_1 (Mulkidjanian, 2010). The electron transport in complex III is known as the Q cycle, which begins with oxidation of ubiquinol from the Q pool to ubiquinone one electron being passed to the Rieske FeS protein and then on to cytochrome c_1 before being used to reduce the electron carrier cytochrome *c* (Mitchell, 1975, Mitchell, 1976). The other electron from the oxidation of ubiquinol reduces cytochrome *b* that passes across the membrane and is the used to reduce a molecule of ubiquinone to semiquinone (Mitchell, 1975, Mitchell, 1976). Another molecule of ubiquinol is then reduced once more, which passes another electron to the carrier cytochrome c_i and then on to cytochrome *c* thereby reducing it, while the other electron is used to reduce the semiquinone molecule to fully reduced ubiquinol that re-enters the Q pool (Mitchell, 1975, Mitchell, 1976). During this process further protons are translocated from the matrix into the inter-membrane space to increase the electrochemical gradient needed for the final production of ATP (Mulkidjanian, 2010).

Complex IV, or cytochrome *c* oxidase, is the terminal oxidase of the electron transport chain (Yoshikawa et al., 2012). In this complex electron transfer begins with oxidation of cytochrome *c* that had been reduced in the Q cycle in complex III (Capaldi, 1990). Electrons are accepted by heme *a* and Cu_A before being used to reduce molecular oxygen to water in the mitochondrial matrix (Capaldi, 1990). During this process more

protons are translocated from the matrix to the inter-membrane space for the final step of ATP production by complex V (ATP synthase) (Capaldi, 1990).

Generation of ATP by complex V involves the concerted action of two main subunits of this enzyme, F_0 and F_1, that function in a fascinating rotary manner to produce the molecules that are so vital to cells (Kinosita, 2012). The electrochemical gradient created by the transfer of protons from the matrix to the inter-membrane space, by complexes I, III, and IV induces flow of protons through F_0 subunit of complex V and results in this subunit rotating in a clockwise manner (Noji et al., 1997). Meanwhile the F_1 subunit rotates anti-clockwise, which causes conformational changes at three sites in this subunit that ultimately couples proton flow through F_0 with production of ATP from ADP and P_i (Noji et al., 1997).

The production of ATP is essential to cells; therefore production of the complexes that make up the electron transport chain is vital for cell survival. The vast majority of the proteins that form these complexes are encoded by nDNA, however, a small number are encoded by mtDNA and make-up an integral part of producing ATP through OXPHOS.

1.1.4 *Mitochondrial DNA*

For many years following the discovery and characterisation of DNA in the nucleus, mitochondria were postulated to contain their own DNA which was finally demonstrated in avian heart and liver (Rabinowitz et al., 1965). Following this discovery came great advances in DNA sequencing techniques, namely sequencing with chain-terminating dideoxynucleotides, which was used to sequence human mtDNA (Sanger et al., 1977, Anderson et al., 1981). From this Anderson et al reported mtDNA to contain two rRNA genes, twenty two transfer RNA (tRNA) genes, and five genes encoding subunits of the electron transport chain with a further eight predicted protein coding genes (Anderson et al., 1981). Later sequencing of the original placental mtDNA

sample used by Anderson et al with newer technology allowed revision of this sequence to remove any discrepancies that had originally been observed (Andrews et al., 1999, Anderson et al., 1981). The information provided from these sequencing experiments, in addition to sequencing of mouse mtDNA by Bibb et al, identified mammalian mtDNA as being highly organised with almost no non-coding nucleotides between coding sequences (Anderson et al., 1981, Bibb et al., 1981b). In the time since these publications it has been possible to establish the exact organisation of human mtDNA which is illustrated in figure 1.4.

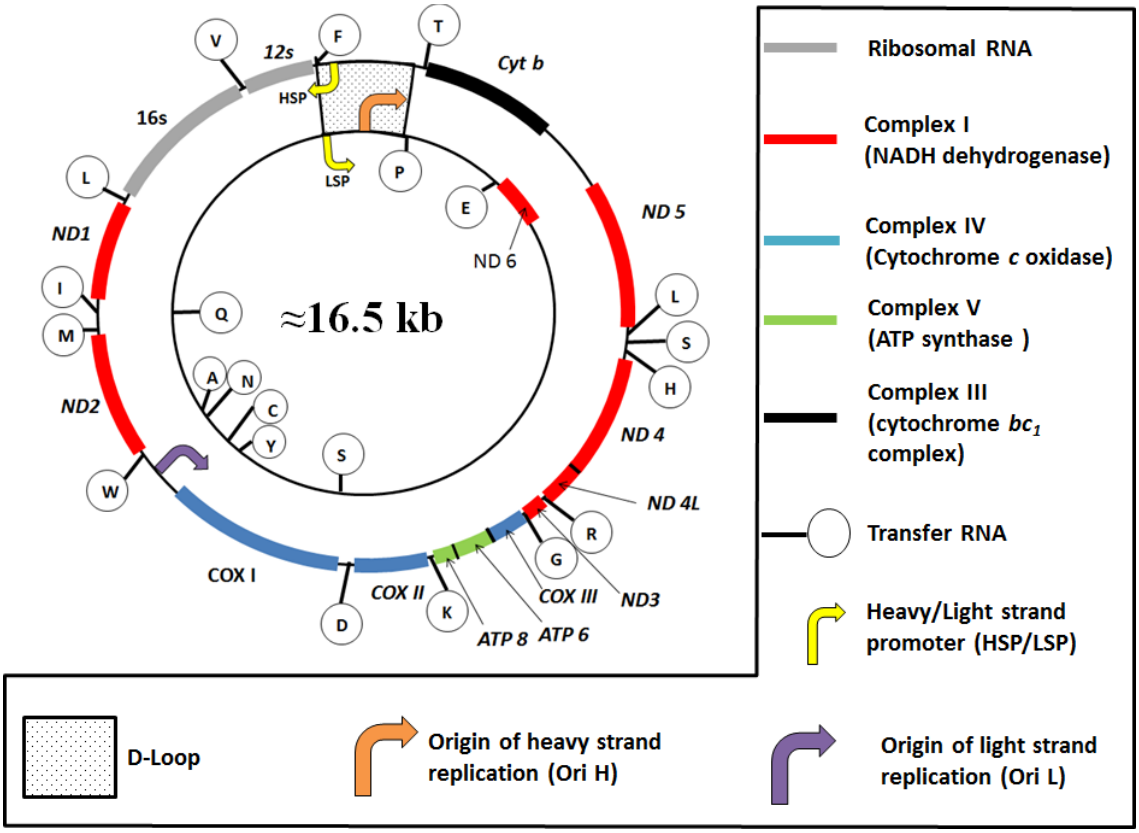

Figure 1.3. *Organisation of the human mitochondrial genome* (adapted from http://www.mitomap.org/MITOMAP/mitomapgenome.pdf).

As can be seen in figure 1.4 the human mitochondrial genome is relatively small and it is also known to be maternally inherited and present in multiple copies in cells (Krishnan et al., 2007). The genome consists of two strands, the guanine rich heavy (H) strand and the guanine poor light (L) strand (Kasamatsu et al., 1971). It is understood that mtDNA molecules are clustered in DNA-protein structures known as nucleoids

where 2-10 copies of mtDNA are packaged by proteins (e.g. mitochondrial transcription factor A (TFAM)) that are also involved in mtDNA maintenance and gene expression (Spelbrink, 2010). Replication and transcription of mtDNA occurs independently of nDNA although all of the factors involved in regulating these processes are encoded by the nuclear genome (Krishnan et al., 2007, Shadel and Clayton, 1997).

Replication of mtDNA was first proposed to occur in a strand uncoupled manner whereby leading strand replication was initiated from Ori H which continued around the genome with lagging strand replication initiated when the leading strand reached Ori L (Robberson et al., 1972). This mode for mtDNA replication was termed the strand-displacement model and was developed as a result of electron microscopic analysis showing that replicating molecules of mtDNA had a single-stranded branch (Robberson et al., 1972). This form of replication was corroborated with the use of ethidium bromide/caesium chloride (EthBr/CsCl) gradients and *in vivo* labelling of mtDNA using radiolabelled thymidine (Berk and Clayton, 1974). These experiments helped to determine the relative densities of replicating molecules of mtDNA that supported previous experiments using electron microscopy and suggested mtDNA replication progressed in an asynchronous manner (Berk and Clayton, 1974). The use of 2-dimensional agarose gel electrophoresis (2-D AGE) was utilised to contradict the strand-displacement model, and instead a bidirectional mode of replication from an origin downstream of Ori H was proposed (Bowmaker et al., 2003, Holt et al., 2000). However, the argument for unidirectional replication initiation was revitalised with the discovery of ribonucleotide incorporation throughout the lagging strand (RITOLS) that was proposed to supersede the bidirectional model (Yasukawa et al., 2006). To date the exact mechanism by which mtDNA is replicated remains to be elucidated, but work in the field is on going as is that involving the expression of genes encoded by mtDNA.

Transcription of human mtDNA is initiated at three points within the genome; the heavy strand promoter (HSP) 1 (H1), the HSP promoter 2 (H2), and the light strand promoter (LSP) (Falkenberg et al., 2007). Transcription from H1 results in the production of a bicistronic unit of mRNA for two rRNA molecules encoded in the genome (Falkenberg et al., 2007). Transcription initiation from H2 and LSP results in the production of a polycistronic mRNA unit from each strand that undergoes cleavage processes to produce the final mRNA molecules that can be used in translation (Falkenberg et al., 2007, Montoya et al., 1981, Ojala et al., 1981). These cleavage processes are thought to take place immediately before and after tRNA sequences in the genome (Ojala et al., 1981). Transcription initiation of mtDNA is dependent on the interaction of the mitochondrial RNA polymerase (POLRMT) with TFAM, B1 (TFB1M), and B2 (TFB2M) (Falkenberg et al., 2002, McCulloch et al., 2002). To date the only transcription termination to be characterised is that from promoter H1 and involves the mitochondrial transcription termination factor (MTERF) with termination of the other mRNA units yet to be identified (Falkenberg et al., 2007, Kruse et al., 1989). Current knowledge of the processing of mitochondrial mRNA transcripts includes polyadenylation by the mitochondrial poly-A-polymerase (MTPAP) before synthesis of each of the 13 OXPHOS proteins encoded by mtDNA is performed on the inner mitochondrial membrane by the mitoribosome (Crosby et al., 2010, Sharma et al., 2003).

As mentioned earlier it has been established that there are multiple copies of mtDNA molecules in cells and that these are packaged in ‘nucleoids’ that can comprise many mtDNA molecules as well as proteins; most notably the TFAM (Kukat et al., 2011, Hallberg and Larsson, 2011). Despite mtDNA appearing to be very well organised, mitochondria still rely heavily on the nuclear encoded proteins and, as with all

biological systems, errors can be made and damage can develop in a variety forms that lead to an abundance of diseases as a result of mitochondrial dysfunction.

1.1.5 *Mitochondrial involvement in disease and ageing*

With mitochondria having a critical role in cells any dysfunction in this organelle can present in a number of diseases. These can be caused by mutations in mtDNA (primary causes), mutations in nuclear genes can also impact on many mitochondrial processes (secondary causes), and somatic damage to DNA/proteins during ageing can influence mitochondrial function (Schapira, 2012). Common mitochondrial diseases that result from mutations in mtDNA include neurogenic ataxia with retinitis pigmentosa (NARP) and Leber's hereditary optic neuropathy (LHON) whilst mutations in nuclear genes encoding proteins such as the mitochondrial DNA polymerase γ (POLG) and the mtDNA helicase twinkle can also cause mitochondrial disease in the form of chronic progressive external opthalmoplegia (CPEO) (Schapira, 2012). Mutations in either mtDNA or nDNA that affect components of the electron transport chain often present in infancy or early childhood and are frequently fatal, thus emphasising the importance of OXPHOS to cells and the whole body (Schapira, 2012). Mutations in the genes encoding Parkin and PTEN-induced putative kinase 1 (PINK1) are known to affect mitochondrial function which is related to the neurodegenerative disorder, Parkinson's disease (PD) (Gegg and Schapira, 2011). Mitochondrial dysfunction has also been observed in patients with Alzheimer's disease (AD) although a causative role for mitochondria in this disease has yet to be proven unequivocally (Howell et al., 2005). The diseases outlined are just a small collection of multiple disorders that involve mitochondrial dysfunction, but the exact role of mitochondria in ageing has yet to be fully established.

In the 1950s it was proposed that oxidative damage caused by reactive oxygen species (ROS) accumulates in cells over time and that this results in impaired cell function which will eventually lead to death (Harman, 1956). This appears to be an attractive explanation for ageing with respect to mitochondria as increased ROS can be generated as a result of electron leakage from the electron transport chain (Lemarie and Grimm, 2011). The increased levels of ROS could cause more damage to mitochondrial components that in turn could generate more ROS and therefore further damage that increases with time; a phenomenon described as the vicious cycle (Jang and Remmen, 2009). However, mouse models in which mtDNA point mutations are greatly increased and lead to early onset of an ageing phenotype do not display increased ROS production, which provides evidence to contradict the vicious cycle of damage proposed for mitochondria (Trifunovic et al., 2004, Trifunovic et al., 2005, Park and Larsson, 2011). Although this evidence would suggest that this vicious cycle of damage in mitochondria does not cause ageing it is clear that there are many negative effects that have been observed in mitochondria with increasing age, such as increased mtDNA mutation load and mtDNA deletion levels (Bender et al., 2006, Krishnan et al., 2007). These mtDNA mutations and deletions clonally expand with age, but whether this is just a sign of ageing or actually contributes to the ageing phenotype is unknown (Krishnan et al., 2007). An alternative hypothesis is that mtDNA mutations occur as a result of replication errors during embryogenesis, and subsequently expand during ageing suggesting that oxidative damage does not have a leading role in mtDNA mutation formation (Larsson, 2010). Even with this in mind it would be naïve to assume that oxidative damage does not affect the ability of mtDNA to provide subunits of the electron transport chain as there are a number of mechanisms by which mtDNA can be damaged (Boesch et al., 2011). The study of mtDNA damage is the main theme of this thesis and will be discussed in greater detail in the following sections.

1.2 **Mitochondrial DNA damage and repair**

Damage to mtDNA can occur in a variety of forms and potentially have devastating effects in cells (Cline, 2012, Boesch et al., 2011). While knowledge for the potential mechanisms of mtDNA damage is well known, the actual study of how damaging agents affect mtDNA and its consequences in disease and ageing is much less characterised in comparison to the nucleus (Boesch et al., 2011). Although a significant proportion of research funding is directed to the study of nDNA damage and repair in comparison to the same subject for mtDNA there is a relative lack of knowledge in this field considering the advances that have been made in researching other areas of mitochondrial biology. Much attention in the area of mitochondrial damage has been devoted to studying the effects of ROS that can damage proteins and DNA within mitochondria (Roede and Jones, 2010). In this section attention will be given to known forms of mtDNA damage as well as the current knowledge surrounding repair of this damage and potential for further findings.

1.2.1 *Forms of mitochondrial DNA damage*

There are a number of agents that can cause DNA damage and with mitochondria producing a considerable amount of ROS this will be reviewed first with respect to mtDNA damage. As discussed previously ROS can be generated endogenously, but they can also be formed from exogenous factors such as pollution and ultra violet (UV) radiation (Boesch et al., 2011). As wells as generating ROS, UV radiation can cause DNA damage as the absorption spectrum of DNA matches the wavelength of UV radiation (100-400nm), which can lead to direct excitation of DNA and form pyrimidine dimers (Batista et al., 2009). This alteration can cause instability of DNA and/or

mutations in the nucleotide sequence (Boesch et al., 2011). Exogenously or endogenously generated ROS include superoxide (O_2^-), hydroxyl radicals ($^{\cdot}OH$), and hydrogen peroxide (H_2O_2) (Boesch et al., 2011). The $^{\cdot}OH$ radical is highly reactive towards DNA and can form damage as well as causing oxidation of unsaturated bonds in polyunsaturated fatty acids (PUFAs) present in the inner mitochondrial membrane (Halliwell and Gutteridge, 1984, Colbeau et al., 1971). The oxidation of PUFAs produces aldehyde products that are usually neutralised by enzymes such as aldehyde dehydrogenase and cause no problem (Esterbauer et al., 1991). However, in circumstances of increased ROS this neutralisation may not occur meaning that these reactive aldehydes are capable of damaging mtDNA (Schlame et al., 2005, Voulgaridou et al., 2011). In the case of O_2^- approximately 0.15% of oxygen consumed by mitochondria forms this radical with complexes I and III being the main sites for its production (St-Pierre et al., 2002, Brand, 2010). ROS can damage mtDNA by forming adducts such as thymine glycol and the well studied 8-hydroxyguanine (8-oxo-G), as well as forming strand breaks and abasic sites in mtDNA (Boesch et al., 2011, Ohno et al., 2009, Evans et al., 2004, Dizdaroglu et al., 2002). In addition to modifying bases within the backbone of mtDNA, oxidation of nucleotides in the deoxynucleotide triphosphate (dNTP) pool can occur which may then become incorporated within mtDNA by POLG upon replication (Boesch et al., 2011, Kamiya and Kasai, 1995). In addition to ROS reactive nitrogen species (RNS) can be formed as a result of a combination of O_2^- and nitric oxide ($NO^{\cdot}$) which forms peroxynitrite ($ONOO^-$) and is highly reactive, potentially being very damaging to mtDNA by oxidising bases and also generating abasic sites (Boesch et al., 2011, Burney et al., 1999). As well as adducts being formed in mtDNA by ROS and RNS it is also possible for adducts to be derived from alkylating agents produced endogenously and also from ultra violet (UV) light,

which forms thymine dimers within the DNA backbone (Boesch et al., 2011, Xiao and Samson, 1993).

The various lesions described here are just some examples that can potentially be very detrimental to the cell and so mitochondria possess repair mechanisms to reverse these forms of mtDNA damage.

1.2.2 *Mitochondrial DNA repair pathways and potential for further identification*

In the mid-1970s a study was carried out to assess the capability of mitochondria to repair UV induced mtDNA damage in the form of pyrimidine dimers that would require the repair mechanism nucleotide excision repair (NER), but it was found that mitochondria did not have this capability (Clayton et al., 1974). From this many concluded that mitochondria did not contain any DNA repair capabilities for some time until this was disproven by demonstrating the existence of base excision repair (BER) in mitochondria (Bogenhagen, 1999, Mason et al., 2003). From this it has been found that mitochondria are able to repair various lesions in mtDNA, which is more than was initially anticipated (Yakes and Van Houten, 1997, Liu and Demple, 2010, Mason and Lightowlers, 2003).

As described in the previous section ROS can be generated from exogenous factors such as pollution or endogenously from processes such as OXPHOS, which can result in many forms of DNA damage (Boesch et al., 2011). Defence against such damaging agents can come in the form of antioxidants such as superoxide dismutases and peroxidases that act to detoxify ROS before damage can occur (Foyer and Noctor, 2009, Turrens, 2003, Chaudiere and Ferrari-Iliou, 1999) However, there are occasions when

damaging ROS escape detoxification and cause a wide variety of DNA lesions that require various repair mechanisms to restore DNA to its original form and avoid any negative impact as a result of this damage (Boesch et al., 2011).

Of the DNA repair pathways in mitochondria BER has been the most studied and was demonstrated to exist for both short-patch and long-patch versions of this pathway (Stierum et al., 1999, Liu et al., 2008). Figure 1.5 illustrates how both these forms of BER operate to repair damage that occurs *in vivo*, and the enzymes that are involved in these processes.

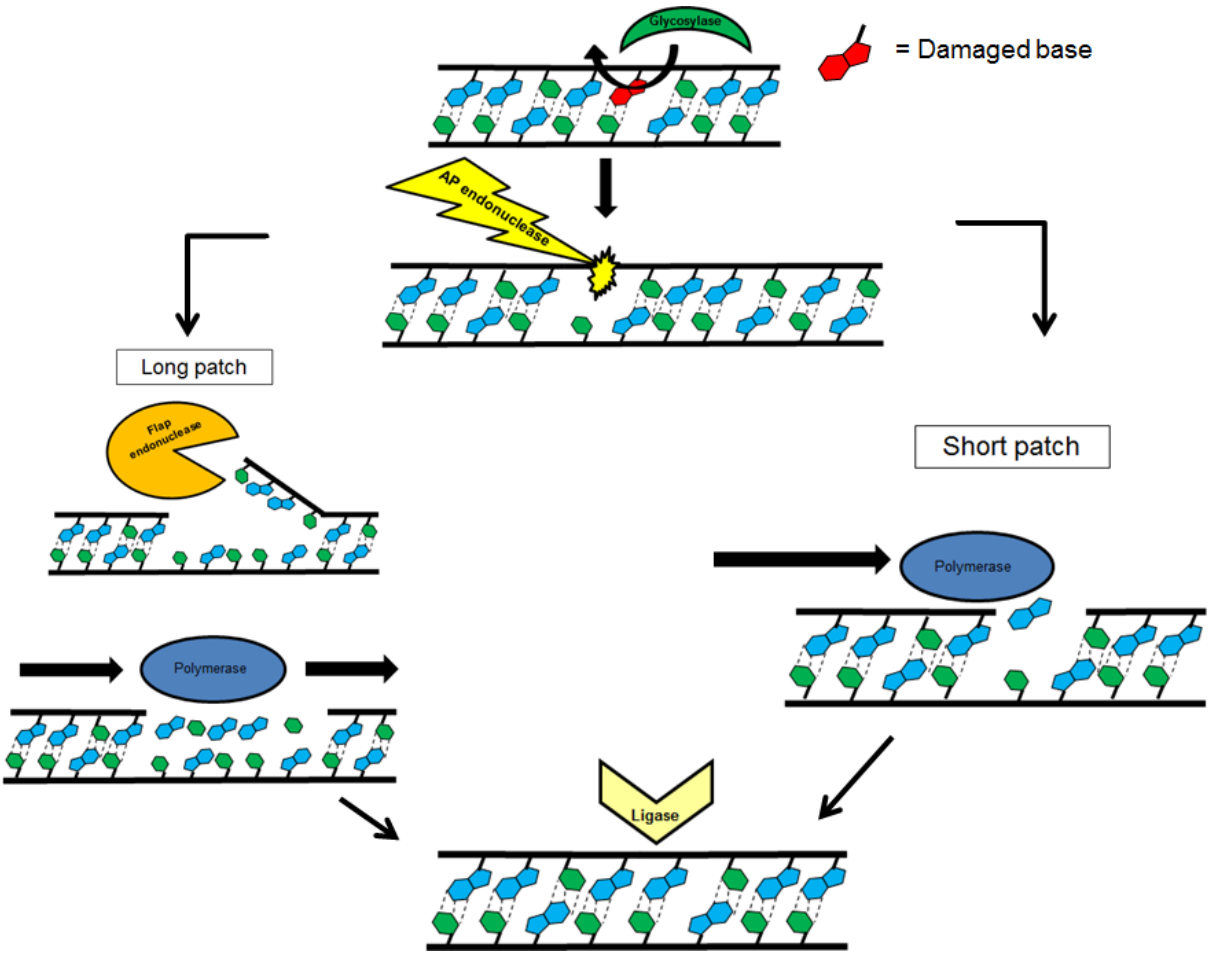

Figure 1.4. *General characterisation of short-patch (SP) and long-patch (LP) BER mechanisms that repair mtDNA damage*. The process is initiated when a damaged base is excised from the DNA backbone by a DNA glycosylase leaving an abasic (AP) site. The DNA backbone is then cleaved by an AP endonuclease followed by infilling of the abasic site by DNA polymerase in SP-BER. In some circumstances the 3' end at the abasic site does not consist of OH following cleavage by the AP endonuclease, which then requires a flap endonuclease to remove 2-10 bases of DNA before infilling can be carried out by the DNA polymerase. Once the correct bases have been replaced a DNA ligase then restores the DNA backbone to its original form (adapted from Boesch et al., 2011).

Along with BER in mitochondria other repair mechanisms have been reported in mitochondria such as mismatch repair (MMR), and removal of oxidised dATP and dGTP from the dNTP pool (Mason et al., 2003, Nakabeppu, 2001b). Removal of these oxidised dNTPs (8-oxo-2′-dATP and 8-oxo-dGTP) is performed by MutT homolog 1 (MTH1) as a protection of oxidised bases being incorporated within replicating mtDNA (Kang et al., 1995, Nakabeppu, 2001a). In cases where oxidised bases are incorporated during replication or when errors are made in this process MMR serves to remove errors

made in the nascent strand of replicating mtDNA by the enzyme YB-1 (Hsieh and Yamane, 2008, Mason et al., 2003, de Souza-Pinto et al., 2009). Direct repair (DR) of DNA without any cleavage of the DNA backbone has also been demonstrated to exist in mitochondria mediated by O^6-methylguanine-DNA methyltransferase (MGMT), which removes methyl groups from modified guanine bases (Myers et al., 1988). Further repair mechanisms have been proposed to be present in mitochondria, such as double strand break repair (DSBR) by non-homologous end joining (NHEJ) and homologous recombination (HR); however these processes have not yet been unequivocally demonstrated in this organelle (Thyagarajan et al., 1996, Bacman et al., 2009, Lakshmipathy and Campbell, 1999a, Fukui and Moraes, 2009). Despite this mitochondria potentially have a more developed repair network than initially anticipated and by turning to repair mechanisms for nDNA it was hoped that more information could be found for the repair capabilities for mtDNA.

1.3 **Tyrosyl-DNA-phosphodiesterase 1**

Tyrosyl-DNA-phosphodiesterase 1 (TDP1) is an enzyme involved in DNA repair in the nucleus (Yang et al., 1996). The repair of nDNA has been well studied when compared to that for mtDNA, and therefore repair in the nucleus is relatively well characterised in comparison to the mitochondrion (Boesch et al., 2011). Table 1.1 shows the DNA repair mechanisms that are known to exist in the nuclear and mitochondrial compartments of the cell.

Table 1.1. DNA repair mechanisms in the nucleus and mitochondrion (adapted from Boesch et al., 2011).

Nucleus						**Mitochondrion**				
BER	NER	MMR	DSBR	DR	SSBR	BER	MMR	DSBR	SSBR	DR

Of the repair mechanisms in mitochondria single strand break repair (SSBR) had yet to be characterised at the beginning of this project. Experiments to determine whether SSBR existed in mitochondria were to be carried out by investigating the function of TDP1, which is involved in SSBR in the nucleus.

1.3.1 *Function of TDP1 enzyme in nucleus*

The discovery of TDP1 came in 1996 when it was found that cleavage complexes formed from type I topoisomerases could be resolved by the activity of TDP1 (Yang et al., 1996). This was established using cell extracts from *Saccharomyces cerevisiae* and a radiolabelled oligonucleotide with a 3' phosphotyrosine to mimic the DNA-topoisomerase 1 (TOP1) lesion that forms *in vivo* (Yang et al., 1996). Following this discovery a plethora of publications has arisen that provide further information on classification of this enzyme and the exact function of TDP1 in repairing DNA-TOP1 lesions in the nucleus. Sequence comparison studies identified TDP1 as a member of phospholipase D (PLD) superfamily due to the presence of two histidine-lysine-aspartic acid (HKD) signature motifs that are characteristic of members of this family (Interthal et al., 2001). The HKD motifs in TDP1 are unusual in that they do not contain the aspartic acid (D) and in place there is an asparagine (N) that categorises TDP1 in a distinct class within the PLD family (Interthal et al., 2001). Other notable findings regarding TDP1 include the discovery that this enzyme can resolve other substrates than 3' phosphotyrosine, such as 3' phosphoglycolate and 3' phosphohistidine, which suggests an important role for TDP1 in cells (Interthal et al., 2005, Inamdar et al., 2002). Also, it was found that in repairing DNA-TOP1 SSBs TDP1 acts in concert with other proteins including X-ray repair cross-complementing protein 1 (XRCC1), polynucleotide kinase (PNK), and DNA ligase IIIα (LIG3α) (Plo et al., 2003, El-

Khamisy et al., 2005, Debethune et al., 2002). However, arguably the most important finding came with the identification that mutations in TDP1 (A1478G) are the causative factor in the autosomal recessive disorder spinocerebellar ataxia with axonal neuropathy 1 (SCAN1) (Takashima et al., 2002). It was found that this mutation in TDP1 caused a change in the active site of the enzyme resulting in a loss of function that produces SCAN1 (Takashima et al., 2002, Raymond et al., 2004).

1.3.2 *Spinocerebellar ataxia with axonal neuropathy 1*

Identification of SCAN1 was established with the mutational analysis that characterised the A1478G mutation in TDP1 as being responsible for causing this disease in a large Saudi Arabian family (Takashima et al., 2002). Discovery of this mutation in TDP1 came as a result of members of this family displaying a co-occurrence of spinocerebellar ataxia and peripheral neuropathy, but no indication of mutations in genes that had already been associated with ataxia and neuropathy (Takashima et al., 2002). All members of the family with this disease had normal intelligence, but accompanying the ataxia and neuropathy was mild cerebellar atrophy with hypercholesterolemia and hypoalbuminemia (Takashima et al., 2002). As the number of diagnosed individuals was relatively low further studies surrounding this disease were limited, therefore when a *Tdp1 -/-* mouse was developed the opportunity for greater insight into the role of TDP1 *in vivo* was presented (Katyal et al., 2007). In these mice a mutation in the *Tdp1* gene caused the subsequent protein to be unstable which effectively resulted in a loss of function (Katyal et al., 2007). Although the mutation in these mice was not exactly the same as in the SCAN1 patients the phenotype of these animals was very similar (ataxia, hypoalbuminemia etc.), which made them the ideal model for studying the role of TDP1 *in vivo* (Katyal et al., 2007). It was found that in

cerebellar neurons and primary astrocytes in these mice SSBs persisted and were unrepaired in comparison to wild type controls, which led to an age-dependent cerebellar atrophy as a consequence (Katyal et al., 2007). This demonstrates significance of DNA repair enzymes in normal cellular functioning and how a slight alteration in the interactions between enzymes associated with DNA can have drastic effects on the whole body level.

1.3.3 *Relationship with topoisomerase 1*

Although the function of TDP1 has been discussed the mechanism of formation of the DNA-TOP1 lesions has yet to be explained as has the history behind the identification of topoisomerases. The first topoisomerase, named protein ω at the time, was identified in *Escherichia coli* and was found to relax DNA from its superhelical structure in these organisms (Wang, 1971). From this a variety of topoisomerases have been characterised with several functions that alter the structure of DNA in preparation for transcription and replication (Vos et al., 2011). Although many different topoisomerases have been identified one characteristic that remains for all is that scission of DNA by these enzymes is mediated by a nucleophilic tyrosine (Vos et al., 2011). Furthermore, all topoisomerases are classified within two groups, type I and type II, and are subdivided within these groups into subtypes A, B, and C depending on sequence similarity between different topoisomerases and/or structural similarities that may exist between proteins (Vos et al., 2011).

For type IA topoisomerases DNA is incised on one strand and the second strand is passed through the gap of this intermediate before the first strand is resealed, which altogether relaxes supercoiled DNA (Tse et al., 1980). In contrast type IB, in which

TOP1 belongs, and IC topoisomerases nick a strand of DNA and rotate this strand around the other before resealing takes place (Koster et al., 2005). The difference between type IB and IC topoisomerases comes in the structure of these enzymes and that type IC topoisomerases are not found in eukaryotes (Slesarev et al., 1993). Type IIA topoisomerases function in a similar way to type IA topoisomerases with the most notable difference being that in type IIA both strands of DNA are cleaved whereas in type IA only one strand is broken (Liu et al., 1980). A second class of type II topoisomerases exists (type IIB), however the exact mechanism by which this group of topoisomerases functions remains to be elucidated (Vos et al., 2011).

The focus of this thesis involves TOP1, which has a relationship with TDP1 in that it is removed from DNA by this enzyme, as discussed earlier (Yang et al., 1996). Lesions where TOP1 becomes covalently bound to DNA can occur when TOP1 collides with DNA or RNA polymerases or when TOP1 incises DNA in close proximity to another form of DNA damage; resulting in this enzyme being covalently linked to the 3' end of the DNA substrate (Caldecott, 2008). Figure 1.6 illustrates one mechanism by which these DNA-TOP1 lesions are formed and how TDP1 acts to repair these lesions.

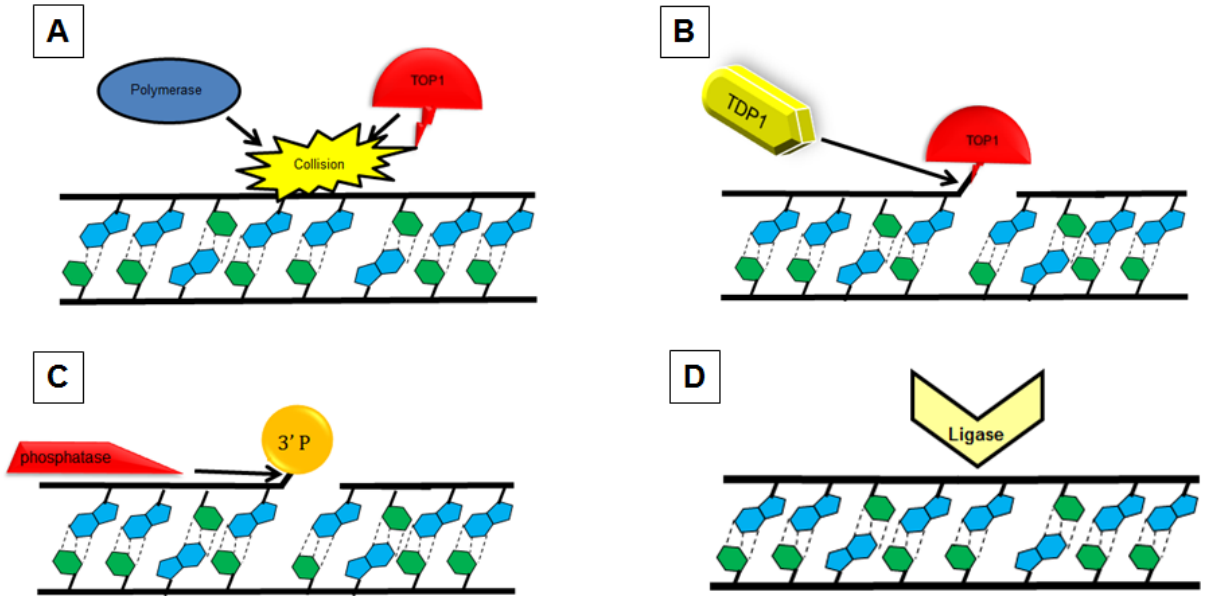

Figure 1.5. *The mechanism of formation of DNA-TOP1 lesions, and repair by TDP1*. **(A)** DNA or RNA polymerases can collide with TOP1 resulting in the protein being covalently bound to the 3' end of the DNA by a phosphotyrosine bond, which requires TDP1 to act in cleaving this bond seen in **(B)**. Once the topoisomerase has been removed by TDP1 the status of the 3' end of DNA at the (SSB) is 3' phosphate, which requires action of a phosphatase **(C)** to restore the 3' end to OH in preparation for re-ligation by a DNA ligase **(D)** (adapted from Caldecott. 2008).

Figure 1.6 demonstrates the importance of TDP1 to repair of DNA-TOP1 lesions and with the identification of a mitochondrial form of TOP1 (TOP1MT) the possibility that TDP1 may function in the mitochondrion was implied (Zhang et al., 2001).

1.3.4 *Mitochondrial topoisomerase 1*

The first indication of topoisomerase activity in mitochondria was discovered in rat liver mitochondria and the enzyme activity was found to be distinct from the activity of nuclear TOP1 (Fairfield et al., 1979). However, it was not for another twenty years before the actual gene encoding TOP1MT was found, which was established as a paralog of the nuclear TOP1 and contained a mitochondrial targeting sequence (Zhang et al., 2001, Zhang et al., 2007). With this finding it may have been assumed that much of the substrate specificity and mode of activity characteristics for TOP1MT were the same as for the nuclear TOP1; however this was proposed not to be true with a study

involving alternative localisation of both forms of the topoisomerase (Dalla Rosa et al., 2009). In this study TOP1MT was overexpressed and targeted to the nucleus, and TOP1 was overexpressed and targeted to mitochondria with controls including overexpression of each enzyme in their correct organelle (Dalla Rosa et al., 2009). The results showed that with expression of each enzyme to the opposite organelle the activity of both topoisomerases was not seen or greatly reduced, and when TOP1 was targeted to mitochondria mtDNA depletion was observed (Dalla Rosa et al., 2009). This suggests that the substrate specificity and/or structure of the catalytic subunit of each enzyme is different meaning that assumptions of TOP1MT activity based on information regarding TOP1 should be made with caution (Dalla Rosa et al., 2009). Despite this it has been possible to identify the binding sites of TOP1MT within the mitochondrial genome as including an area of the displacement loop (D-loop) and a region adjacent to this illustrated in figure 1.7 (Zhang and Pommier, 2008).

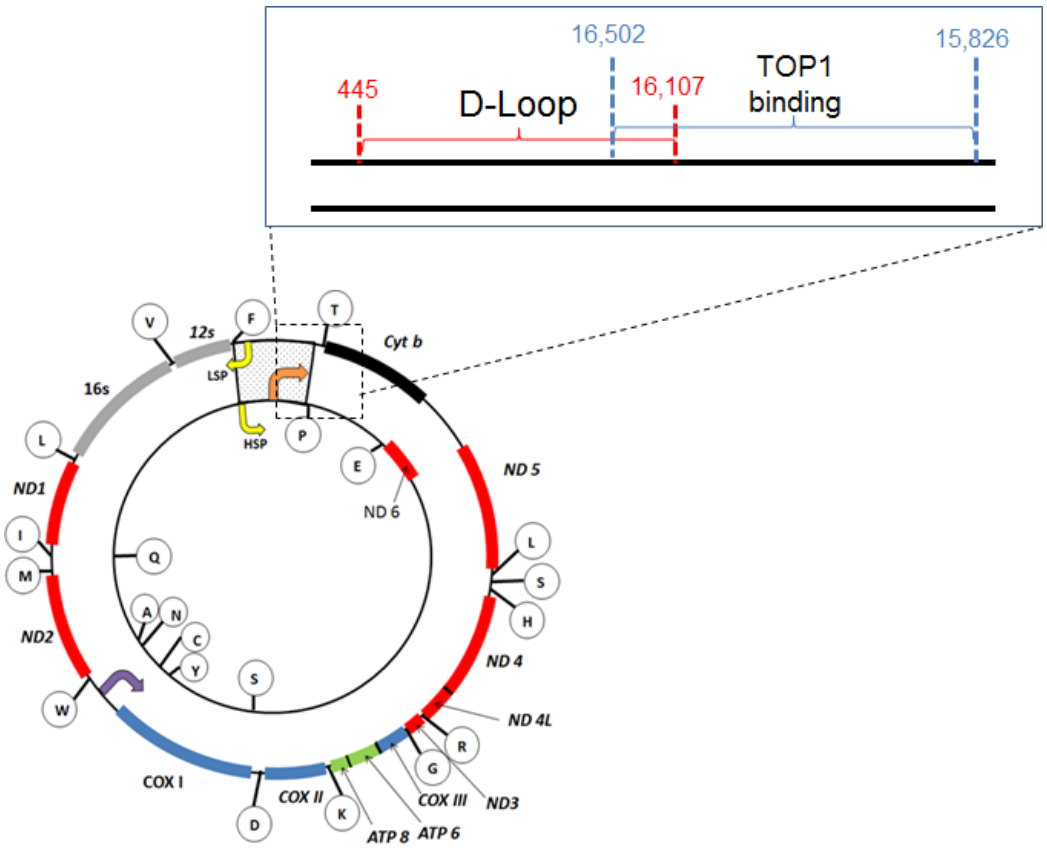

Figure 1.6. *The binding sites of TOP1MT on mtDNA*. This figure demonstrates that TOP1MT binds to a region of mtDNA adjacent to and including part of the D-loop (adapted from Zhang and Pommier, 2008, http://www.mitomap.org/MITOMAP/mitomapgenome.pdf).

All together the results indicating that mitochondria contain their own topoisomerase illustrates how mechanisms surrounding the regulation of mtDNA are more intricate than initially thought, which leaves the possibility for finding further information on factors that are involved with this genome.

1.4 Overall aims of study

The overall aim of this study was to determine whether TDP1 was present and active in mitochondria and if so exactly what role this enzyme has in mtDNA repair, which was covered by asking the following questions:

- Is TDP1 present and active in the mitochondrion?
- Is TDP1 essential in mtDNA repair and cell survival?
- Does next generation sequencing aid in discovering the exact role of TDP1 in mtDNA repair?

It was also determined that if TDP1 was found to be present and active in mitochondria the protein associations of this enzyme would be assessed by asking:

- Does phosphorylation of amino acid 81 in TDP1 promote association with mitochondrial DNA ligase IIIα?

It was anticipated that by using these questions as a basis to study TDP1 it would be possible to delineate the role of this enzyme in mitochondria, providing greater insight as to the organisation of the DNA repair machinery of this organelle.

Chapter 2. General materials and methods

2.1 Materials

2.1.1 *Chemicals and reagents*

All reagents used for the experiments presented in this thesis were supplied by Sigma-Aldrich®, unless stated otherwise.

2.1.2 *Bacterial strains*

- α-Select Competent Cells (Bioline):

Bacterial strain used to transform cloned DNA into bacteria in preparation for experiments with mammalian cell lines.

2.1.3 *Mammalian cell lines*

- Flp-In™ T-Rex™ HEK293 cells (life technologies):

Mammalian cell line containing a Tet repressor and Flp Recombination Target (FRT) site that allows stable integration and tetracycline-inducible expression of a gene of interest, from a specific locus within the genome of the host. Stable integration of the gene of interest within the Flp-In™ T-Rex™ HEK293 host genome at the same location ensures homogenous expression of the desired protein upon expression with tetracycline.

- FD105 M21 fibroblasts

These cells were derived from an ataxia oculomotor apraxia-1 (AOA1) patient and immortalised using human telomerase reverse transcriptase (hTERT). The cells were then stably transfected with a plasmid encoding and expressing aprataxin (APTX); the protein involved in causing AOA1 when its function is compromised as a result of mutated *APTX* (El-Khamisy et al., 2009).

- SCAN1 lymphoblastoids

These cells were taken from a SCAN1 patient and immortalised using Epstein-Bar virus (EBV) (performed by Dr El-Khamisy). These cells contained the A1478G mutation in *TDP1* that causes SCAN1 (Takashima et al., 2002).

2.1.4 *Mouse strains*

- *Tdp1* -/- mice

These mice were generated from C57 black 6 (C57BL/6) mice and contained a single substitution at nucleotide 1369 in *Tdp1* causing premature termination of transcription and loss of stability of TDP1. Heterozygous *Tdp1* +/- mice were kept on an outbred 129Ola and C57BL6 mouse background (Katyal et al., 2007).

2.1.5 *Vectors*

Table 2.1. Vectors used and their application in this thesis.

Name	Application
pEGFP-NI (Clontech Laboratories Inc.)	Contained the *TOP1mt* and *TOP1mt*^{Y559A} genes to be used for transfecting Flp-In™ T-Rex™ HEK293 cells. Vector contained gene for resistance to **Kanamycin**.
pCI-neo (Promega)	Contained the *mtTDP1*^{S81E}*/FLAG* and *mtTDP1*^{S81A}*/FLAG* genes for transfecting Flp-In™ T-Rex™ HEK293 cells. Vector contained a gene for resistance to **Ampicillin**.
pcDNA5/FRT/TO (life technologies)	Vector was used for cloning with *TOP1mt* and *TOP1mt*^{Y559A} genes for subsequent transfection into Flp-In™ T-Rex™ HEK293 cells. Vector contained a gene for resistance to **Ampicillin**.
pOG44 (life technologies)	Vector used in co-transfection of Flp-In™ T-Rex™ HEK293 cells along with pcDNA5/FRT/TO and desired construct. Vector contained a gene for resistance to **Ampicillin**.
pcDNA5/FRT/TO/mtPARN	Vector contained a gene for mitochondrially targeted PARN. The *PARN* gene was removed by restriction digest, leaving the mitochondrial presequence from ATP9 of *Neurospora crassa* behind. This would then be used for cloning with the *mtTDP1*^{S81E}*/FLAG* and *mtTDP1*^{S81A}*/FLAG* genes for transfecting Flp-In™ T-Rex™ HEK293 cells. The vector also contained a gene for resistance to **Ampicillin**.

2.1.6 *DNA oligonucleotides*

Table 2.2. DNA oligonucleotides used in this thesis.

Name and orientation	Sequence (5' to 3')	Restriction site	Application
TOP1mt (F)	CACACA**GGATCC**TGGCAGATGCGCGTGGTG	BamHI	Molecular cloning
TOP1mt (R)	ACTCGA**CTCGAG**CTACTTATCGTCGTCATCCTTGTAATCGAATTCAAAGTCTTCTCCTGC	XhoI	Molecular cloning
TDP1 (F)	ACAA**GCGCGC**CTACTCTTCCCAGGAAGGCGATTATGGG	BssHII	Molecular cloning
TDP1 (R)	ACTCGA**GCGGCCGC**TACTTATCGTCGTCATCCTTGTAATCGGAGGGCACCCACATGTTC	NotI	Molecular cloning
pcDNA5 (F)	GTTTAGTGAACCGTCAGATCG	N/A	Plasmid sequencing
pcDNA5 (R)	CCTACTCAGACAATGCGATGC	N/A	Plasmid sequencing

B2M (F)	CCAGCAGAGAATGGAAAGTCAA	N/A	qRT-PCR
B2M (R)	TCTCTCTCCATTCTTCAGTAAGTCAACT	N/A	qRT-PCR
B2M FAM probe (life technologies)	ATGTGTCTGGGTTTCATCCATCCGACA	N/A	qRT-PCR
ND1 (F)	CCCTAAAACCCGCCACATCT	N/A	qRT-PCR
ND1 (R)	GAGCGATGGTGAGAGCTAAGGT	N/A	qRT-PCR
ND1 VIC probe (life technologies)	CCATCACCCTCTACATCACCGCCC	N/A	qRT-PCR
Human mtDNA A (F) 550bp-570bp	AACCAAACCCCAAAGACACCC	N/A	Deep sequencing
Human mtDNA A (R) 9839bp-9819bp	CCTGAAGTGCAGTAATAACC	N/A	Deep sequencing
Human mtDNA B (F) 9592bp-9611bp	TCCCACTCCTAAACACATCC	N/A	Deep sequencing
Human mtDNA B (R) 646bp-625bp	CCCGAGTGTAGTGGGGTATTTG	N/A	Deep sequencing
Mouse mtDNA A (F) 2665bp-2684bp	AGAGAAGGTTATTAGGGTGG	N/A	Deep sequencing
Mouse mtDNA A (R) 10756bp-10737bp	CATGAAGCGTCTAAGGTGTG	N/A	Deep sequencing
Mouse mtDNA B (F) 9822bp-9844bp	AAAAAAATTAATGATTTCGACTC	N/A	Deep sequencing
Mouse mtDNA B (R) 2335bp-2315bp	ACTTTGACTTGTAAGTCTAGG	N/A	Deep sequencing

*Bases in bold represent restriction sites introduced by the primers into each gene. With exception to probes for qRT-PCR all oligonucleotides were supplied by Eurogentec.

2.1.7 *siRNA duplexes*

Table 2.3. siRNA duplexes used for siRNA knockdowns in Flp-In™ T-Rex™ HEK293 cells.

Name	Sequence
Non-targeted	5’-CGUUAAUCGCGUAUAAUACGCGUAU-3’ 3’-GCAAUUAGCGCAUAUUAUGCGCA-5’
TDP1 siRNA duplex	5’-UGCAUAGCAUAAUGAGAUAUCUUGG-3’

A	3’-ACGUAUCGUAUUACUCUAUAGAA-5’
TDP1 siRNA duplex B	5’-GGAUAGAUGUCAUUCACAAGCACGA-3’ 3’-CCUAUCUACAGUAAGUGUUCGUG-5’
TDP1 siRNA duplex C	5’-CGAUGAAUCAAAGUGGUUAUGUUCT-3’ 3’-GCUAVUUAGUUUCACCAAUACAA-5’

*Supplied by OriGene. All contained 2x dT 3’ end overhangs.

2.2 General methods

2.2.1 *Bacterial culture*

i) Transformation of chemically competent cells

α-select bacterial cells (Bioline Reagents Ltd.), kept in 200µl aliquots at -80^{o}C, were thawed on ice and 40µl was transferred to pre-chilled 1.5ml reaction tubes per transformation reaction. Any remaining cells from the aliquot were replaced at -80^{o}C, but freeze-thaw cycles never exceeded more than 1 per aliquot. Between 1-4µl of ligation reaction for molecular cloning, or 10ng for purified plasmid DNA was added to 40µl α-select bacterial cells for each sample and incubated on ice for 30 mins. During this time Super Optimal Broth with Catabolite repression (SOC) media was pre-warmed to 37^{o}C. Cells were heat pulsed at 42^{o}C for 45 secs before being incubated on ice for 2 mins, followed by addition of 900µl SOC to each sample and incubation for 1 hour at 37^{o}C with rotary shaking. The cell suspension was then plated on agar plates with the desired antibiotic resistance and incubated overnight at 37^{o}C. Plates displaying colonies following this incubation were stored at 4^{o}C.

SOC media
10mM NaCl
2.5mMKCl
10mM $MgCl_2$
10mM $MgSO_4$
20mM Glucose
0.5% Yeast Extract
2% Tryptone

ii) Plasmid DNA isolation from bacteria

Bacterial cells containing a desired plasmid for purification were grown overnight at 37^{o}C in 5ml Luria Bertani broth (LB) medium containing the correct antibiotic resistance. Cells suspensions were centrifuged at 1500xg for 15 mins and supernatant discarded before plasmid purification was performed using the GeneJET™ Plasmid Miniprep Kit (Fermentas) and the manufacturer's instructions.

LB medium
1.0% NaCl
1.0% Tryptone
0.5% Yeast Extract
Adjust to pH 7.0 with NaOH

2.2.2 *Tissue culture*

i) Cell storage

Cells were incubated at 37^{o}C with humidified 5% CO_2 in sterile conditions in filter-topped flasks or 6-well plates.

ii) Cell maintenance

When cells reached 80-90% confluence during general culturing (i.e. not an experiment to gather data) growth media was removed and cells were removed from their 75cm^2 flask using 5ml PBS/1mM EDTA, or 5ml PBS/1mM EDTA+1x trypsin in the case of fibroblasts. The cell suspension was neutralised with an equal volume of pre-warmed supplemented growth media before being centrifuged at 260xg for 4 mins. The supernatant was discarded and the cell pellet was resuspended in 1ml pre-warmed supplemented growth media before 100µl (at least 200µl for fibroblasts) of the suspension was replaced in its original flask with 15ml supplemented growth media.

Once split three times cells were placed in a fresh 75cm^2 flask and for cell lines of, or generated from Flp-In^{TM} T-Rex^{TM} HEK293 cells the correct concentrations of hygromycin (life technologies) and/or blasticidin (Melford) were added.

iii) Freezing cells for long term storage

To freeze cells for long term storage cell lines were grown to 70-80% confluence in 75cm^2 flasks and harvested using 5ml PBS/1mM EDTA or 5ml PBS/1mM EDTA+1x trypsin for fibroblasts. The cell suspension was neutralised using and equal volume of supplemented growth media before being centrifuged at 260xg for 4 mins. The supernatant was discarded and the cell pellet carefully resuspended in 1ml 10% DMSO in FBS before being transferred to a 2ml cryovial and placed a -80^{o}C in a freezing container with isopropanol for 24 hours. After this time the cells could be transferred to a container with liquid nitrogen.

iv) Thawing cells from long term storage

Cells stored in liquid nitrogen were removed and thawed in their cryovials in a 37^{o}C water bath. The 1ml cell suspension was then transferred to 5ml pre-warmed supplemented growth media and centrifuged at 260xg for 4 mins. The cell pellet was then resuspended in 1ml pre-warmed supplemented growth media and transferred to a 75cm^2 flask with 15ml pre-warmed supplemented growth media. Cells were incubated as in 2.2.2 (i) for 5 hours before the media was replaced and cells placed back in the incubator.

v) Cell counting

Cell counting was performed using an improved Neubauer Haemocytometer (Hawksley) using 100µl cell suspension mixed with 100µl 50% Trypan Blue/PBS. Cells that were unstained by the Trypan Blue were counted in each quadrant of one side of the cell counter. The total number was then divided by 4 (for each quadrant) and then multiplied by 2 (to account for dilution in 50% Trypan Blue/PBS). This number was then multiplied by 10000 to give the total number of cells per ml of cell suspension. The process of counting was then repeated using the quadrants on the opposite side of the cell counter to verify that the number of cells were the same on either side.

vi) Mycoplasma testing and treatment

Every 6 weeks mycoplasma testing was carried out using MycoAlert™ Mycoplasma Detection Kit (Lonza) as per the manufacturer's guidelines. If mycoplasma was present treatment with Plasmocin^{TM} (InvivoGen) was carried out for 2 weeks or until undetectable.

vii) Transformation of Flp-In^{TM} T-Rex^{TM} HEK293 cells

To generate stable cell lines with inducible expression of desired proteins for this thesis the Flp-In^{TM} T-Rex^{TM} HEK293 system (life technologies) was used. Cells were seeded at $3x10^5$ cells in wells of a 6-well plate in 2ml supplemented DMEM for the desired plasmid, and a negative and positive control (pcDNA5/FRT/TO without any gene integration through cloning). Once cells were adhered to the well surface 500µl DMEM was mixed carefully with 1µl pOG44 (1µg), 1µl of the desired plasmid (100ng), and

10µl SuperFect Transfection Reagent (Qiagen) in 1.5ml reaction tubes. The same reaction was also set up with pcDNA5/FRT/TO alone as a positive control, and another reaction without any pcDNA5/FRT/TO vector was also set up. The reactions were incubated at room temperature for 10 mins before being applied to the cell containing wells once the 2ml supplemented DMEM had been removed. Cells were incubated as in 2.2.2 (i) for 2.5 hours before the vector/DMEM mix was removed and replaced with 2ml supplemented DMEM. Cells were then incubated for 48 hours before selection of successfully transformed cells began with the use of hygromycin B (life technologies) at 100ng/ml final concentration and blasticidin S (Melford) at 10ng/ml final concentration.

viii) Poly-L-ornithine treating flasks

To aid in adhering cells the surfaces of 25cm^2 flasks for use in transient siRNA transfections 1.5ml Poly-L-ornithine was added to each flask required for the experiment and then incubated as in 2.2.2 (i) for 30 mins. After this time the Poly-L-ornithine was removed and flask surfaces were washed with 2ml PBS before 5ml supplemented growth media was added along with the desired cell number.

2.2.3 *Protein manipulation*

i) Isolation of cytoplasmic protein from human cell lines

Cells grown in 6-well plates or 25cm^2 flasks were harvested using 0.5ml and 2ml PBS/EDTA, respectively, before being neutralised in an equal volume of supplemented growth media. Cells were centrifuged at 260xg for 4 mins and the resulting supernatant was discarded. Cell pellets from 6-well plates were resuspended in 50µl pre-chilled lysis

buffer, and cell pellets from 25cm^2 flasks were resuspended in 150µl pre-chilled lysis buffer. Samples were then vortexed for 30 secs and centrifuged at 2000xg for 4 mins at 4^{o}C. The supernatant was then transferred to fresh pre-chilled 1.5ml reaction tubes and used to quantify protein concentration by Bradford analysis, or snap frozen in liquid nitrogen and stored at -80^{o}C.

Lysis buffer

50mM	Tris-HCl pH 7.5
0.15M	NaCl
2mM	$MgCl_2$
1mM	PMSF
1%	NP-40
1x	Protease inhibitor mix (Roche Applied Science)*

* Diluted to 1x concentration from 7x stock solution depending on volume of lysis buffer required.

ii) Isolation of mitochondria from human cell lines

Cells were grown in 300cm^2 flasks (1-6 flasks depending on quantity of mitochondria required) until 80-90% confluent, and were harvested by removing growth media followed by addition of 15ml 1mM EDTA/PBS or 15ml 1mM EDTA/PBS+1x trypsin for fibroblast cells. The cell suspension was neutralised with supplemented growth media and centrifuged at 260xg for 4 mins before the subsequent pellet was resuspended in 2ml ice cold homogenisation buffer. All steps from this point were carried out at 4^{o}C. The cell suspension was then transferred to a 2ml glass/teflon homogeniser (Glas-Col) for HEK293 cells or glass/glass homogeniser for fibroblast cells. The cell suspension was subjected to 20 homogenisation passes before being centrifuged at 400xg for 10 mins. The supernatant was transferred to a new tube and the pellet was resuspended in 2ml homogenisation buffer for the homogenisation and

centrifugation steps to be repeated twice more. All supernatants were centrifuged at 12000xg for 10 mins and supernatants discarded. Pellets were combined in 100µl homogenisation buffer and centrifuged at 12000xg once again. This pellet was resuspended in 500µl homogenisation buffer to wash and centrifuged at 12000xg for another 10 mins. The pellet could then be snap frozen in liquid nitrogen and stored at -80^{o}C, or resuspended in 100-500µl homogenisation buffer (without BSA or PMSF) if purification was desired.

Homogenisation buffer
0.6M Mannitol
10mM Tris-HCl pH 7.4
1mM EGTA
1mM PMSF
0.1% BSA

iii) Isolation of mitochondria from mouse brain

Once the mouse brain was harvested it was placed immediately in a beaker containing 20ml isolation medium. Using pre-chilled scissors the brain was cut into small pieces that were then washed by carefully decanting the isolation medium followed by addition of another 10ml isolation medium. The brain suspension was then transferred to a 40ml Dounce homogeniser (Fisher Scientific) and subjected to 8 homogenisation passes before being transferred to a pre-chilled SS34 centrifuge tube and centrifuged for 3 mins at 2000xg using the Sorvall RC-5C. The supernatant was decanted into a clean pre-chilled SS34 tube and centrifuged at 12500xg for 10 mins. The supernatant was removed and the pellet resuspended in 1ml 3% ficoll medium using a pre-chilled glass rod being careful not to disturb any blood spot in the pellet. The suspension was then carefully layered onto 10ml 6% ficoll medium and centrifuged at 11500xg for 15 mins. The supernatant was decanted sharply and the remaining pellet was resuspended in 10ml isolation medium before being centrifuged at 11500xg for a further 10mins. The

pellet could then be snap frozen in liquid nitrogen and stored at -80^{o}C or could be purified if desired.

Isolation medium
250mM Sucrose
10mM Tris-HCl pH 7.4
0.5mM EDTA

Ficoll medium
240mM Mannitol
60mM Sucrose
50µM EDTA
10mM Tris-HCl pH 7.4
6% or 3% Ficoll (added immediately before use)

iv) Mitochondrial purification

Mitochondrial purification was carried out in order to remove any nuclear and/or cytosolic contaminants following mitochondrial isolation from human cells or from mouse brain. This was performed by initially treating with 1U RNase free DNaseI (Epicentre®) per 5mg mitochondrial protein at room temperature for 15 mins supplemented with 10mM $MgCl_2$. Following this 20µg RNase free Proteinase K (Life Technologies) was added per 5mg mitochondrial protein and incubated on ice for 30 mins. The reaction was stopped with addition of 1mM PMSF (final concentration) before being centrifuged at 12000xg for 10 mins. Mitochondria were washed with 500µl homogenisation buffer containing 1mM PMSF and centrifuged as previous.

v) Mitochondrial localisation assay

To ensure that expressed proteins using the Flp-In^{TM} T-Rex^{TM} HEK293 system (life technologies) were localised to mitochondria a localisation assay was performed using Proteinase K (life technologies). Mitochondria that had been isolated from appropriate cell lines as described in 2.2.3 (ii) were quantified by Bradford analysis as in 2.2.3 (vi) and transferred in homogenisation buffer to 3 1.5ml reaction tubes for each cell line in 100µg per tube. The following reactions were set up with a total volume of 50µl:

Table 2.4. Reaction set up for mitochondrial localisation assay.

	Untreated	**Proteinase K alone**	**Proteinase K + Triton X-100**
Mitochondria	100µg	100µg	100µg
Proteinase K	-	4µg	4µg
Triton X-100	-	-	1%

The Proteinase K was stopped using 5µl 10mM PMSF and then mixed with an equal volume of 2x dissociation buffer, snap frozen in liquid nitrogen, and stored at -80^{o}C to be used for SDS-PAGE and western blot analysis. The use of 4µg Proteinase K would prove to be too much and so this experiment was repeated for the HEK293/*TOP1mt/FLAG* and HEK293/*TOP1mt*^{Y559A}*/FLAG* cell lines with 0.5µg and 2µg Proteinase K It was found that 2µg was sufficient and so this was used for the HEK293/*mtTDP1*^{S81E}*/FLAG*, and HEK293/*mtTDP1*^{S81A}*/FLAG* cell lines.

2x dissociation buffer
0.125M Tris-HCl, pH 6.8
4% SDS
0.15M DTT
15% Glycerol
0.01% Bromophenol blue
0.01% Benzonase (Novagen)

vi) Protein quantification through Bradford assay

The Bradford assay was used to quantify protein within samples and this was performed by firstly setting up the following reactions in 1.5ml reaction tubes to set the standard curve:

Table 2.5. Reaction set up to make standard curve for Bradford analysis on the microplate reader Elx 800 (BIO-TEK).

	BSA (µg)					
	0	2	5	10	15	20
H_2O	800µl	798µl	795µl	790µl	785µl	780µl
Bradford reagent (Bio-Rad)	200µl	200µl	200µl	200µl	200µl	200µl
BSA (1µg/µl)	-	2µl	5µl	10µl	15µl	20µl

Once this had been set up, 1µl of each sample for protein quantification was then mixed in 799µl H_2O and 200µl Bradford reagent before 200µl of all reactions were added to two wells of a 96-well plate for each sample. The plate was then put into the microplate reader Elx 800 (BIO-TEK) set at a wavelength of 595nm for protein quantification.

vii) SDS-PAGE

To prepare samples for western blotting protein was separated by SDS-PAGE. Protein samples were transferred to 1.5ml reaction tubes in the desired concentration and then mixed with and equal volume of 2x dissociation buffer. Each reaction was then heated at 95^{o}C for 3 mins before being centrifuged at 12000xg for 2 mins and loaded onto the gel. For the results outlined in this thesis either 10% or 12% polyacrylamide resolving gels were used along with a 4% stacking gel in every case. The following tables demonstrate the reagents used to cast these gels:

Table 2.6. 4% SDS-PAGE stacking gel reagents and volumes.

	5ml	**10ml**	**15ml**	**20ml**
29:1 30%: bisacrylamide (NBS Biologicals)	0.625ml	1.25ml	1.875ml	2.5ml
0.5M Tris-HCl pH 6.8	1.25ml	2.5ml	3.75ml	5ml
H_2O	3.025ml	6.05ml	9.075ml	12.1ml
10% SDS	50µl	100µl	150µl	200µl
TEMED	5µl	10µl	15µl	20µl
10% APS	50µl	100µl	150µl	200µl

Table 2.7. 10% SDS-PAGE resolving gel reagents and volumes.

	5ml	**10ml**	**15ml**	**20ml**
29:1 30%: bisacrylamide (NBS Biologicals)	1.665ml	3.33ml	4.995ml	6.66ml
3.75M Tris-HCl pH 8.5	0.5ml	1ml	1.5ml	2ml
H_2O	2.725ml	5.45ml	8.175ml	10.9ml
10% SDS	50µl	100µl	150µl	200µl
TEMED	5µl	10µl	15µl	20µl
10% APS	50µl	100µl	150µl	200µl

Table 2.8. 12% SDS-PAGE resolving gel reagents and volumes.

	5ml	**10ml**	**15ml**	**20ml**
29:1 30%: bisacrylamide (NBS Biologicals)	1.998ml	3.998ml	5.994ml	7.992ml
3.75M Tris-HCl pH 8.5	0.5ml	1ml	1.5ml	2ml
H_2O	2.392ml	4.784ml	7.176ml	9.568ml
10% SDS	50µl	100µl	150µl	200µl
TEMED	5µl	10µl	15µl	20µl
10% APS	50µl	100µl	150µl	200µl

Once samples had been loaded onto the gel the were electrophoresed at 80V in 1x running buffer until the samples reached the resolving gel in which the voltage was set to 120V. A molecular weight marker (Thermo Scientific) was also run to determine the rate at which protein was moving through the gel and when it should be stopped. Once complete the gel could then be used for its desired purpose.

2x dissociation buffer

125mM Tris-HCl, pH 6.8
4% SDS
0.15M DTT
15% Glycerol
0.01% Bromophenol blue
0.01% Benzonase (Novagen)

1x running buffer

192mM Glycine
25mM Tris-HCl pH 7
0.1% SDS

viii) Western blotting

Once SDS-PAGE was complete the gel was removed and transferred to 20ml 1x transfer buffer and incubated at room temperature with rocking for 10 mins to equilibrate. During this time a section of Immobilon transfer membrane (Millipore) was cut to an appropriate size to cover the SDS-PAGE gel, and then activated with incubation in 15ml Methanol for 30 secs with agitation. Once activated the membrane was placed in 20ml 1x transfer buffer and incubated with rocking until the 10 min incubation for the SDS-PAGE gel was complete. At this point 2 sections of 3mm chromatography paper (Whatman™) were cut to an appropriate size in comparison to the gel/membrane and placed in a transfer cassette, followed by addition of the gel on top, then the transfer membrane, and lastly 2 more sections of 3mm chromatography paper. The cassette was then closed and placed into the transfer unit (Hoefer® or Bio-Rad), making sure the gel end of the cassette was closest to the cathode, and ≈1.5L 1x transfer buffer was added. The transfer unit was then placed in 4°C with a magnetic stirrer to aid circulation of the buffer before the transfer from gel to membrane was mediated at 100V or 500mA for 1.5 hours, or if 2 gels were run, 2 hours. Once the transfer was complete the membrane the membrane was washed in 1x TTBS for 10 mins at room temperature with rocking before being blocked in 5% milk/TTBS for 1 hour or overnight at 4°C with rocking. After blocking, membranes were washed 3 times in 1x TTBS and then exposed to the primary antibody, washed 3 times in 1x TTBS, and

then secondary antibodies (after another washing step) at the indicated concentration and indicated times as shown in tables 2.7 and 2.8.

Table 2.9. Primary antibodies used for western blotting.

Antibody	Source	Dilution in 5% milk/TTBS (µl antibody: µl milk)	Incubation time (hours)	Incubation temperature (^{o}C)	Expected size ≈: western blot (kDa)
α β-Actin	Mouse	1:10,000	1	20	42
α COX I (Abcam)	Mouse	1:1000	1	20	40
α COX II (Abcam)	Mouse	1:1000	1	20	24
α FLAG	Mouse	1:1000	1	20	Dependant on protein
α Lamin (Cell Signalling)	Rabbit	1:1000	overnight	4	51
α NDUFA9 (Abcam)	Mouse	1:1000	1	20	35
α Neu N (Cell Signalling)	Rabbit	1:1000	overnight	4	46
α TDP1 (Abcam)	Rabbit	1:1000	overnight	4	70
α TOM 20 (Santa Cruz Biotechnology)	Rabbit	1:750	overnight	4	17
α Porin (Abcam)	Mouse	1:10,000	1	20	39
α XRCC1 (Cell Signalling)	Rabbit	1:1000	overnight	4	82

Table 2.10. Secondary antibodies used for western blotting.

Antibody	Source	Dilution in 5% milk/TTBS (µl antibody: µl milk)	Incubation time (hours)	Incubation temperature (^{o}C)
α mouse (Dako)	Rabbit	1: 2000	1	20
α rabbit (Dako)	Swine	1: 3000	1	20

Once incubation with the secondary antibody was complete the membrane was washed 3 time in 1x TTBS before being exposed to ECL Plus (GE Healthcare) for 5 mins followed by scanning and imaging using the Storm 850. The blot could then be analysed by using ImageQuant.

1x transfer buffer
25mM Tris-HCl (pH 7.6)
192mM glycine
20% methanol
0.03% SDS

1x TTBS
50mM Tris-HCl (pH 7.6)
150mM NaCl
0.05% Tween-20

2.2.4 DNA manipulation

i) DNA amplification by polymerase chain reaction

In order to amplify desired regions of DNA for cloning or to prepare samples for sequencing polymerase chain reaction (PCR) was carried out. This was performed by setting up PCR reactions in 0.2ml reaction tubes using the KOD polymerase kit (Novagen) in the following manner (negative and positive reactions were also set up):

Table 2.11. Reagents of a standard PCR.

Plasmid DNA (10ng)	1µl
10x PCR Buffer 20 mM Tris-HCl pH7.5 0.5 mM DTT 50 µg/ml BSA	5µl
10x dNTPs (2mM each)	5µl
$MgSO_4$ (25mM)	2µl
Forward primer (10µM)	1µl
Reverse primer (10µM)	1µl
H_2O	34µl
KOD Polymerase (1U/µl)	1µl

Once the reaction had been set up it could then be subjected to the PCR programme as follows:

Table 2.12. General PCR programme.

Step	Time	Temperature (^{o}C)	Cycle number
Initial denaturation	2 mins	94	1
Denaturation Annealing Extension	30 secs 30 secs 1-3 mins*	94 50-65* 70	35
Final extension	10 mins	70	1

*annealing temperatures and extension times depended on primers and length of DNA fragment to be analysed

Once the PCR programme was complete the samples could then be subjected to gel electrophoresis as described in 2.2.4. (iv).

ii) Real-time polymerase chain reaction (qRT-PCR) to assess mtDNA copy number

The copy number of mtDNA was assessed using qRT-PCR following expression/knockdown experiments in mammalian cells as described in chapter 4. In order to attain this data 10ng whole cell DNA from each experiment was mixed with the following reagents and oligonucleotides (table 2.13) in a 96-well plate in triplicate, and subjected to the qRT-PCR programme (table 2.14) in the StepOnePlus™ Real-Time PCR System. For validity of results samples using 100ng, 10ng, 1ng, 100pg, and 10pg DNA were also added to the reagents in table 2.13 in triplicate so that a standard curve could be made on final analysis for validity of results.

Table 2.13. Reagents and oligonucleotides used per qRT-PCR reaction.

Reagent	Volume (µl)
Taqman® Universal Master Mix II (life technologies)	10
B2M (F) primer (10µm) (Eurogentec)	0.6
B2M (R) primer (10µm) (Eurogentec)	0.6
ND1 (F) primer (10µm) (Eurogentec)	0.6
ND1 (R) primer (10µm) (Eurogentec)	0.6
B2M FAM probe (life technologies)	0.4
ND1 VIC probe (life technologies)	0.4
H_2O	4.8

Table 2.14. qRT-PCR programme used to determine mtDNA copy number.

Temperature (^oC)	Time	Cycle number
50	2 mins	1
95	10 mins	1
95 60	15 secs 1 min	45

Once the data had been gathered by the StepOnePlus™ Real-Time PCR System it was transferred to a Microsoft Excel 2010 folder where the critical threshold (CT) values from ND1 were subtracted by the CT value from B2M. The relative number of reads of ND1 to B2M could then be assessed by using $2^{\Delta\Delta CT}$ on the ND1 minus B2M value.

iii) Restriction digests of DNA

Restriction digests were performed in molecular cloning to prepare PCR amplified regions of DNA for ligation with digested vectors in preparation for transfection into Flp-In™ T-Rex™ HEK293 cells. Restriction digests for experiments in this thesis were conducted using 1U BamHI, XhoI, NotI, and BssHII (all from New England Biolabs), which were incubated at 37^{o}C overnight with the appropriate vector/DNA fragment.

Enzymes were inactivated by heat treating reactions at 70^{o}C for 15 mins once digest was complete.

iv) DNA ligation

For ligation of vectors with these specific inserts ligation was carried out in 10µl reactions containing 50ng vector: 100ng insert. In these 1µl T4 DNA Ligase (New England Biolabs) was used with 1µl 10x ligase buffer (50mM Tris-HCl pH 7.5, 10mM MgCl2, 1mM ATP, 10mM DTT) and reactions were incubated overnight at 16^{o}C.

v) Gel electrophoresis of DNA

To separate products of DNA to determine whether PCR or restriction digest reactions were successful, samples were subjected to gel electrophoresis. For this gels were cast at 0.8% molecular grade agarose (Bioline) in 1x TAE containing 50ng/ml ethidium bromide. When DNA was to be extracted from the gel following electrophoresis, gels were cast at 1% NuSieve® GTG® agarose (Lonza) in 1x TAE containing 50ng/ml ethidium bromide. Samples were then loaded onto the appropriate gel with 5µl 1kb DNA ladder (New England Biolabs) and electrophoresis was carried out by applying 70V for 45 mins. Images of the gel could then be taken and any further manipulations were then performed.

1x TAE
40mM Tris-acetate
1mM EDTA
pH 8.3

vi) Phenol/chloroform extraction of DNA constructs from agarose

Following some PCR and restriction digest reactions it was necessary to remove DNA of the correct molecular weight for further experiments. This was achieved by cutting the desired DNA from the NuSieve® GTG® agarose (Lonza) (described above),

transferring it to a 1.5ml reaction tube, and melting it a 68^{o}C. An equal volume of TE buffer was then added followed by addition of an equal volume of phenol pH 7.9 and vortexing for 30 secs. The sample was then centrifuged at maximum speed in a microcentrifuge for 3mins before the upper aqueous phase was transferred to a fresh 1.5ml reaction tube. An equal volume of phenol was added and the vortexing/centrifuge step was repeated with the upper aqueous phase being transferred to a new 1.5ml reaction tube again. An equal volume of 1:1 phenol: chloroform (24 parts chloroform, 1 part isoamyl alcohol) was then added and the vortexing/centrifuge step was repeated before an equal volume of chloroform was added followed by vortexing/centrifuging once more. The upper aqueous phase was taken and placed into a fresh 1.5ml reaction tube and incubated on ice for 15 mins, and then centrifuged at 16,000xg for 15 mins at 4^{o}C. The upper aqueous phase was transferred to a new 1.5ml reaction tube with 10% 3M NaOAc, 1µl linear acrylamide, and 2 volumes of 100% ethanol. This reaction was then incubated overnight at -20^{o}C before being centrifuged at 16,000xg for 30 mins, the supernatant discarded and tube air dried, followed by the DNA being resuspended in 20µl H_2O.

TE buffer
10mM Tris-HCl pH 8
1mM EDTA

vii) Phenol/chloroform extraction of DNA from mammalian cells in culture

To extract DNA from mammalian cells in culture the cells were harvested with PBS/EDTA and centrifuged at 260xg before the supernatant was discarded. The cell pellet was then resuspended in 200µl TE buffer, 20µl 20% SDS, and 25µl Proteinase K (20µg/µl) (life technologies). The reaction was then incubated overnight at 37^{o}C with shaking, followed by addition of 245µl phenol pH 7.9, vortexing for 30 secs and centrifuging at maximum speed in a microcentrifuge for 3 mins. The upper aqueous

phase was transferred to a fresh 1.5ml reaction tube and an equal volume of phenol was added and the vortexing/centrifuge step was repeated with the upper aqueous phase being transferred to a new 1.5ml reaction tube again. An equal volume of 1:1 phenol: chloroform (24 parts chloroform, 1 part isoamyl alcohol) was then added and the vortexing/centrifuge step was repeated before an equal volume of chloroform was added followed by vortexing/centrifuging once more. The upper aqueous phase was taken and placed into a fresh 1.5ml reaction tube and 10% 3M NaOAc, 1µl linear acrylamide, and 2 volumes of 100% ethanol were added. This reaction was then incubated overnight at -20^{o}C before being centrifuged at 16,000xg for 30 mins, the supernatant discarded and tube air dried, followed by the DNA being resuspended in 20µl H_2O.

viii) Nucleic acid quantification

Quantification of DNA was performed using a ND1000 spectrophotometer (Labtech) at OD_{260} for duplex DNA (50µg/OD_{260}) following the manufacturer's guidelines. Using mM extinction coefficients of 50 for dsDNA, 33 for ssDNA, and 40 for RNA.

ix) DNA sequencing

In order to confirm that plasmid DNA had the correct sequence for transfection into Flp-In^{TM} T-Rex^{TM} HEK293, sequencing was carried out. This service was kindly provided by members of the Mitochondrial Diagnostic Service within the Mitochondrial Research Group.

Chapter 3. Is TDP1 present and active in the mitochondrion?

3.1 Introduction

As outlined in 1.3.2 the mutation in *TDP1* (A1478G) causes a conversion of amino acid 493 from histidine to arginine, thus modifying the active site of TDP1 resulting in a loss-of-function (Takashima et al., 2002). This mutation affects cerebellar neurons which is manifested in SCAN1; a rare autosomal recessive neurodegenerative disorder (Takashima et al., 2002). A common feature of mitochondrial disorders is spinocerebellar ataxia, alluding to the possibility that a loss of function mutation in *TDP1* could have an effect in mtDNA repair and contribute to the phenotype observed in patients (Stumpf and Copeland, 2011).

The observation that TDP1 resolves DNA-TOP1 complexes independently of DNA replication demonstrated the importance of TDP1 in neurons as they are post-mitotic (El-Khamisy et al., 2005). Generation of *Tdp1 -/-* mice showed that TDP1 was required in neural homeostasis and that these mice displayed a very similar phenotype to that observed in SCAN1 patients (Katyal et al., 2007). In order to investigate whether TDP1 was present and active in mitochondria a collaboration was set up between our own group and a group leader at the University of Sussex; Dr SF El-Khamisy. Being an author on several papers regarding TDP1, and having access to SCAN1 patient cell lines as well as the *Tdp1 -/-* mice, it was anticipated that this collaboration would help in our shared objective.

Activity assays were used as a means to determine whether TDP1 was present and active in mitochondria from fibroblasts, a SCAN1 patient cell line, and from *Tdp1 -/-* mouse brain. Once these experiments had been conducted it was hoped that a sound conclusion could be made to the question:

Is TDP1 present and active in the mitochondrion?

3.2 Methods

3.2.1 *In vitro activity assay using mitochondrial extracts*

To determine whether TDP1 was active in mitochondria an *in vitro* assay was used with mitochondrial extracts from both human cells and mouse brain. The assay employs a duplex DNA substrate composed of three oligonucleotides of which one (18mer) is radiolabelled and has a 3' phosphotyrosine. This phosphotyrosine is intended to mimic the covalent bond *in vivo* that is formed between DNA and TOP1. Under this circumstance TDP1 cleaves the phosphotyrosine bond, thus removing TOP1 from the 3' end of DNA allowing further processing by a phosphatase before re-ligation can commence. In this *in vitro* assay the phosphotyrosine bond of the 18mer is cleaved, removing tyrosine and resulting in a 3' phosphate. If the duplex substrate is then subjected to denaturing gel electrophoresis the radiolabelled 18mer oligonucleotide without tyrosine has increased electrophoretic mobility, which then allows exposure to a phosphorscreen and scanning by Storm 8500 to confirm this result. Therefore, if TDP1 is present and active within a sample the tyrosine should be cleaved which lowers the molecular weight of the substrate resulting in further migration on the denaturing gel.

Mitochondria from human cells were isolated as described in 2.2.3 (ii), and from mouse brain as in 2.2.3 (iii). Both human and mouse mitochondrial extracts were purified as in 2.2.3 (iv) before the activity assay was performed. Three oligonucleotides were used for this assay:

18-mer	5'-TCCGTTGAAGCCTGCTTT-P-Y-3'
25-mer	5'-GACATACTAACTTGAGCGAAACGGT-3'
43-mer	3'-TAGGCAACTTCGGACGAAACTGTATGATTGAACTCGCTTTGCC-5'

(25-mer complimentary to nucleotides 18-43 of 43-mer, and 18-mer complimentary to nucleotides 1-18 of 43-mer. See figure 3.1 A)

The 18-mer (Midland Scientific), with a 3'-phosphotyrosine terminus (18-Y) to imitate DNA lesion *in vivo*, was radiolabelled by phosphorylation using T4 PNK (New England Biolabs) in 25µl reactions containing 5µCi (γ-^{32}P) ATP at 7000Ci/mM for 1 hour at 37^{o}C. T4 PNK was inactivated by incubation at 68^{o}C for 10 mins. Following removal of unincorporated nucleotides the three oligonucleotides were annealed in equimolar concentrations at 55^{o}C and then kept on ice. Mitochondrial samples were lysed using 1x lysis buffer on ice for 15 mins before being centrifuged at 10,000xg for 5 mins at 2^{o}C before the supernatant was transferred to a clean reaction tube. Mitochondria and control whole cell extract containing nuclear protein were quantified by Bradford analysis as described in 2.2.3 (vi). In 10µl reactions the desired amount of protein extract was incubated with 25nM substrate for 1 hour at 37^{o}C in 1x reaction buffer. Reactions were stopped with addition of 1x loading buffer before being heated at 90^{o}C for 10 mins and fractionated by denaturing electrophoresis. Once ran, the gel was exposed to a phosphorscreen and results visualised using the Storm 8500 and ImageQuant to assess relative conversion rates of 3'-phosphotyrosine to 3'-phosphate.

1x lysis buffer
20mM Tris-HCl pH7.5
10mM EDTA
1mM EGTA
100mM NaCl
1% Triton X-100
protease inhibitors (Roche)

1x reaction buffer
25mM Hepes pH8
130mM KCl
1mM DTT

1x loading buffer
44% deionized formamide
2.25mM Tris-borate
0.05mM ETDA
0.01% xylene cyanol
1% bromophenol blue

3.3 Results

3.3.1 *TDP1 is present and active in fibroblast mitochondrial extracts*

Mitochondria isolated from FD105 M21 fibroblasts were used for the activity assay described in 3.2.1 as well as whole cell extract containing nuclear protein as a control. Reasons for using this cell line are outlined in the discussion of this chapter. The results from this experiment are illustrated in figure 1 (performed by Dr. El-Khamisy).

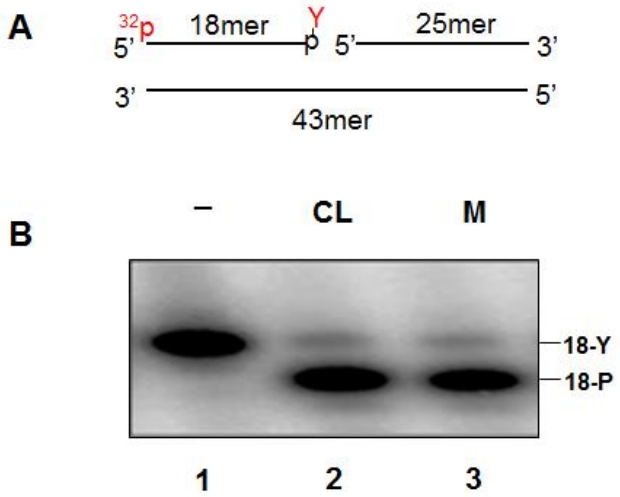

Figure 3.1. *Activity assay to assess TDP1 presence and activity in fibroblast mitochondria***.** Mitochondria were prepared from FD105 M21 fibroblasts as described in 2.2.3 (ii) and purified as in 2.2.3 (iv), and whole cell protein was isolated as in 2.2.1 (i). Whole cell lysate containing nuclear protein (**CL**) and mitochondrial protein (**M**) (10µg) were incubated with radiolabeled duplex substrate and subsequent repair products fractionated by denaturing electrophoresis then exposed to phosphorscreen as described in 3.2.3. Duplex substrate without any protein addition (-) was also fractionated as a control. **(A)** Schematic to demonstrate the radiolabeled duplex substrate used in the assay as described in 3.2.3. **(B)** Substrate following denaturing electrophoresis to indicate whether TDP1 is active in both mitochondrial and nuclear protein. The 18-Y and 18-P to the right of **B** describe 18-mer with 3'-phosphotyrosine terminus and 3'-phosphate terminus, respectively.

The results shown in figure 3.1 **B** demonstrate TDP1 presence and activity in mitochondria, which can be seen in lane **3** by the increased electrophoretic mobility of the 18mer oligonucleotide after incubation with mitochondrial extracts from FD105 M21 fibroblasts. This result is verified in lane **2** as there is similar migration of the substrate following incubation with control whole cell lysate containing nuclear protein in which TDP1 is certainly present. In lane **1**, substrate without any protein addition was also fractionated on the gel to illustrate the electrophoretic mobility of the 18mer oligonucleotide without removal of tyrosine.

3.3.2 *TDP1 is active in LCL mitochondrial extracts*

Having established TDP1 was present and active in FD105 M21 fibroblasts it was then decided to repeat the same activity assay using extracts from wild type and SCAN1 patient lymphoblastoid cell lines. The aim of this experiment was to determine the relative activity of TDP1 in mitochondria in comparison to whole cell lysate and to also confirm that the A1478G mutation in *TDP1* affected activity in mitochondria; thus demonstrating TDP1 in mitochondria is encoded by the same gene as TDP1 in the nucleus. As earlier the same activity assay was carried out (described in 3.2.1) using the same duplex substrate, which is illustrated in figure 3.2 **A**. Mitochondrial and whole cell lysate containing nuclear protein were isolated for this experiment with the results being shown in figure 3.2 **B**, **C**, and **D** (performed by Dr. El-Khamisy).

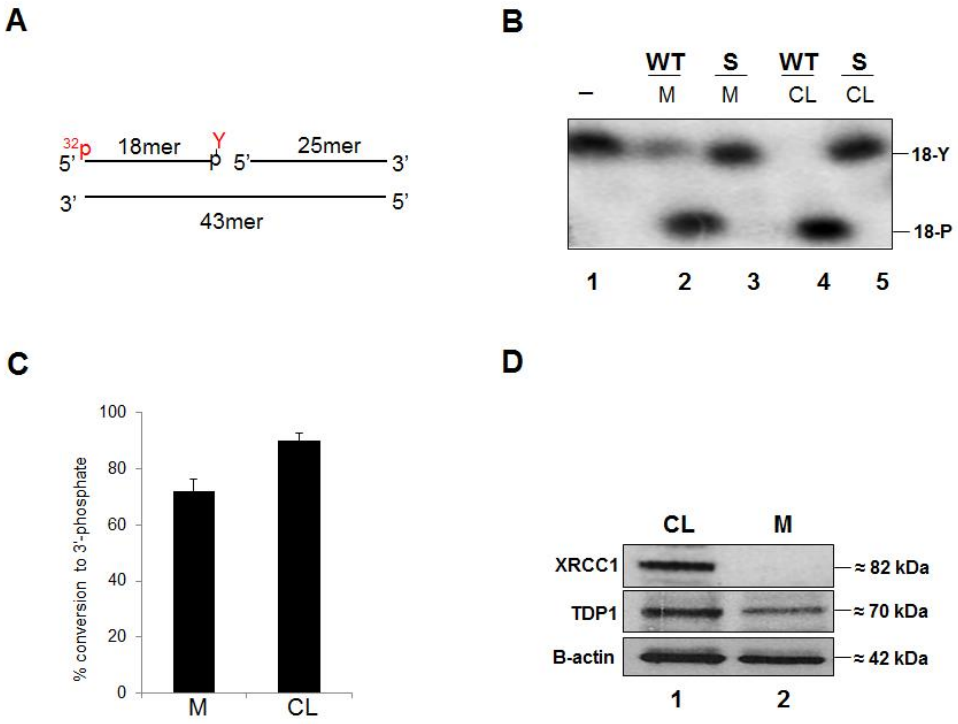

Figure 3.2. *Activity assay to assess TDP1 presence and activity in LCL mitochondria*. Mitochondrial protein was prepared as described in 2.2.3 (ii) from SCAN1 patient and wild type lymphoblastoid cell lines. Following purification as described in 2.2.3 (iv) mitochondrial and whole cell lysate containing nuclear protein (10µg) were incubated with radiolabeled duplex substrate and subsequent repair products were fractionated by denaturing electrophoresis then exposed to phosphorscreen as described in 3.2.3. **(A)** Schematic to demonstrate the radiolabeled duplex substrate used in the assay as described in 3.2.3. **(B)** Substrate following denaturing electrophoresis to indicate whether TDP1 is active in both mitochondrial and nuclear protein. The 18-Y and 18-P to the right of **B** represent 18-mer with 3'-phosphotyrosine terminus and 3'-phosphate terminus respectively. **(C)** Percentage conversion of 3'-phosphotyrosine to 3'-phosphate from both mitochondrial (M) and whole cell lysate containing nuclear protein (CL) from lanes 2 and 4 of **B**, as determined by ImageQuant. Error bars represent the difference observed from two independent experiments for the activity assay. **(D)** Whole cell and mitochondrial protein (20µg) separated by SDS-PAGE as described in 2.2.3 (vii) followed by western blot analysis as in 2.2.3 (viii) to determine purity of mitochondrial protein used in the assay.

Figure 3.2 **B** confirms TDP1 presence and activity in human mitochondria similar to that observed in 3.3.1. In **B** lanes 2 and 4 suggest cleavage of tyrosine from the radiolabelled 18mer constituent of the duplex substrate resulting in further migration on electrophoresis. Extracts from the SCAN1 patient cell line show no TDP1 activity in lanes 3 and 5 of **B**, consistent with the control reaction in lane 1 without any protein addition to the duplex substrate. The graph in **C** illustrates the relative conversion of 3' phosphotyrosine to 3' phosphate from lanes 2 and 4 of **B**. The graph demonstrates that

there is greater cleavage of tyrosine using whole cell lysate (column 2) in comparison to mitochondrial extract alone (column 1). Western blot analysis in **D** demonstrates that there was no nuclear contamination in the mitochondrial extract used in the assay as the nuclear protein XRCC1 is detected in whole cell extract (lane 1), but not in mitochondrial extract (lane 2).

3.3.3 *TDP1 is active in mouse brain mitochondrial extracts*

Having demonstrated TDP1 presence and activity in in mitochondria from human cell lines in 3.3.1 and 3.3.2, it was decided to determine whether this was also true in mouse mitochondria. Using mitochondria isolated from wild type and *Tdp1* -/- mouse brain mitochondria the activity assay described in 3.2.1 was performed with the duplex substrate illustrated in figure 3.3 **A**. Whole cell lysate containing nuclear protein was also prepared and used in the assay for which the results are shown in figure 3.3 **B**, **C**, and **D** (performed with Dr. El-Khamisy).

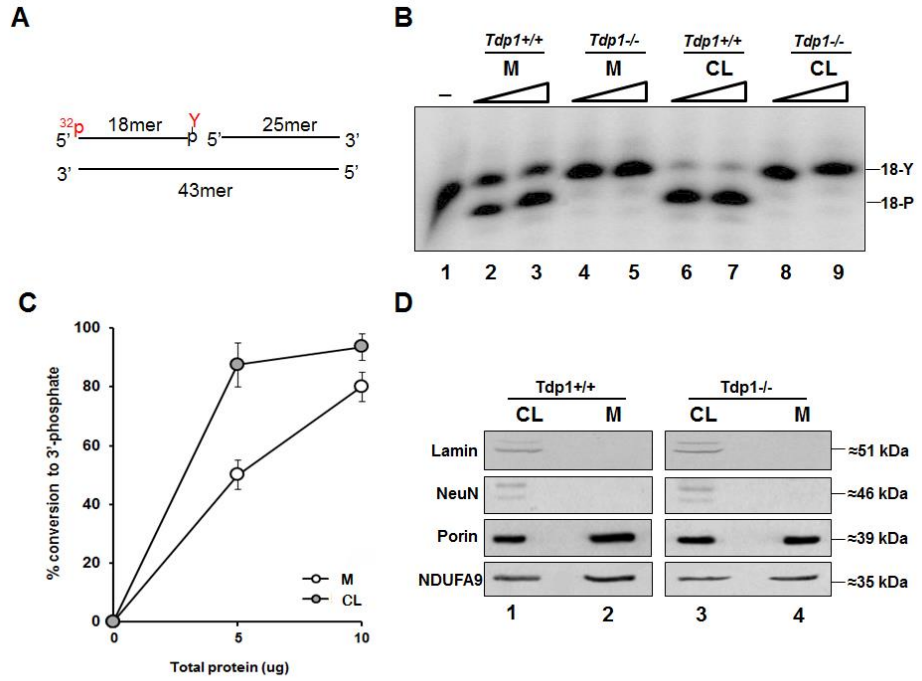

Figure 3.3. *Activity assay to assess TDP1 presence and activity in mouse brain mitochondria*. Mitochondrial protein was isolated from *Tdp1 -/-* and *Tdp1 +/+* mouse brain as described in 2.2.3 (iii) and purified as in 2.2.3 (iv). Once purified, mitochondrial and whole cell lysate containing nuclear protein (5µg and 10µg) were incubated with the radiolabelled duplex substrate followed by fractionation using denaturing electrophoresis and exposure to phosphorscreen as described in 3.2.3. **(A)** Schematic to demonstrate the radiolabeled duplex substrate used in the assay as described in 3.2.3. **(B)** Substrate following denaturing electrophoresis to indicate whether TDP1 is active in both mitochondrial and whole cell lysate containing nuclear protein. The 18-Y and 18-P to the right of **B** represent 18-mer with 3'-phosphotyrosine terminus and 3'-phosphate terminus respectively. **(C)** Percentage conversion of 3'-phosphotyrosine to 3'-phosphate using mitochondrial (**M**) and whole cell lysate (**CL**) from mouse brain at both 5µg and 10µg concentration. These conversion are with reference to those observed in lanes 2, 3, 6, and 7 of **B** and were calculated using ImageQuant. Error bars represent the difference observed from two independent experiments for the activity assay. **(D)** Whole cell (lanes 1) and mitochondrial (lanes 2) protein (20µg) from *Tdp1 +/+* and *Tdp1 -/-* mouse brain separated by SDS-PAGE as described in 2.2.3 (vii) followed by western blot analysis as in 2.2.3 (viii) to determine purity of mitochondrial protein used in the assay.

Figure 3.3 **B** demonstrates TDP1 presence and activity in mouse brain mitochondria by the increased electrophoretic mobility of the radiolabelled 18mer component of the duplex substrate used for this assay. This indicates that the tyrosine from the substrate was cleaved by TDP1 using 5µg and 10µg mitochondrial and whole cell extract containing nuclear protein from wild type mouse brain (shown in lanes 2, 3, 6, and 7). Activity was not observed in mitochondrial and whole cell extract from *Tdp1 -/-* mouse

brain (shown in lanes 4, 5, 8, and 9). In **C** the percentage conversion from 3' phosphotyrosine to 3' phosphate is shown for each amount of protein (5µg and 10µg) for both mitochondrial (**M**) and whole cell lysate (**CL**). This result shows that using 5µg whole cell lysate on 25nM of substrate for the assay was almost enough to cause complete conversion from 3' phosphotyrosine to 3' phosphate, which was in contrast to the mitochondrial extract where only ≈40% conversion was observed at the same concentration. This suggests that the amount of TDP1 in the whole cell lysate is considerably higher than in the mitochondrial extract alone. A consideration for future could be to increase the concentration of substrate used in the assay so that similar increases in conversion may be seen on doubling the concentration of protein used in the assay for both whole cell lysate and mitochondrial extract. Western blot analysis, shown in **D**, excludes nuclear contamination of mitochondrial extracts used in the assay by the absence of Lamin and NeuN in mitochondrial protein (lanes 2) in contrast to whole cell protein (lanes 1) for wild type and *Tdp1* -/- mice. Equal loading was demonstrated using antibodies to the mitochondrial proteins porin and NDUFA9.

3.4 Discussion and conclusions

In assessing the role of TDP1 in mtDNA repair, it was necessary to establish that TDP1 was present and active in mitochondria. At this stage of the project there had been no previous reports of TDP1 in mitochondria, and therefore the decision to investigate TDP1 presence and activity in mitochondria was based on three basic principles, which are that:

- Mammalian mitochondria have their own DNA (Anderson et al., 1981, Bibb et al., 1981a)
- Mitochondria have mechanisms to repair their DNA (Boesch et al., 2011), and

- Mutations in TDP1 can cause cerebellar ataxia; a common feature of mitochondrial disease (Takashima et al., 2002, Stumpf and Copeland, 2011)

With this in mind the assays undertaken in this chapter to examine TDP1 presence and activity in the mitochondrion has provided convincing data from which a sound conclusion can be drawn.

Presence and activity of TDP1 in human mitochondria

Activity of TDP1 in mitochondrial samples from human cell lines was first demonstrated using FD105 M21 fibroblasts. These cells had been isolated from an ataxia with oculomotor apraxia type 1 (AOA1) patient and been immortalised by our collaborators who also stably transformed these cells with a plasmid encoding and expressing aprataxin (APTX). Mutations in *APTX* are responsible for causing AOA1 and these 'corrected' cells were originally intended to aid in determining whether APTX was present and active in mitochondria. This project was discontinued when another group reported presence and activity of APTX in mitochondria; thus explaining the lack of any data regarding APTX in this thesis (Sykora et al., 2011). Despite mitochondria from FD105 M21 fibroblasts originally intended for experiments investigating APTX, some of the mitochondrial extract could also be used to determine whether TDP1 was present and active in mitochondria as there were no mutations in the *TDP1* gene in these cells. Figure 3.1 shows TDP1 activity in mitochondrial extract from FD105 M21 fibroblasts as there is increased electrophoretic mobility of the radiolabelled 18mer component of the duplex substrate used in the assay. This increased electrophoretic mobility was generated as a result of TDP1 removing tyrosine from the DNA substrate as it would *in vivo* where the phosphodiester linkage between DNA and TOP1MT is

broken allowing re-ligation of DNA to its normal conformation (Zhang et al., 2001). The activity seen from mitochondria is similar to that from whole cell extract containing nuclear protein in which TDP1 activity has already been characterised (Yang et al., 1996). This provided preliminary data supporting the hypothesis that TDP1 is present and active in mitochondria, and once this had been established a more comprehensive investigation into TDP1 presence and activity in human and mouse mitochondria was begun.

With the data in figure 3.1 suggesting TDP1 presence and activity in fibroblast mitochondria it was decided to assess whether this was also true in lymphoblasts. Our collaborators had a SCAN1 patient lymphoblast cell line as well as wild type control cells that were used in the same *in vitro* assay as earlier. Figure 3.2 demonstrates that the tyrosine was cleaved from the DNA substrate and increased its electrophoretic mobility as a result of TDP1 activity in mitochondrial extract from wild type cells similar to whole cell extract containing nuclear protein from the same cell line. In the SCAN1 patient cell line the A1478G mutation in *TDP1* causes a change in the active site of the protein converting amino acid 493 from histidine to arginine, which disrupts the symmetrical arrangement of the active site and results in a loss-of-function (Takashima et al., 2002). Crystal structure characterisation of TDP1 identified the histidine at amino acid residue 493 as a vital component of two symmetrical domains in the active site of the enzyme, which explains why there is no detectable activity from either mitochondrial or whole cell extracts from the SCAN1 cell line (Davies et al., 2002b). Figure 3.4 illustrates the proposed reaction mechanism for TDP1 when processing DNA-TOP1 cleavage complexes, and demonstrates the importance of His493 in TDP1 (Davies et al., 2002a).

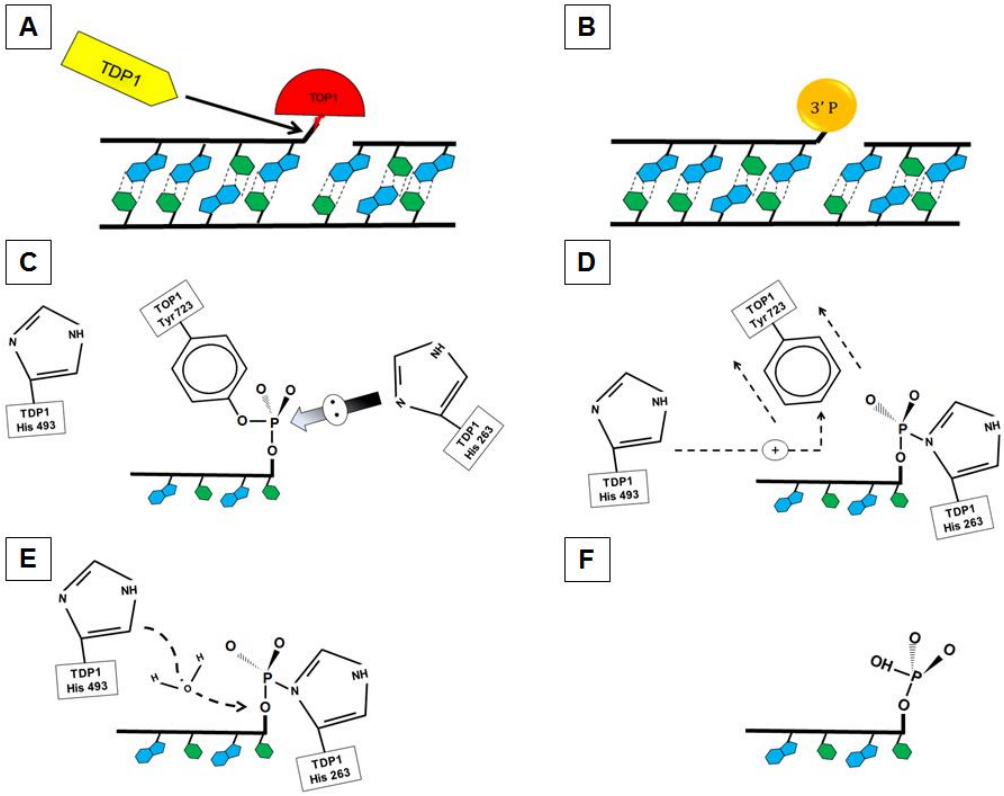

Figure 3.4. *Proposed mechanism for TDP1 activity on mtDNA-TOP1MT substrate* in (**A**), which leads to its conversion to 3' phosphate seen in (**B**). The process of removing TOP1MT from the 3' end of mtDNA begins with nucleophilic attack from His 263 of TDP1 as in (**C**) leading to covalent attachment of this amino acid to the mtDNA molecule and release of TOP1MT that is also protonated by His 493 of TDP1 as illustrated in (**D**). In (**E**) His 493 activates a water molecule that then hydrolyses the 3' phosphohistidine thus releasing and regenerating the active site of TDP1 and leaving behind 3' phosphate (**F**) for further processing by a phosphatase (adapted from Davies et al., 2002a).

The His493 residue is conserved between species which highlights its importance for normal enzyme function and offers an explanation as to the lack of cleavage of tyrosine from the DNA substrate used in the activity assays in this chapter (Davies et al., 2002b, Interthal et al., 2001). This result also demonstrates that the mutation in *TDP1* in SCAN1 patients affects function in the mitochondria as well the nucleus, which suggests that TDP1 is encoded by the same gene for activity on nDNA and mtDNA (Takashima et al., 2002, El-Khamisy et al., 2005).

Possible mechanisms for TDP1 import into mitochondria

Based on the data in this chapter that appears to suggest TDP1 is encoded by the same gene, it is therefore necessary to discuss some the possible mechanisms by which TDP1 gains entry to the mitochondrion. For many years import into mitochondria was thought to be carried out through two general pathways involving a mitochondrial targeting sequence (MTS) (Becker et al., 2012). Many proteins have an N-terminal mitochondrial targeting sequence (MTS) that is usually cleaved by mitochondrial processing peptidase (MPP) upon entry into the mitochondrion (Bolender et al., 2008, Zhang et al., 2001). An example of a protein of significance to TDP1 that enters mitochondria by this mechanism is TOP1MT, where the mitochondrial isoform is encoded by a separate gene to the nuclear TOP1 (Zhang et al., 2001). In other instances, such as for several inner mitochondrial membrane proteins, there is no N-terminal targeting sequence, and alternatively there are internal targeting sequences throughout the polypeptide chain (Becker et al., 2012). In these cases the mitochondrial proteins are bound to cytosolic chaperones, which are recognised by the outer membrane protein, Tom70, and passed across the membrane on the way to their final destination (Becker et al., 2012). However, *TDP1* does not appear to contain a predicted MTS which opens the possibility that it is transported into mitochondria through an alternative mechanism (Das et al., 2010).

In some other cases, such as for 8-oxoG DNA glycosylase (OGG1) and 2-OH-A/adenine DNA glycosylase (MYH), proteins are encoded in the same genes as their nuclear counterpart and are instead spliced for localisation to mitochondria (Nakabeppu, 2001b, Zhang et al., 2001). Another well characterised example where alternative splicing acts as the mechanism for targeting a DNA repair enzyme to mitochondria is

that of uracil-DNA glycosylase (UNG) (Nilsen et al., 1997, Otterlei et al., 1998). This protein has two isoforms UNG1 (mitochondrial) and UNG2 (nuclear) are transcribed from distinct transcription initiation sites and are spliced for targeting to their chosen organelle (Nilsen et al., 1997). Each isoform has a targeting sequence, which is a classic strong mitochondrial targeting sequence for UNG1, whereas the nuclear targeting sequence (NTS) for UNG2 was found to be unusually long and complex (Otterlei et al., 1998). Although such mechanisms for import exist for some mtDNA repair enzymes there are no such alternatively spliced isoforms found for TDP1 (Das et al., 2010).

In more rare circumstances, as for the mitochondrial DNA ligase (LIG3α), an upstream initiation site for translation controls targeting to mitochondria where the targeting sequence is then cleaved meaning that the resulting polypeptide in mitochondria has approximately the same molecular weight as LIG3α in the nucleus (Lakshmipathy and Campbell, 1999b). However, TDP1 does not contian an upstream translation initiation site and so it is unlikely that this mechanism causes its localisation to mitochondria, but it is important to consider these more rare targeting mechanisms in relation to TDP1 (Das et al., 2010). Another interesting observation was made in yeast (*Saccharomyces cerevisiae*) where an uncharaterised protein (Pir1p) interacts with the C-terminal end of AP endonuclease 1 (Apn1p) to initiate localisation to mitochondria (Vongsamphanh et al., 2001). Although this mechanism for import has yet to be identified in humans it acts to demonstrate the variety of possible mechanisms for protein entry into mitochondria.

Despite not comprehending the exact way in which TDP1 is imported into mitochondria, an interesting point from the data presented in this chapter is that TDP1 is present and active in mitochondria in unstressed conditions, whereas many dual localised repair proteins (e.g. AP-endonuclease 1 (APE1)) are recruited to mitochondria

upon stress (Mitra et al., 2007, Boesch et al., 2011). This would suggest that TDP1 is continuously localised to mitochondria due to DNA-TOP1MT lesions occuring on a regular basis during initiation of mtDNA replication and transcription (Zhang et al., 2001). While the data in figures 3.1 and 3.2 show clear actvity of TDP1 in mitochondrial extracts from human cells, this protein had not yet been identified in mitochondria of other mammalian organisms; therefore this was to be evaluated.

Presence and activity of TDP1 in mouse mitochondria

Our collaborators developed a *Tdp1* -/- mouse for use in their own research, which has been shown to exhibit a very similar phenotype (e.g. cerebellar atrophy and ataxia) to that observed in SCAN1 patients (Katyal et al., 2007). The *Tdp1* -/- mice were generated using a mutated form of *Tdp1* which contained a single substitution at nucleotide 1369 causing premature termination of transcription (Katyal et al., 2007). The resulting polypeptide is unstable and its function is therefore lost as it lacks a significant section of TDP1 including the His493 residue vital to the active site of the protein (Katyal et al., 2007). These mice with wild type controls were utilised to detect TDP1 presence and activity in mouse mitochondria, and to determine whether the *Tdp1* gene encoded nuclear and mitochondrial forms of TDP1 as in humans. Figure 3.3 shows increased electrophoretic mobility of the DNA substrate following treatment with mitochondrial and whole cell protein from wild type mouse brain, suggesting that the tyrosine was cleaved from the substrate similar to previous experiments. However, mitochondrial and whole cell extracts from *Tdp1* -/- mouse brain did not cleave the tyrosine from the DNA substrate suggesting that TDP1 in mice is encoded by the same gene for nuclear and mitochondrial localisation similar to in humans. This provides

further evidence of TDP1 presence and activity in mitochondria of higher eukaryotes; a phenomenon yet to be reported at the time of these experiments.

Discovery of this novel mtDNA repair enzyme has many interesting implications for discerning the extent of the mtDNA repair machinery and how much disrupting this contributes to ageing and disease. It could be postulated that impaired mtDNA repair due to the loss of function of TDP1 is a contributing factor to progression of SCAN1 along with dysfunctional nDNA repair; although unequivocal experimental data for this does not exist and would be very difficult to attain (Takashima et al., 2002). However, in discovering that this enzyme is present and active in mitochondria as well as previously identified repair proteins, there is confirmation that mtDNA repair mechanisms do exist and may be more intricate than initially thought (Cline, 2012, Boesch et al., 2011, Clayton et al., 1974). Delineating the involvement and role of more repair enzymes and more repair mechanisms in mitochondria may prove difficult. Despite this, the identification of more enzymes involved in mtDNA repair is increasing and so it was decided to perform more experiments relating to this field of mitochondrial research for which there is relatively little known (Boesch et al., 2011, Cline, 2012). The focus of this thesis was to determine the extent to which DNA-TOP1MT lesions form and what role TDP1 has in repairing this damage.

Altogether, the data shown in this chapter provide compelling evidence of TDP1 presence and activity in the mitochondrion. This was demonstrated using a variety of human and mouse samples, therefore strengthening this conclusion and developing a base to further investigate the specifics behind the role of TDP1 in mtDNA repair.

Chapter 4. Is TDP1 essential in mtDNA repair and cell survival?

4.1 Introduction

The results in chapter 3 provide very strong evidence that TDP1 is present and active in human and mouse mitochondria. The next step in investigation was to answer the question:

Is TDP1 essential in mtDNA repair and cell survival?

While attempting to address this question another group reported the presence and activity of TDP1 in mitochondria. In this publication the group used immunofluorescence on cells (MCF-7 breast carcinoma cells), and subcellular fractionation with a Proteinase K protection assay to demonstrate TDP1 presence in mitochondria. Mouse embryonic fibroblasts (MEFs) with *Tdp1* knockout were also used to demonstrate absence of TDP1 activity in comparison to controls similar to the experiments conducted in chapter 3 using *Tdp1 -/-* mice and SCAN1 patient cells. An *in vitro* repair assay was also utilised to show an association between TDP1 and DNA Ligase IIIα (LIG3α), and to show that TDP1 can remove 3' phosphoglycolate using mitochondrial lysates in contrast to those with TDP1 immunodepletion. Further investigation into the involvement of TDP1 in mtDNA repair was carried out using a long-range quantitative PCR based assay following hydrogen peroxide (H_2O_2) treatment in cells with or without *Tdp1* knockout. The data from this suggested the loss of TDP1 caused dramatically more mtDNA damage with H_2O_2 treatment in comparison to controls. From this the group concluded that mitochondrial base excision repair

(mtBER) was dependent on TDP1, implying that this enzyme was a critical member of the mtDNA repair network (Das et al., 2010).

Although the data from this paper shows clearly that TDP1 is present and active in mitochondria, similar to our previous observations, the conclusion that mtBER depends on this enzyme is a conclusion that does not appear to be true based on our own observations (Das et al., 2010). If mtBER depended on TDP1 it would be reasonable to assume the mtDNA mutation rate would be relatively high, yet the phenotype of SCAN1 patients and *Tdp1 -/-* mice is relatively mild in comparison to patients and mice with high mtDNA mutation load (Stumpf and Copeland, 2011, Trifunovic et al., 2004). It has also been shown that other enzymes involved in mtBER, namely LIG3, play a critical role in maintaining the integrity of mtDNA and also show very severe phenotypes in mice, which contrasts to *Tdp1 -/-* mice (Simsek et al., 2011, Gao et al., 2011). Also, demonstrating that TDP1 can resolve 3' phosphoglycolate in mitochondria corroborates that already observed in the nucleus, but this in itself does not demonstrate that TDP1 can resolve all DNA lesions involved in BER (Das et al., 2010, Interthal et al., 2005). The authors neglected the possibility that other 3' damaged termini are likely to exist in mtDNA other than 3' phosphotyrosine and 3' phosphoglycolate; not to mention 5' damaged termini that require repair such as 5' adenine monophosphate and 5' hydroxyl, to name just two (Caldecott, 2008). Experience of the principal supervisor of this project (Professor R.N.Lightowlers), with regard to the long range quantitative PCR assay used to assess mtDNA damage in the publication, revealed that this assay can be highly variable and any results provided using this should be viewed with caution. With this in mind it was decided to continue with the aim of trying to determine whether TDP1 was essential for mtDNA repair and cell survival to either confirm or contradict the conclusion that mtBER depends on TDP1 (Das et al., 2010).

Approaching this began with analysis of *Tdp1 -/-* mouse brain to determine whether there was any mitochondrial dysfunction detectable through COX/SDH histochemistry. This would determine whether there is any severe mtDNA damage resulting in COX deficiency in the cerebellum of these mice. Our collaborators had also observed increased retinal degeneration in *Tdp1 -/-* mice with methylmethane sulfonate (MMS) treatment, and so it was intended to assess mitochondrial involvement in this as there is mounting evidence for mitochondrial dysfunction in retinal diseases (Barot et al., 2011).

Experiments were also conducted using mammalian cells in culture. Some of these included transient siRNA transfections to knockdown TDP1 and determine whether this provided any data on the involvement of TDP1 in mtDNA repair. Our collaborators had also generated a mutant form of the mitochondrial topoisomerase (*TOP1mt*^{Y559A}) to be used in the cell culture experiments. This construct contains a mutation changing amino acid 559 from tyrosine to alanine (Y559A), thus affecting the active site of the enzyme causing it to remain covalently bound to mtDNA upon nicking (Redinbo et al., 1998, Zhang et al., 2001). This would then require TDP1 for removal, therefore expressing TOP1mt^{Y559A} in cells in culture was intended to provide more information on the role of TDP1 in mtDNA repair.

4.2 Methods

4.2.1 *Ionizing radiation treatment of mice*

In order to generate mtDNA damage in the brain that would require TDP1 for repair mice were treated with ionizing radiation (IR). This was achieved in a 7 day experiment by dosing 1.5 years *Tdp1 -/-* and wild type mice with 3Gy caesium 137 on day 1 and day 4, and 10Gy on day 7 with brain being harvested 3 hours after the last exposure.

This dose is similar to that given to human patients receiving radiotherapy in treatment of brain tumours (10Gy/week). Radiation was delivered using a Cammael 1000 source.

4.2.2 *Methylmethane sulfonate (MMS) treatment of mice*

Treatment using MMS was carried out to stall mtDNA replication forks in *Tdp1 -/-* and wild type mice that may then require TDP1 for repair, with particular focus being on the retina of these mice. This was undertaken by intraperitoneal injection of 6-8 week-old mice with 75mg/kg MMS and collecting tissue after 5 days. Mice were kept under daily observation following MMS treatment and were culled humanely if found to be in any discomfort.

4.2.3 *Cytochrome c oxidase (COX)/succinate dehydrogenase (SDH) histochemistry*

To assess whether significant mtDNA damage was occurring in mice dual COX/SDH histochemistry was performed. The principal behind using this technique is that there are three subunits of COX encoded in the mitochondrial genome and therefore damage to mtDNA may cause reduced expression of these proteins, which consequently affects the activity of COX. In contrast SDH is fully encoded in nDNA and its activity should not be affected by mtDNA damage. This technique uses cytochrome *c* which is reduced when mixed with DAB, but is then oxidised when placed on the tissue section if COX is active. A brown colour is then produced as DAB donates more electrons to cytochrome *c* as it is oxidised by COX. A second reaction medium is then used on the section of tissue which contains sodium succinate, sodium azide, NBT and PMS. The NBT acts as a final electron acceptor following dehydrogenation of sodium succinate by SDH followed by transport of electrons by PMS to NBT, and the sodium azide inhibits COX to ensure no further activity is seen from this complex. As the NBT is reduced it produces a blue colour that will only be seen if there is reduced COX activity from the previous staining procedure (Old and Johnson, 1989).

For this thesis sections of mouse brain and eye that had been cut to 10µm using a cryostat (Leica Biosystems) were firstly incubated in 100µl COX reaction medium for the following times for each tissue type at 37^{o}C (See appendix for optimisation of incubation times):

- Mouse brain – 35 mins
- Mouse eye – 30 mins

Following this incubation sections were washed three times in 100µl PBS for 5 mins each time and then incubated in 100µl SDH reaction medium for the following time at 37^{o}C:

- Mouse brain – 40 mins
- Mouse eye – 35 mins

Washing was repeated a further three times using 100µl PBS for 5 mins each time. For mouse eye sections counterstaining with 100µl Vector Methyl Green (Vector laboratories) was carried out for 10 mins at 65^{o}C to help distinguish retinal morphology before sections were washed three times in 100µl PBS for 5 mins each time and then dehydrated in the following percentages of EtOH in H_2O for the indicated times:

- 70% EtOH – 5 mins
- 95% EtOH – 5 mins
- 100% EtOH – 5 mins
- 100% EtOH – 10 mins

Sections were allowed to air dry for 5 mins before being mounted using DPX^{TM} and a coverslip, followed by image acquisition using a light microscope (Zeiss).

COX reaction medium

100µM	Cytochrome *c*
4mM	DAB
0.2M	Phosphate buffer pH 7

SDH reaction medium

1.3M	Sodium succinate
1.875mM	NBT
2mM	PMS
100mM	Sodium azide
0.2M	Phosphate buffer pH 7

4.2.4 *TOP1mt/FLAG and TOP1mt^{Y559A}/FLAG expression experiments*

Following stable transfection of *TOP1mt/FLAG* and *TOP1mt^{Y559A}/FLAG* into Flp-In^{TM} T-Rex^{TM} HEK293 cells as described in 2.2.2. (vii) it was necessary to determine

whether clones exhibiting resistance to antibiotics blasticidin S and hygromycin B expressed the desired proteins upon induction. This was accomplished by seeding $5x10^5$ cells in 2ml supplemented DMEM in 2 wells of a 6-well plate for each clone of both HEK293/*TOP1mt/FLAG* and HEK293/*TOP1mt*^{Y559A}*/FLAG* and adding 1µg/ml (final concentration) tetracycline in one well for each clone leaving the other without tetracycline as a control. Cells were incubated as outlined in 2.2.2 (i) for 18 hours before cytoplasmic protein was isolated as described in 2.2.3 (i). In order to determine whether expression of TOP1mt/FLAG and TOP1mt^{Y559A}/FLAG was successful in each clone SDS-PAGE (2.2.3 (vii)) and western blotting (2.2.3 (viii)) were performed using the cytoplasmic isolate for each sample.

Once successful expression of each protein had been established (figure 4.5), clone D for HEK293/*TOP1mt/FLAG* and clone A for HEK293/*TOP1mt*^{Y559A}*/FLAG* were selected for further experimentation as these clones appeared to produce the strongest signal on western blot analysis using the M2 anti-FLAG antibody in comparison to other clones for each cell line. Expressing both proteins for 6 days would enable analysis of whether TOP1mt^{Y559A}/FLAG had any significant effect on cell growth, mtDNA encoded protein levels, or levels of mtDNA copy number in comparison to TOP1mt/FLAG. To facilitate this each cell line was seeded in triplicate at $5x10^4$ cells in 2 poly-L-ornithine treated $25cm^2$ flasks with 5ml supplemented DMEM to allow unrestricted growth. Tetracycline at 1µg/ml final concentration was added to one flask for both cell lines in each of the three replicates and incubated as described in 2.2.2 (i) for 72 hours. After this period media was removed from each flask and replaced with fresh supplemented DMEM containing 1µg/ml tetracycline and incubated for a further 72 hours as in 2.2.2 (i).

Cells were harvested using 1ml PBS/1mM EDTA, transferred to a 2ml reaction tube, and neutralised using 1ml supplemented DMEM. Samples were centrifuged at 260xg for 4mins, supernatant discarded, and cells carefully re-suspended in 1ml PBS. From this 100µl cell suspension was mixed with 100µl 50% Trypan Blue/PBS and used for cell counting with an improved Neubauer Haemocytometer (Hawksley) to determine any impact on cell growth. The remaining cell suspension was centrifuged once more at 260xg for 4mins, supernatant discarded, and cytoplasmic protein isolated as described in 2.2.3 (i) before SDS-PAGE (2.2.3 (vii)) and western blotting (2.2.3 (viii)) were carried out to detect levels of mtDNA encoded proteins (COXI and COXII) in the absence of TDP1 compared to controls.

This experiment was repeated with exception to the cytoplasmic protein isolation followed by SDS-PAGE and western blotting. On this occasion the remaining cell suspension was used for whole cell DNA extraction as described in 2.2.4 (vii) and used for qRTPCR analysis as in 2.2.4 (ii).

4.2.5 *siRNA transfection optimisation*

With the intention of performing TDP1 knockdown experiments it was necessary to determine if the Trisilencer-27 siRNA kit (OriGene) was capable of reducing the levels of TDP1 that would then be undetectable by western blot analysis. If TDP1 was not detected by western blot analysis then it could be assumed that the protein was no longer present in these cells. To assess this, 3 concentrations (0.1nM, 1nM, and 10nM final) of each siRNA construct provided in the kit were used including a negative control (non-targeted) to determine whether the highest concentration of a non-specific siRNA had any impact on the levels of TDP1. In 1.5ml reaction tubes 4µl lipofectamine (life technologies) was mixed with 500µl Opti-MEM RNAiMAX (life technologies)

and 1.25µl stock siRNA. For each siRNA construct used, including the negative control, 3 stocks had been prepared for each final concentration desired:

Stock	**0.2µM**	**2µM**	**20µM**
Final concentration	0.1nM	1nM	10nM

An untransfected control reaction was also prepared using the same reagents with exception to addition of any siRNA construct. Each reaction was incubated for 15mins at room temperature before being added to $1x10^5$ Flp-In™ T-Rex™ HEK293 cells in 6-well plates with 2ml supplemented DMEM and incubated for 72 hours as described in 2.2.2 (i). Cytoplasmic protein was then isolated as described in 2.2.3 (i) and TDP1 levels determined by SDS-PAGE (2.2.3 (vii)) and western blotting (2.2.3 (viii)).

4.2.6 *siRNA transfection of Flp-In™ T-Rex™ HEK293*

With siRNA transfection optimisation completed as described in 4.2.4 it was concluded that siRNA would be used at 10nM final concentration with constructs B and C reducing the levels of TDP1 to the extent that it was not detectable by western blot analysis (figure 4.6). Knockdown of TDP1 was then performed over 6 days in Flp-In™ T-Rex™ HEK293 cells to determine whether there were any effects on cell growth, mtDNA encoded protein levels, or mtDNA copy number in the absence of TDP1. This was undertaken by mixing 8µl lipofectamine (life technologies) with 1ml Opti-MEM RNAiMAX (life technologies) and 2.5µl 20µM construct C siRNA in a 1.5ml reaction tube. The same reaction was set up replacing construct C siRNA with 2.5µl 20µM non-targeted siRNA as a negative control. A reaction without any siRNA was also prepared and all reactions were made in triplicate. Reactions were incubated for 15mins at room temperature before being added to $5x10^4$ Flp-In™ T-Rex™ HEK293 cells in poly-L-

ornithine treated 25cm^2 flasks with 4ml supplemented DMEM to allow for unrestricted cell growth. Cells were incubated for 72 hours as described in 2.2.2 (i) before the siRNA transfection was repeated and cells incubated for a further 72 hours.

Cells were counted, and protein and DNA extracted and analysed as in 4.2.3. This experiment was also repeated for further cell counting and isolation of DNA.

4.2.7 *siRNA transfection with TOP1mt/FLAG and TOP1mt^{Y559A}/FLAG expression experiment*

In an attempt to generate a greater degree of mtDNA-TOP1 lesions to investigate TDP1 function in mtDNA repair an experiment combining TDP1 knockdown with expression of TOP1mt/FLAG and TOP1mt^{Y559A}/FLAG was conducted. From this it would be possible to observe whether there was a greater impact on cell growth, levels of mtDNA encoded proteins, or mtDNA copy number when the specific damage that TDP1 is responsible for repairing was being generated in the absence of this enzyme. Using HEK293/*TOP1mt/FLAG* clone D and HEK293/*TOP1mt^{Y559A}/FLAG* clone A cell lines cells were seeded at 5x10^4 in poly-L-ornithine treated 25cm^2 flasks in 5ml supplemented DMEM for unrestricted growth. The same siRNA transfection as in 4.2.5 was carried out for each cell line in triplicate and cells had expression of TOP1mt/FLAG and TOP1mt^{Y559A}/FLAG induced as in 4.2.3.

After the experiment was complete cells were counted, and protein and DNA extracted and analysed as in 4.2.3. This experiment was repeated to increase validity of results.

4.3 Results

4.3.1 *No COX negativity in Tdp1 -/- mouse brain or eye*

In order to determine whether there was severe mtDNA damage occurring in *Tdp1 -/-* mice COX/SDH histochemistry was carried out on mouse brain and eye. The rationale for using this technique was that severe mtDNA damage can cause reduced production of mRNA encoding COX proteins and thus reduce COX activity, which can be detected upon histochemical analysis.

i) No COX negativity in *Tdp1 -/-* mouse brain

Dual COX/SDH histochemistry was performed on wild type and *Tdp1 -/-* mouse brain sections with particular attention to the granule and Purkinje cell layers of the cerebellum. The reason for this was that SCAN1 causes defects in the cerebellum in patients which is also observed in *Tdp1 -/-* mice (Katyal *et al*. 2007). The results from this method of analysis are illustrated in figure 4.1.

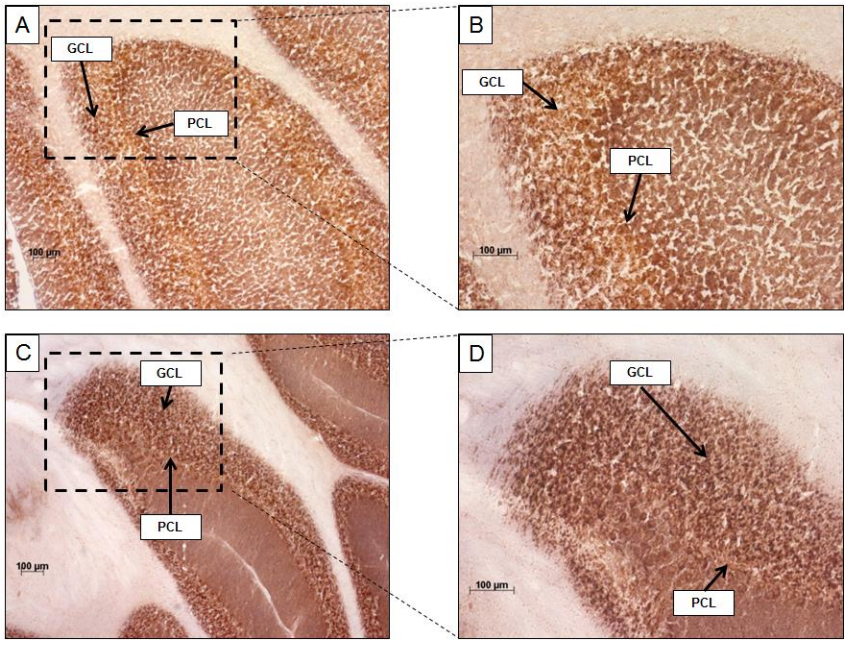

Figure 4.1. *COX/SDH histochemistry (described in 4.2.3) of mouse brain cerebellum*.
Sections cut to 10µm.
GCL – Granule cell layer
PCL – Purkinje cell layer
(A and B) *Tdp1 +/+*
(C and D) *Tdp1 -/-*

The images in figure 4.1 **C** and **D** show no sign of COX deficiency and therefore demonstrate that there was no severe mtDNA damage occurring in *Tdp1 -/-* mouse brain cerebellum. There are no blue coloured cells visible in **C** or **D** similar to that in the wild type mouse brain in **A** and **B**, suggesting that any mtDNA damage in cells without TDP1 was not enough to cause a biochemical defect.

ii) No COX negativity in *Tdp1 -/-* mouse brain following ɣ-irradiation

Following the results observed in 4.3.1 (i) ɣ-irradiation was used as a means to generate increased mtDNA damage that would potentially have a greater impact in *Tdp1 -/-* mice. Once this had been performed COX/SDH histochemistry was carried out on wild type and *Tdp1 -/-* mouse brain sections to determine whether there were any COX deficient cells in any sections that would suggest severe mtDNA damage. Results for this experiment are shown in figure 4.2.

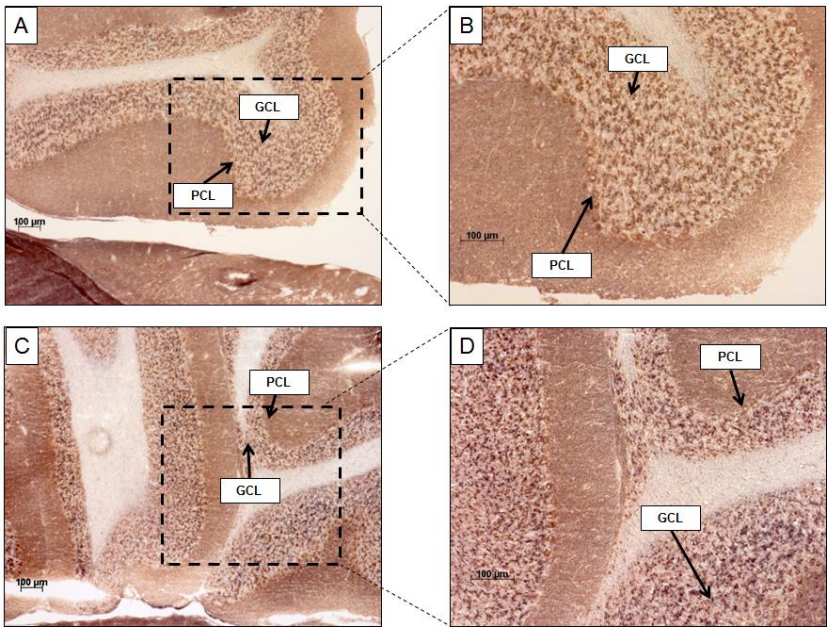

Figure 4.2. *COX/SDH histochemistry (described in 4.2.3) of mouse brain cerebellum following ɣ-irradiation (described in 4.2.1).* Sections cut to 10µm.
GCL – Granule cell layer
PCL – Purkinje cell layer
(A and B) *Tdp1 +/+*
(C and D) *Tdp1 -/-*

Images **C** and **D** in figure 4.2 demonstrate that in the absence of TDP1 there is no severe mtDNA damage that is visible by COX/SDH histochemistry in the cerebellum following ɣ-irradiation. These images are similar to those observed in **A** and **B** for the wild type control. However, *Tdp1 -/-* mice did show an early onset of ataxia following γ-irradiation, which would suggest that this treatment did have an effect in mice lacking TDP1.

iii) No COX negativity in *Tdp1 -/-* mouse eye

Analysis by COX/SDH histochemistry was carried out in wild type and *Tdp1 -/-* mouse eye sections as our collaborators had observed greater retinal degeneration under a particular treatment (MMS), and mitochondrial involvement in this was to be investigated. Firstly, COX/SDH histochemistry was performed on eye sections taken from wild type and *Tdp1 -/-* mice without any treatment. The results from this are illustrated in figure 4.3.

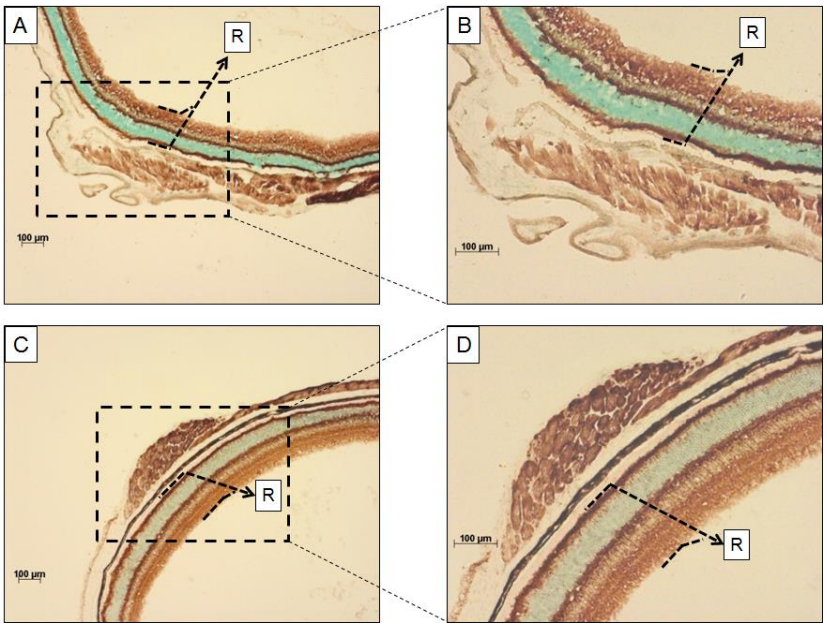

Figure 4.3. *COX/SDH histochemistry and methyl green counterstaining (described in 4.2.3) of mouse eye retina*. Sections cut to 10µm.
R - Retina
(A and B) *Tdp1 +/+*
(C and D) *Tdp1 -/-*

The images shown in figure 4.3 demonstrate that without stress there is no severe mtDNA damage in the absence of TDP1 that would cause a biochemical defect leading to blue coloured cells following COX/SDH histochemistry (**C** and **D**). These results are the same as for eye sections taken from wild type mice with the blue layer of cells (photoreceptors) visible in all images being as a result of counterstaining with methyl green to aid in determining eye morphology. There is also no noticeable retinal degeneration in sections from *Tdp1 -/-* mice, similar to that in sections from the wild type control.

iv) No COX negativity in *Tdp1 -/-* mouse eye following MMS treatment

Using MMS to stall replication forks in mice and thus potentially cause severe mtDNA damage leading to COX deficiency was the next step in analysing the role for TDP1 in mtDNA repair. Treatment using MMS was carried out in wild type and *Tdp1 -/-* mice before COX/SDH histochemistry was performed to determine whether there was increased retinal degeneration and/or COX deficiency in mice lacking TDP1. Results from this experiment are shown in figure 4.4.

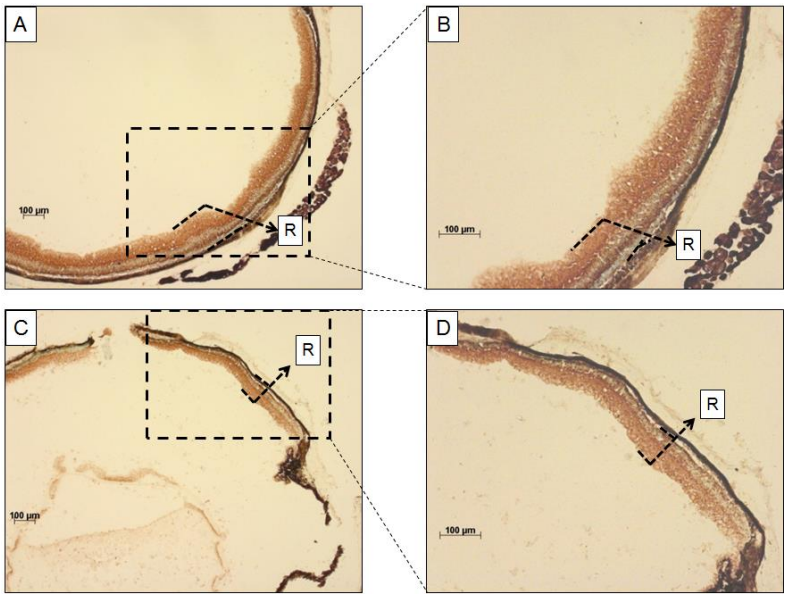

Figure 4.4. *COX/SDH histochemistry and methyl green counterstaining (described in 4.2.3) of mouse eye retina following MMS treatment (described in 4.2.2).* Sections cut to 10µm.
R - Retina
(A and B) *Tdp1 +/+*
(C and D) *Tdp1 -/-*

The images in figure 4.4 **C** and **D** show no blue cells that would suggest COX deficiency due to increased mtDNA damage in *Tdp1 -/-* mouse retina following MMS treatment. However, there is dramatic retinal degeneration visible in **C** and **D** in comparison to that in **A** and **B** suggesting that there is a severe effect in *Tdp1 -/-* mice as a result of MMS treatment, but that the majority of this was probably due to DNA damage/replication stalling in the nucleus which explains the cell loss observed in **C** and **D**.

4.3.2 *Expression of TOP1mt/FLAG and TOP1mt^{Y559A}/FLAG following stable transfection*

With COX/SDH histochemical analysis in 4.3.1 not providing any evidence for severe mtDNA damage with various treatments in *Tdp1 -/-* mice it was decided to concentrate further studies for the role of TDP1 in mtDNA repair using cells in culture. This began with stable transformation of Flp-In^{TM} T-Rex^{TM} HEK293 cells with a FLAG-tagged wild type form of *TOP1MT* (*TOP1mt/FLAG*) and a mutant form of the gene (*TOP1mt^{Y559A}/FLAG*). The mutant form of the gene has a mutation changing amino acid 559 from tyrosine to alanine, thus altering the active site of the enzyme and causing it to remain covalently bound to mtDNA upon nicking, which does not detach like the wild type form of the protein. This would then require TDP1 for removal, and therefore by transfecting these genes into Flp-In^{TM} T-Rex^{TM} HEK293 cells it was predicted that a greater understanding of TDP1 in mtDNA repair would be acquired.

Transfection of *TOP1mt/FLAG* and *TOP1mt*^{Y559A}*/FLAG* into Flp-In™ T-Rex™ HEK293 cells was completed and results for successfully expressing clones are shown in figure 4.5.

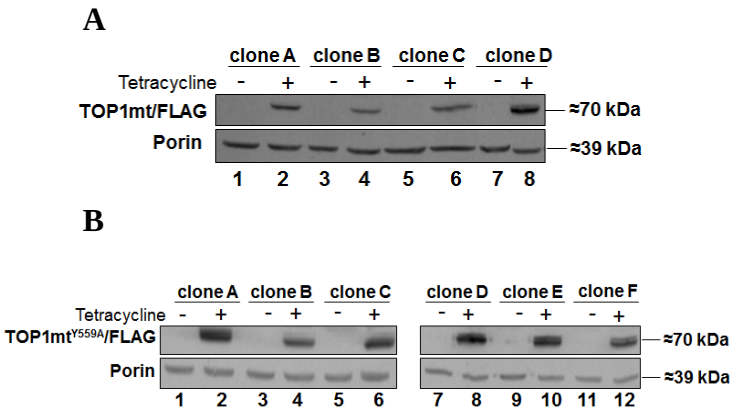

Figure 4.5. *Analysis of TOP1mt/FLAG and TOP1mtY559A/FLAG expression*. Western blot analysis as described 2.2.4 (viii) using 20µg cytoplasmic protein isolated as described in 2.2.4 (i) to determine expression of desired protein following stable transfection of Flp-In™ T-Rex™ HEK293 cells as described in 2.2.2 (vii). Expression of each protein was induced with addition of 1µg/ml (final concentration) tetracycline from 5x10^5 cells in 2ml supplemented DMEM in 6-well plates, followed by incubation for 18 hours in conditions outlined in 2.2.2 (i). A separate well containing 5x10^5 cells for each clone in 2ml supplemented DMEM was left without tetracycline as controls **(A)** Analysis of 4 clones following transfection of *TOP1mt/FLAG*. **(B)** Analysis of 6 clones following transfection of *TOP1mt*^{Y559A}*/FLAG*.

Western blot analysis in figure 4.5 **A** shows successful expression of TOP1mt/FLAG in 4 clones following the transfection and induction with tetracycline (lanes 2, 4, 6, and 8). The uninduced controls (lanes 1, 3, 5, and 7) show no signal as anticipated. Also, western blot analysis in **B** illustrates successful expression of TOP1mt^{Y559A}/FLAG from 6 clones following transfection and induction with tetracycline (lanes 2, 4, 6, 8, 10, and 12); whereas the uninduced controls (lanes 1, 3, 5, 7, 9, and 11) show no signal. Equal loading for each western blot was proven using α-porin antibody. Following this it was concluded that clone D for HEK293/*TOP1mt/FLAG* and clone A for HEK293/

TOP1mt^{Y559A}*/FLAG* would be used for further experiments as they appeared to show the strongest expression based on the western blots in figure 4.5.

4.3.3 *Localisation of TOP1mt/FLAG and TOP1mt*^{Y559A}*/FLAG to mitochondria*

Once successful expression of TOP1mt/FLAG and TOP1mt^{Y559A}/FLAG had been established in 4.3.2, it was necessary to confirm that each of the clones selected for further experiments (clone D for HEK293/*TOP1mt/FLAG* and clone A for HEK293/ *TOP1mt*^{Y559A}*/FLAG*) had expression of their respective proteins targeted to mitochondria. This was achieved using a Proteinase K (life technologies) protection assay described in 2.2.3 (v) for which the results are shown in figure 4.6.

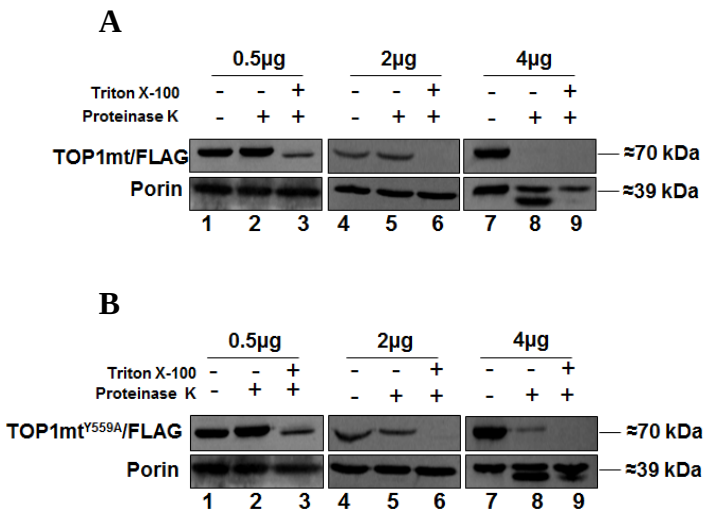

Figure 4.6. *Analysis of TOP1mt/FLAG and TOP1mtY559A/FLAG mitochondrial localisation*. Western blot analysis as described 2.2.3 (ix) using 10µg mitochondrial protein isolated as described in 2.2.3 (ii) to determine mitochondrial localisation of both TOP1mt/FLAG and TOP1mt^{Y559A}/FLAG following stable transfection of Flp-In^{TM} T-Rex^{TM} HEK293 cells as described in 2.2.2 (vii). Expression of each protein was induced in each cell line with addition of 1µg/ml (final concentration) tetracycline followed by incubation for 18 hours in conditions outlined in 2.2.2 (i). Localisation of both proteins was assessed by addition of 0.5µg, 2µg, and 4µg Proteinase K (life technologies) with or without Triton X-100 as described in 2.2.3 (v). **(A)** Analysis of TOP1mt/FLAG clone D **(B)** Analysis of TOP1mt^{Y559A}/FLAG clone A.

Successful localisation of both proteins is demonstrated in figure 4.6. In **A** and **B** 2µg was the optimal concentration of Proteinase K (life technologies) to show that both TOP1mt/FLAG and TOP1mt^{Y559A}/FLAG were protected by the mitochondrial outer membrane in samples without Triton X-100 (lanes 5 in **A** and **B**), whereas those

samples with this detergent added showed no signal for the expressed protein using the M2 α-FLAG antibody (lanes 6 in **A** and **B**). It was found in optimising this assay that 0.5µg Proteinase K was not enough to cause degradation of either TOP1mt/FLAG or TOP1mt^{Y559A}/FLAG with Triton X-100 addition (lanes 3 in **A** and **B**), and that 4µg was too much and caused widespread degradation of proteins including porin (lane 8 in **A** and lanes 8 and 9 in **B**). Nevertheless, based on the results using 2µg Proteinase K it was concluded that on expression of TOP1mt/FLAG or TOP1mt^{Y559A}/FLAG these proteins were both localised to mitochondria, and could then be used in further experiments.

4.3.4 *No decreased cell growth, reduction of mtDNA encoded proteins, or reduction in mtDNA copy number upon TOP1mt^{Y559A}/FLAG expression*

With the knowledge that TOP1mt/FLAG or TOP1mt^{Y559A}/FLAG were expressed and localised to mitochondria in HEK293/*TOP1mt/FLAG* and HEK293/ *TOP1mt^{Y559A}/FLAG*, respectively, it was decided to express each protein within their cell line for 6 days to determine whether this had any impact on cell growth, levels of mtDNA encoded proteins, or mtDNA copy number in comparison to uninduced controls. The results from this experiment are outlined in figure 4.7.

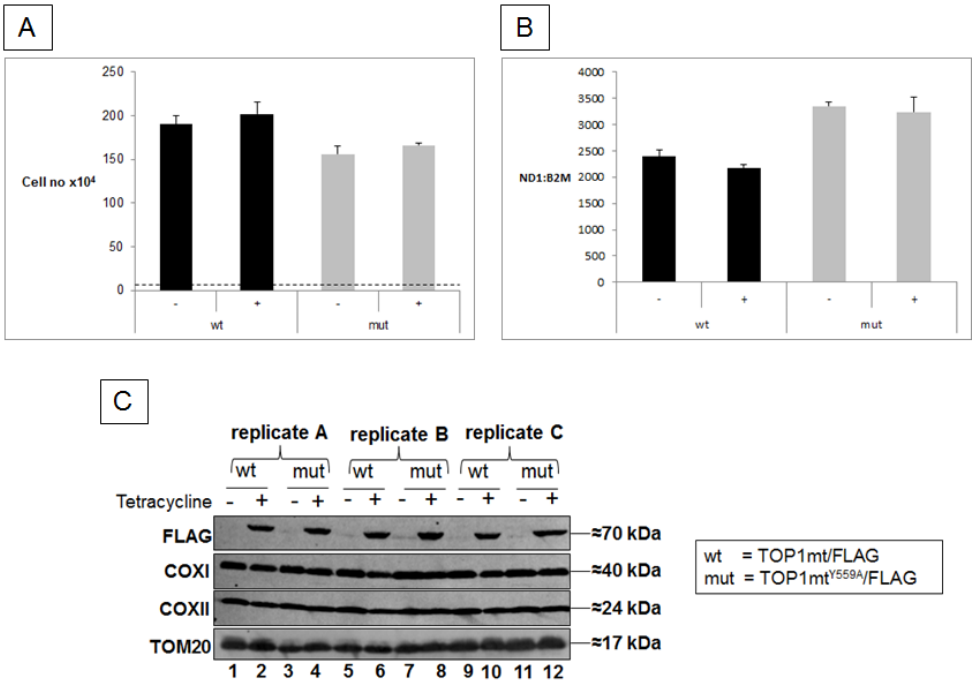

Figure 4.7. *Expression of TOP1mt/FLAG and TOP1mt^{Y559A}/FLAG for 6 days* by addition of 1µg/ml (final concentration) tetracycline at the 0 hours and 72 hours of experiment start. Both cell lines were seeded at 5x10^4 in 25cm^2 flasks in triplicate in 5ml supplemented DMEM without any limiting factors on cell growth. **(A)** Cell counts (mean +/- SEM from each triplicate) performed using an improved Neubauer Haemocytometer (Hawksley) upon expression (+) of both TOP1mt/FLAG (wt) and TOP1mt^{Y559A}/FLAG (mut) in comparison to non-expressed (-) controls. Dashed line indicates approximate starting number of cells (5x10^4 cells). **(B)** Real-time PCR (qRT-PCR) as described in 2.2.4 (ii) to determine mtDNA copy number by the ratio of *ND1* reads in comparison to reads of a nuclear control *B2M* (mean +/- SEM from each triplicate). For this, whole cell DNA extraction as described in 2.2.5 (x) was performed following expression (+) of both TOP1mt/FLAG (wt) and TOP1mt^{Y559A}/FLAG (mut) in comparison to non-expressed (-) controls. **(C)** Western blot analysis as described 2.2.3 (viii) using 20µg cytoplasmic protein isolated as described in 2.2.3 (i) to determine levels of mtDNA encoded proteins (COXI and COXII) upon expression (+) of both TOP1mt/FLAG (wt) and TOP1mt^{Y559A}/FLAG (mut) in comparison to non-expressed (-) controls.

The graph in figure 4.7 **A** shows that there was no significant decrease in cell growth with expression of TOP1mt^{Y559A}/FLAG for 6 days in comparison to uninduced controls. As expected, the results upon expression of TOP1mt/FLAG for the same time period showed no reduction in cell growth. When analysis by qRT-PCR was carried out using DNA isolated from these cells there was no significant reduction in mtDNA copy number with expression of TOP1mt^{Y559A}/FLAG in comparison to controls. Not surprisingly, when cytoplasmic protein was isolated and western blotting performed in

C, there was no reduction in the levels of mtDNA encoded proteins (COXI and COXII) with expression of TOP1mt^{Y559A}/FLAG (lanes 4, 8, and 12) in comparison to expression of TOP1mt/FLAG and uninduced controls. Both COXI and COXII have a half-life of six days and so it may have been expected that if this treatment caused severe mtDNA damage the transcript levels of corresponding mRNAs could have been reduced resulting in 50% reduction of signal on western blot analysis, but this was not observed. This suggested that expression of TOP1mt^{Y559A}/FLAG alone over 6 days was not enough to cause severe mtDNA damage and affect cell growth, mtDNA encoded protein levels, or mtDNA copy number.

4.3.5 *TDP1 siRNA transfection optimisation*

With expression of TOP1mt^{Y559A}/FLAG alone not leading to any detectable mtDNA damage or negative effect in cells, alternative methods for evaluating the role of TDP1 in mtDNA repair were considered. One of these was to knock down TDP1 in Flp-In^{TM} T-Rex^{TM} HEK293 cells using siRNA and evaluate its effect in a similar way as in 4.3.4. To begin this line of experiments the TDP1 siRNA constructs (OriGene) were required to be tested to measure their effectiveness at different concentrations. This was implemented with a 3 day knockdown using siRNA constructs A, B, and C at 0.1nM, 1nM, and 10nM final concentration whilst also using a non-targeted siRNA control at the same concentration to determine whether there was any off target knockdown of TDP1 using this construct. The results from this knockdown are shown in figure 4.8.

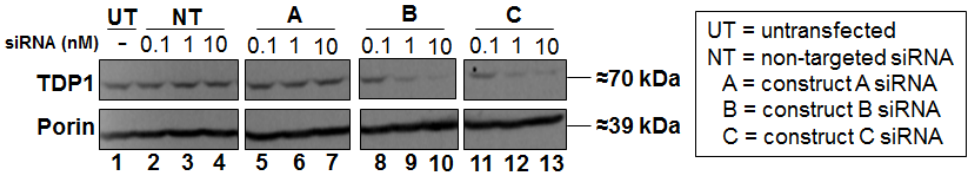

Figure 4.8. *Analysis of TDP1 knockdown in Flp-In™ T-Rex™ HEK293 cells*. Western blot analysis as described 2.2.3 (viii) using 20µg cytoplasmic protein isolated as described in 2.2.3 (i) to determine TDP1 knockdown following siRNA transfection in Flp-In™ T-Rex™ HEK293 cells as described in 4.2.4. Three TDP1 siRNA constructs (A, B, and C) and a non-targeted (NT) control were used over 3 days at 0.1nM, 1nM, and 10nM final concentration in parallel with untransfected cells (UT).

Figure 4.8 establishes that TDP1 siRNA constructs B and C knockdown TDP1 to levels that are undetectable by western blot analysis at 1nM and 10nM concentration. Construct A shows no knockdown of TDP1 similar to the non-targeted control and untransfected cells. Equal loading of protein on the blot was proven using the α-porin antibody. Based on this data construct C would be used alongside the non-targeted siRNA at 10nM final concentration in further experiments.

4.3.6 *No decreased cell growth, reduction in mtDNA encoded proteins, or reduction in mtDNA copy number with TDP1 knockdown Flp-In™ T-Rex™ HEK293 cells*

Using TDP1 siRNA construct C TDP1 was knocked down over a 6 day period at 10nM final concentration in wild type Flp-In™ T-Rex™ HEK293 cells to determine whether there were any negative effects detectable with reference to cell growth, levels of mtDNA encoded proteins, or mtDNA copy number. The results from this experiment are displayed in figure 4.9.

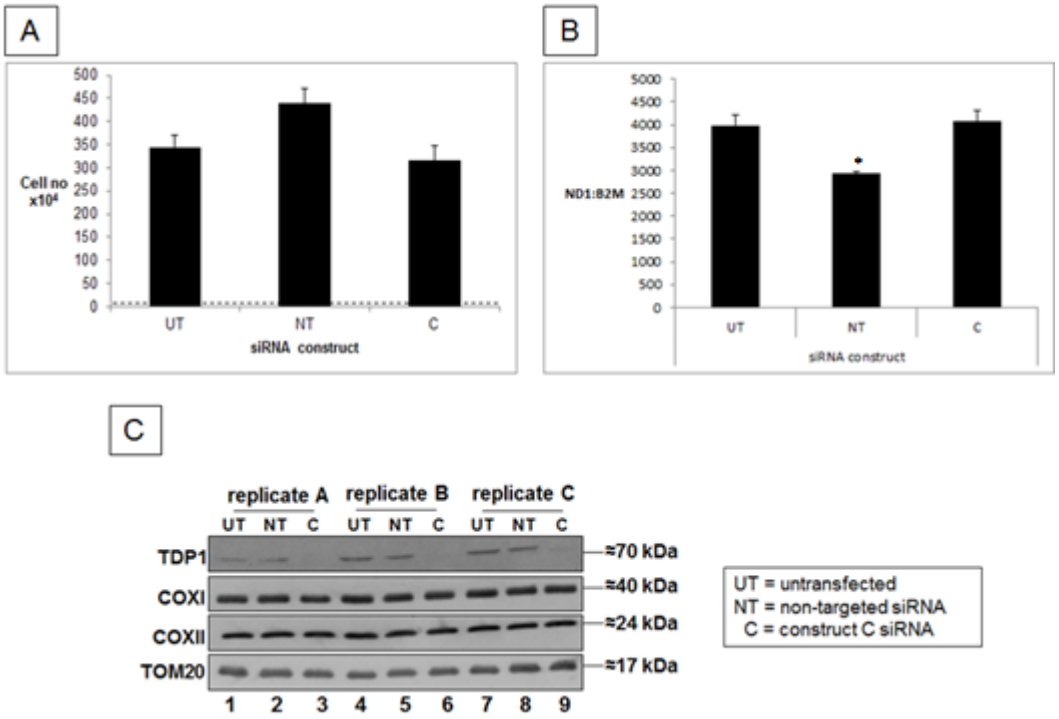

Figure 4.9. *Analysis of TDP1 knockdown (described in 4.2.5) for 6 days in Flp-In™ T-Rex™ HEK293 cells* seeded at 5x10^4 in 25cm^2 flasks in triplicate in 5ml supplemented DMEM without any limiting factors on cell growth. Knockdown was performed at 10nM siRNA final concentration and repeated after 72 hours from experiment start. **(A)** Cell counts (mean +/- SEM from each triplicate) performed using an improved Neubauer Haemocytometer (Hawksley) in untransfected (UT), non-targeted (NT), and siRNA construct C cells after 6 days. Dashed line indicates approximate starting number of cells (5x10^4 cells). **(B)** Real-time PCR (qRT-PCR) as described in 2.2.4 (ii) to determine mtDNA copy number by the ratio of *ND1* reads in comparison to reads of a nuclear control *B2M* (mean +/- SEM from each triplicate). Whole cell DNA extraction as described in 2.2.4 (vii) was performed from in untransfected (UT), non-targeted (NT), and siRNA construct C cells after 6 days (* = P<0.05). **(C)** Western blot analysis as described in 2.2.3 (viii) using 20µg cytoplasmic protein isolated as described in 2.2.3 (i) to determine levels of mtDNA encoded proteins (COXI and COXII) in untransfected (UT), non-targeted (NT), and siRNA construct C cells after 6 days.

The results in figure 4.9 **A** show no significant decrease in cell growth despite knockdown of TDP1 over 6 days. In **B** qRT-PCR shows no reduction in mtDNA copy number with loss of TDP1 over the same time period, and in **C** western blotting demonstrates that there is no reduction in the levels of COXI or COXII with TDP1 knockdown (lanes 3, 6, and 9). The statistically significant result showing reduced mtDNA copy number in non-targeted cells is most probably an anomalous result as there are no other negative effects observed using cell counts or western blot analysis.

4.3.7 *Significantly decreased cell growth with TDP1 knockdown and expression of TOP1mt/FLAG and TOP1mt^{Y559A}/FLAG, but no reduction in mtDNA encoded proteins, or reduction mtDNA copy number*

The experiments conducted in 4.3.4 and 4.3.6 indicate that expressing TOP1mt^{Y559A}/FLAG and knocking down TDP1, as separate treatments, are not enough to cause severe mtDNA damage that presents in decreased cell growth, reduction in levels of mtDNA encoded proteins, or lowered mtDNA copy number. With this in mind it was decided to knockdown TDP1 and express TOP1mt^{Y559A}/FLAG for 6 days to determine whether combining these treatments had a negative impact on cells, which may aid in realising the exact role for TDP1 in mtDNA repair. Knockdown of TDP1 with expression of TOP1mt/FLAG was also performed as a control, as well as cells without TDP1 knockdown but expression of both TOP1mt/FLAG and TOP1mt^{Y559A}/FLAG. Results from this experiment are shown in figure 4.10.

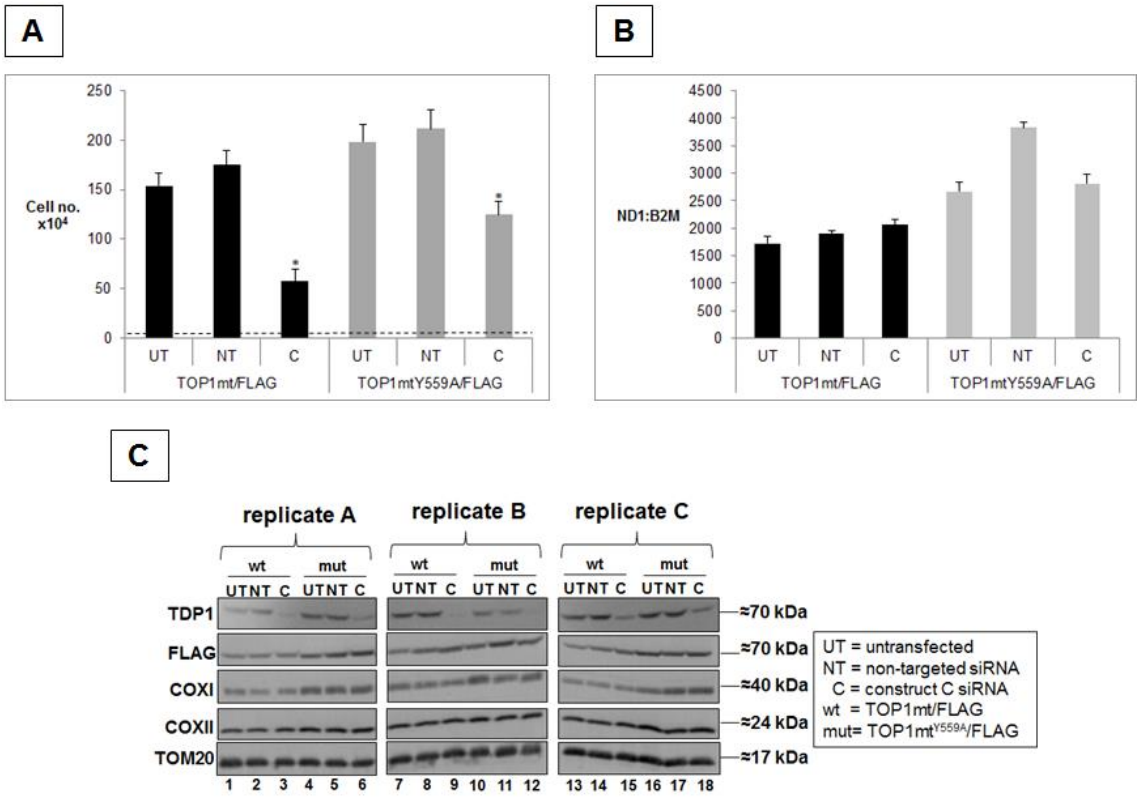

Figure 4.10. *Analysis of TDP1 knockdown and TOP1mt/FLAG and TOP1mt^{Y559A}/FLAG for 6 days.* siRNA transfection at 10 nm (final concentration) and expression of TOP1mt/FLAG and TOP1mt^{Y559A}/FLAG by addition of 1µg/ml (final concentration) tetracycline over 6 days in HEK293/TOP1mt/FLAG and HEK293/TOP1mt^{Y559A}/FLAG cells. Cells were seeded at 5x10^4 in 25cm^2 flasks in triplicate. The siRNA transfection and addition of tetracycline was repeated after 72 hours from experiment start. **(A)** Cell counts (mean +/- SEM from each triplicate) performed using an improved Neubauer Haemocytometer (Hawksley) for untransfected (UT), non-targeted (NT), and siRNA construct C cells with expression of both TOP1mt/FLAG (wt) and TOP1mt^{Y559A}/FLAG (mut) after 6 days. Dashed line indicates approximate starting number of cells (5x10^4) (* = P<0.05). (UT/NT vs C) **(B)** Real-time PCR (qRT-PCR) as described in 2.2.4 (ii) measuring the ratio of *ND1* reads in comparison to reads of the nuclear control *B2M* to determine mtDNA copy number (mean +/- SEM from each triplicate). Whole cell DNA extraction as described in 2.2.4 (vii) was performed from untransfected (UT), non-targeted (NT), and siRNA construct C cells with expression of both TOP1mt/FLAG (wt) and TOP1mt^{Y559A}/FLAG (mut) after 6 days. **(C)** Western blot analysis as described 2.2.3 (viii) using 20µg cytoplasmic protein isolated as described in 2.2.3 (i) to determine levels of mtDNA encoded proteins (COXI and COXII) in untransfected (UT), non-targeted (NT), and siRNA construct C cells with expression of both TOP1mt/FLAG (wt) and TOP1mt^{Y559A}/FLAG (mut) after 6 days.

In figure 4.10 **A** cell counting revealed that over 6 days there was significantly less cell growth in cells that had TDP1 knocked down, and TOP1mt/FLAG and TOP1mt^{Y559A}/FLAG expressed. This suggests that there is sufficient mtDNA damage occurring in these cells to have a negative impact on cell proliferation, which is not

observed in control cells for the experiment. This was unexpected for cells expressing TOP1mt/FLAG, but it must be that lesions occur more often than originally thought when TOP1mt/FLAG is expressed and TDP1 would then be required for repair. Western blotting in **B** indicates that in spite of the decreased cell growth there was no reduction in either COXI or COXII in protein from cells that had TDP1 knocked down, and that were expressing TOP1mt/FLAG or TOP1mt^{Y559A}/FLAG (lanes 3, 6, 9, 12, 15, and 18). Similarly there was no decrease in mtDNA copy number in these cells (**C**), suggesting that the damage to mtDNA was not enough to cause a reduction in mtDNA levels or the levels of mtDNA encoded proteins despite a reduction in cell growth. There was a slight increase in mtDNA copy number in cells that had been transformed with *TOP1mt^{Y559A}/FLAG* in comparison to cells with the wild type form of this protein. However when comparing mtDNA copy number in HEK293/*TOP1mt^{Y559A}/FLAG* cells between the TDP1 knockdown, and non-targeted and untreated controls there does not appear to be any discernible cause for this with regard to mtDNA damage as a result of these treatments. Therefore no conclusions can be drawn from the result in this instance.

4.4 Discussion

With TDP1 presence and activity being demonstrated in chapter 3 and verified by another group, the experiments in this chapter were designed to assess whether TDP1 is essential to mtDNA repair and cell survival (Das et al., 2010). By using *Tdp1* -/- mice and mammalian cell lines it was anticipated our experiments would aid in confirming or counteracting the argument that:

- Mitochondrial base excision repair is dependent on TDP1 (Das et al., 2010)

If this was true TDP1 would be a significant member of the mtDNA repair network, and therefore our line of experiments would help to interpret how essential TDP1 is to mitochondria.

Impact of TDP1 loss in mice

From their inception *Tdp1 -/-* mice have been utilised to study the impact of TDP1 loss with regard to nDNA. It was established that these mice were very similar in phenotype to SCAN1 patients in terms of their neurological (e.g. cerebellar atrophy and ataxia) and extraneurological (e.g. hypoalbuminemia) symptoms. Therefore using various mechanisms to generate specific TOP1-DNA damage through camptothecin (CPT) and topotecan (TPT), as well as more general single strand break (SSB) and double strand break (DSB) damage using γ-irradiation, it was possible to find that TDP1 was crucial to SSB repair (SSBR) of nDNA in primary neural cells. From this the cerebellar atrophy observed in the mice and patients was attributed to the unrepaired SSBs as a result of loss of function of TDP1 (Katyal et al., 2007).

In light of these findings and the claim that mtBER is dependent on TDP1 it is important to make clear the distinction between SSBR and BER (Katyal et al., 2007, Das et al., 2010). In SSBR the DNA backbone can be broken and form a lesion (e.g. 3' phosphotyrosine and 5' AMP) but the base at that particular position may or may not be damaged in addition (Caldecott, 2008). This is different to BER that has many steps including one for SSBR (Boesch et al., 2011). In brief, the process begins with the removal of a damaged base by a DNA glycosylase, incision of the DNA backbone by an apurinic/apyrimidinic (AP) endonuclease, infilling of the abasic site by a DNA polymerase, before DNA is finally restored to its original conformation with ligation of the backbone by a DNA ligase (Boesch et al., 2011). Although the final ligation step in this process involves SSBR by a DNA ligase, it does not necessarily involve the activity of TDP1 as the specific substrate required for this enzyme (3' phosphotyrosine) does

not match the 3' hydroxyl present before the final ligation takes place (Boesch et al., 2011, Caldecott, 2008). By researching previous studies performed in mice that investigated mtDNA repair, it may be possible to determine the some of the expected outcomes of our own experiments if mtBER depends on TDP1.

Mouse knockouts of enzymes with specific involvement to mtBER (e.g. oxoguanine DNA glycosylase (OGG1) and thymine glycol-DNA glycosylase (NTH1)) have shown relatively mild to no observable phenotype, but have reduced mtDNA repair capacity (de Souza-Pinto et al., 2001, Karahalil et al., 2003). The phenotype observed in *Tdp1 -/-* mice, in comparison, is more severe and based on this it would appear that this would support the argument that mtBER depends on TDP1 (Katyal et al., 2007). However, when *Tdp1 -/-* mice are compared to other mouse models with knock-outs for enzymes that are known to be involved in all mtBER, the consequences of TDP1 loss appear to be relatively mild. The mitochondrial DNA ligase (LIG3α) is involved in all mtBER and mitochondrial SSBR, and in this case *Lig3α -/-* mice displayed a very severe phenotype including mtDNA loss and debilitating ataxia (Gao et al., 2011). Although TDP1 does not have the same function as LIG3α there would surely be a more significant phenotype in *Tdp1 -/-* mice and SCAN1 patients if mtBER was dependent on TDP1 as the mutation rate of mtDNA would be relatively high, which can have a dramatic effect at the molecular and whole organism level (Hirano, 2008, Trifunovic et al., 2004). In the case of the well reported mtDNA mutator mouse, an alteration in the mitochondrial DNA polymerase γ (POLG) to affect the proof reading capability of the enzyme caused increased mtDNA mutation rate and early ageing onset (Trifunovic et al., 2004). Such dramatic changes on the whole organism level are not seen in *Tdp1-/-* mice, which potentially questions the dependency of mtBER on TDP1. However, data was required to illustrate this so by assessing the activity of complexes of the electron

transport chain, with subunits encoded in mtDNA, it was hoped that more information could be provided on the role of TDP1 in mtDNA repair.

The results in figure 4.1 and 4.2 show no sign of severe mtDNA damage in the cerebellum of *Tdp1 -/-* mice in comparison to wild type controls despite introducing more DNA damage through γ-irradiation. Although γ-irradiation is used to generate DSBs in DNA, the vast majority (>95%) of DNA damage using this technique is SSBs (Katyal et al., 2007). This does not necessarily cause the specific DNA-TOP1 lesion, but it should lead to these lesions as they can be formed when TOP1 incises DNA at the site of an already damaged nucleotide (Caldecott, 2008). In the absence of TDP1 the delivery of DNA damage through γ-irradiation has already been shown to have an effect in mice with regard to nDNA, and so it was believed that lesions of DNA-TOP1MT would occur in the mitochondrion using this method (Katyal et al., 2007). However, with COX/SDH histochemistry there is no evidence to suggest that there is severe mtDNA damage in the cerebellum of *Tdp1 -/-* mice indicating that any mtDNA damage is not occurring at a high enough rate in the absence of TDP1 to have an effect on the expression of COX subunits encoded in this genome. This suggests that TDP1 is not critical to general SSB repair of mtDNA as a result of γ-irradiation.

Studies using *Tdp1 -/-* mice were continued with investigation using COX/SDH histochemistry in the retina as our collaborators observed retinal degeneration with a particular treatment, and mitochondrial dysfunction has been associated with retinal diseases (Barot et al., 2011). In unstressed conditions there did not appear to be any retinal degeneration or mitochondrial dysfunction in *Tdp1 -/-* mice as a result of increased mtDNA damage due to TDP1 loss; as was expected. Further experiments were carried out using the alkylating agent methylmethane sulfonate (MMS) that adds methyl groups to DNA bases, which would then require BER enzymes for repair (Wyatt

and Pittman, 2006). If mtBER was dependent on TDP1 it may be the case that mtDNA damage would be severe enough to be detected by COX/SDH histochemistry in *Tdp1 -/-* mice. However, there is quite dramatic retinal degeneration in *Tdp1 -/-* mice that can be seen in figure 4.4 with no sign of mitochondrial dysfunction. One possible explanation for this could be that the DNA damage occurring in these mice in the absence of TDP1 is mainly within the nucleus, thus accounting for the cell loss observed in figure 4.4. This method of generating DNA damage is most probably not the best mechanism to investigate mtDNA repair and so no definitive conclusions could be made.

One criticism of using COX/SDH histochemistry to detect mtDNA damage is that it may not be very sensitive to observe this phenomenon in mice. In humans it has been shown that immunohistochemistry using antibodies against subunits of complex I of the respiratory chain allows for a more sensitive analysis of respiratory chain defects (Lax et al., 2012). With many complex I subunits in mtDNA it would appear as though this would be perfect for analysis of mtDNA damage in mice. However, this was attempted in relation to a separate project by a member of the Mitochondrial Research Group (Dr.N.Lax) with much experience in immunohistochemistry, and unfortunately it was not possible to optimise this technique for mouse brain as there was too much background signal produced when using this tissue. Investigating the involvement of TDP1 in mtDNA was then continued with further experiments using mammalian cells in culture.

Investigations in mammalian cell lines

In order to attempt to delineate the exact role of TDP1 in mtDNA repair, mammalian cells (HEK293) were manipulated to gain a greater understanding of the importance of TDP1 on the molecular level. Using cells in culture has many practical advantages over experiments involving mice and so this would aid in producing more data for analysis.

One of the challenges of studying mtDNA damage in cells in culture and in mice is to generate DNA damage that is specific to the mitochondrial genome as many other methods (e.g. γ-irradiation, MMS, and H_2O_2) impact on nDNA as well as mtDNA. In these instances damage to nDNA may affect any results observed, and so to overcome this the Flp-In™ T-Rex™ system (life technologies) was utilised in order to gain cell lines that had been transformed with a wild type form of TOP1MT (*TOP1mt/FLAG*) and a mutant form (*TOP1mt*^{Y559A}*/FLAG*). The mutant form of the protein has an altered active site, which causes it to remain covalently bound to mtDNA upon nicking and does not become detached as the wild type form would; meaning that TDP1 is then required for removal. This mutant was designed based on previously studied mutants for the nuclear TOP1, and in consideration of this the active amino acid residue at position 559 in the mitochondrial topoisomerase was changed from tyrosine to alanine to cause altered function (Redinbo et al., 1998, Zhang and Pommier, 2008). Expressing the FLAG-tagged TOP1mt^{Y559A} was intended to increase DNA damage specific to mtDNA that would then require TDP1 for repair, and help to understand the exact role of this repair enzyme in mtDNA repair. However, when this mutant was expressed for a six day period there was no indication of a negative impact in cells as a result, which can be seen in figure 4.7. This may not be too surprising given that TDP1 was still present and active in the mitochondria of these cells meaning that it could repair any damage formed as a result of this expression. Knockdown of TDP1 was also performed to determine whether there would be any negative effects on cells with the loss of TDP1. Figure 4.9 demonstrates that there was no negative impact in cells with the loss of TDP1.

Although the cells with TDP1 knockdown were not stressed, mtDNA damage would likely still occur in these cells suggesting that TDP1 is not a critical member of mtDNA repair as when vital mtDNA repair enzymes are lost, such as the mitochondrial DNA ligase (LIG3α), cells cannot survive (Simsek et al., 2011). This is also similar for other

enzymes specific to mtBER, such as apurinic/apyrimidinic endonuclease 1 (APE1), which causes apoptosis when the enzyme is lost, but when overexpressed to mitochondria apoptosis is reduced (Hegde et al., 2012, Li et al., 2008). Only when combining TDP1 knockdown with expression of either TOP1mt/FLAG or TOP1mt^{Y559A}/FLAG was any impact in cells seen. The reduction in cell number in figure 4.10 indicates that there was reduced cell growth due to TOP1MT being bound to mtDNA in the absence of TDP1, but interestingly this did not have any impact on the levels of mtDNA encoded proteins or mtDNA copy number. This implies that mtDNA integrity is still maintained and can produce mtDNA encoded proteins over a six day period despite these lesions occurring and causing a reduction in cell growth. The reduced cell growth with TDP1 knockdown and TOP1mt/FLAG expression was slightly unexpected in this experiment, but it must be the case that expression of this protein caused these lesions occur more often than initially expected in the absence of TDP1 which resulted in less cell growth. The presence of TDP1 in mitochondria in unstressed conditions, as demonstrated in chapter 3, also supports the assumption that these lesions occur within mitochondria under normal circumstances that requires TDP1 for repair, and would help explain the unexpected result in this case.

The significance of these findings is that TDP1 is confirmed to be involved in mtDNA repair, but based on this data it would be careless to assume that mtBER is dependent on this enzyme or that it is essential for cell survival. It may have been possible to observe reduction in the levels of mtDNA encoded proteins or mtDNA copy number if the length of experiments had been longer, but these data do still show that TDP1 is in some part involved in mtDNA repair. Further analysis of exact mtDNA mutation load through deep sequencing would provide a greater depth of analysis to assess the consequences of losing TDP1. Using DNA samples from the expression/knockdown experiments would help to determine whether mtDNA mutation load was increased with TDP1 loss

as would be expected if mtBER was dependent on this enzyme (Boesch et al., 2011, Das et al., 2010).

Chapter 5. Does next generation sequencing aid in discovering the exact role of TDP1 in mtDNA repair?

5.1 Introduction

The results presented in chapters 3 and 4 suggest that TDP1 is present and active in mitochondria, but the exact role of TDP1 in mtDNA repair remained unclear although it is unlikely that mtBER is dependent on this enzyme as Das et al concluded (Das et al., 2010). In order to delineate the role of TDP1 in mtDNA repair next generation sequencing was utilised as it was anticipated this would provide insight into the exact mutation rate in mtDNA as a result of the expression/knockdown experiments described in chapter 4.

For this Ion Torrent^{TM} technology (life technologies) was used to sequence mtDNA using DNA samples from the experiments described in chapter 4. One of the main advantages of Ion Torrent^{TM} technology is the ability to perform sequencing at a relatively low cost in comparison to traditional Sanger sequencing methods and machines that are typically used in this line of experimentation. Although the coverage of DNA using Ion Torrent^{TM} technology is not as extensive as with other Next-Generation sequencing platforms (≤1Gb compared to ≤120Gb using SOLiD^{TM} technology previously used for sequencing mtDNA) it was decided that this was not an issue for the study of the mitochondrial genome as it is relatively small and would allow for sufficient coverage to detect significant mutation levels in mtDNA if the mutations were present (Rothberg et al., 2011, Ameur et al., 2011, Liu et al., 2012).

The principle behind this form of sequencing technology is that pH changes can be measured and used to determine the sequence of DNA as a result of proton release following incorporation of nucleotides by a DNA polymerase in a growing nucleotide

chain. More specifically, when a nucleotide is incorporated into a nascent strand of DNA by polymerase a single proton is released as a result of hydrolysis of the entering dNTP. For sequencing using Ion Torrent™ technology the DNA sample is loaded onto a chip that is then flooded sequentially with the four dNTPs that, when incorporated into DNA, release a proton that alters the pH in the solution surrounding that particular area. The change in pH is then detected by the chip, converted to a voltage, and processed so that it is recorded by the software. This allowed for the sequencing of mtDNA in a library following a library preparation protocol that briefly consisted of an initial long-range PCR (LR-PCR) to generate two ≈8kb regions of mtDNA that were combined, fragmented into smaller sections, ligated to adapters, and then clonally amplified onto beads. Once this had been complete the samples could be analysed by loading the clonally amplified libraries on beads onto a chip that contained wells for each bead to lie in whilst the chip was flooded with each dNTP. Figure 5.1 illustrates how flooding of a chip with a dNTP leads to incorporation of a nucleotide into nascent DNA that is attached to a bead (Rothberg et al., 2011).

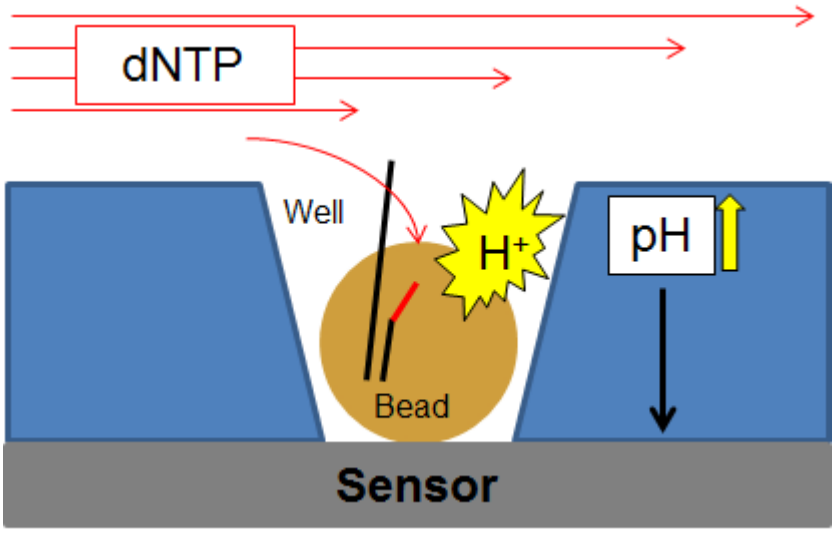

Figure 5.1. *Detection of an incorporated nucleotide using Ion Torrent™ technology*. The chip is flooded with a dNTP that passes over wells and is incorporated into a nascent strand of DNA on a bead if complementary to the parental strand. This incorporation causes the release of a proton that is detected by the chip and recorded by the machine to determine the sequence of the parental strand of DNA (adapted from Rothberg et al., 2011).

It was anticipated that using this form of sequencing technology that it would be possible to determine:

The exact role of TDP1 in mtDNA repair.

Sequencing mtDNA in this manner would be combined with analysis using NextGENe® software (Softgenetics®) that was designed for sequencing analysis from the Ion Torrent™ and would provide data on the number of mtDNA mutations generated as a result of the expression/knockdown experiments described in chapter 4.

5.2 Methods

5.2.1 *mtDNA sequencing using Ion Torrent™*

In order to determine the mutation rate in mtDNA following the expression/knockdown experiments conducted in chapter 4, it was necessary to perform deep sequencing. This was accomplished using Ion Torrent™ technology (life technologies) with sequencing data being analysed using NextGENe® software (Softgenetics®).

The process of generating samples for sequencing began with a LR-PCR step to generate two ≈8kb mtDNA fragments with primers Human mtDNA A (F and R) and Human mtDNA B (F and R) using 500ng DNA extracted following expression/knockdown experiments described in chapter 4. A control sample of mouse mtDNA cloned into the vector pAM1 was a kind gift form the lab of Professor N.G.Larsson which was previously sequenced by Bibb *et al* to discover the sequence and gene organisation of mouse mtDNA (Bibb et al., 1981a). This plasmid was considered to be the correct control to be used to determine the error rate of the sequencing technique as mtDNA from control human cells will contain a natural mutation rate that are not mutations generated as a result the sequencing technology. As with the DNA from human cells two DNA fragments of ≈8kb were generated through LR-PCR with primers Mouse mtDNA A (F and R) and Mouse mtDNA B (F and R) using 50ng plasmid DNA. LR-PCR reactions were performed in 25µl in 0.2ml reaction tubes with the following reagents (TaKaRa) and put through the following PCR programme:

Table 5.1. LR-PCR reagents and programme used to generate mtDNA fragments (≈8kb) in preparation for deep sequencing.

LR-PCR reagents	**LR-PCR programme**			
4µl dNTPs (2.5mM each)	**LR-PCR step**	**Temperature (^{o}C)**	**Time**	**Number of cycles**
2.5µl 10x LR-PCR buffer 25 mM TAPS (pH9.3 at 25℃) 50 mM KCl 2 mM MgCl2 0.1 mM DTT	Initial denaturation	94	1 min	1
1µl Forward primer (10µm)	Denaturation	98	10 secs	35
1µl Reverse primer (10µm)	Annealing	60	30 secs	
0.5µl LA Taq DNA polymerase	Extension	68	10 mins	
15µl H_2O	Final extension	68	10 mins	1
1µl DNA 500ng for human cell DNA 50ng for pAM1 plasmid				

Once the LR-PCR was complete samples were electrophoresed on a 1% NuSieve® GTG® agarose gel (Lonza) for 45 mins at 70V. Following this mtDNA fragments at the correct molecular weight (≈8kb) were excised from the gel and mtDNA was purified by phenol/chloroform extraction as described in 2.2.4 (vi). Quantification of DNA concentration was then determined as described in 2.2.4 (viii) and then 50ng of each mtDNA fragment (A and B from the LR-PCR) were combined at equal molarity in 35µl H_2O in 1.5ml LoBind® reaction tubes (eppendorf).

Samples were then incubated at 37°C for 40 mins after 5µl Ion Shear™ Plus 10x Reaction Buffer (life technologies) had been added. Once complete samples were then purified by firstly transferring them to 2ml LoBind® reaction tubes (eppendorf) for better fitting with the DynaMag™-2 magnetic rack (life technologies). To purify 99µl Agencourt® AMPure® XP Reagent (Beckman Coulter) were added to each sample followed by a pulse spin and incubation at room temperature for 5 mins. Samples were then subjected to another pulse spin before being placed in the DynaMag™-2 magnetic rack (life technologies) and incubated for 3 mins. The supernatant was then discarded and 500µl freshly prepared 70% EtOH was added in each tube whilst still in the rack. Samples were incubated for 30 secs and each reaction tube was turned twice in the rack during this time. The supernatant was then discarded and this wash step was repeated. To remove residual EtOH samples were subjected to a pulse spin and replaced in the magnetic rack for 30 secs before any leftover EtOH was removed and samples incubated with open lids for ≥5 mins. Once this incubation was complete 25µl Low TE (life technologies) was added to each pellet and samples were then vortexed for 10 secs before being subjected to a pulse spin and incubated in the magnetic rack for 1 min. Each supernatant was then transferred to 0.2ml reaction tubes in preparation for ligation of adapters.

In order for final sequencing in later stages it was necessary to ligate barcoded adapters for identification of each sample when final analysis of the sequencing data was required. To ligate barcoded adapters the following reactions were set up with different barcode numbers, and subjected to the following programme:

Table 5.2. Components and programme to ligate barcoded adapters to sheared DNA. All reagents were supplied by life technologies.

Ligation reaction component	**Volume**	**Ligation programme**	
Sheared DNA	25µl	**Temperature (^{o}C)**	**Time (mins)**
10x ligation buffer	10µl	25	15
Ion P1 adapter	2µl		
Ion Xpress™ Barcode (x)	2µl	72	5
dNTP mix	2µl		
H_2O	49µl		
DNA ligase	2µl		
Nick Repair Polymerase	8µl		

Once the ligation programme was complete reactions were transferred to 2ml LoBind® reaction tubes (eppendorf) and 180µl AMPure® XP Reagent (Beckman Coulter) was added before purification was carried out as described earlier. The purified DNA (now in 20µl Low TE (life technologies)) was then used for size selection of DNA of 150bp length as per the manufacturer's instructions using the E-Gel® iBase™ unit and E-Gel® Safe Imager™ transilluminator combo kit with a 2% E-Gel® SizeSelect™ 2% Agarose Gel.

Once DNA fragments of the correct length had been selected it was then necessary to amplify these in preparation for sequencing. This was performed by setting up the following amplification reaction and subjecting samples to the following PCR programme:

Table 5.3. Reagents and PCR programme to amplify 150bp DNA fragments in preparation for deep sequencing. All reagents were supplied by life technologies.

Amplification reaction component	**Volume**	**PCR programme**			
Size-selected DNA	25µl	**Step**	**Temperature (^{o}C)**	**Time**	**Number of cycles**
Library amplification mix	5µl	Denaturation	95	5 mins	1
Platinum® PCR SuperMix High Fidelity	100µl	Denaturation Annealing Extension	95 58 70	15 secs 15 secs 1 min	8

Once the PCR programme was complete samples were transferred to 2ml LoBind reaction tubes (eppendorf) and DNA was purified using 195µl AMPure® XP Reagent (Beckman Coulter) as described earlier. Following purification the DNA was quantified using the 2100 Bioanalyzer (Agilent Technologies) as per the manufacturer's instructions, and then DNA from all samples were combined to 26pM concentration to form a combined library for the final sequencing steps. This was kindly performed by Dr. Helen Tuppen. Briefly, the combined library was subjected to another PCR step to enrich the samples using the Ion OneTouch™ system (life technologies) before the library was loaded onto the Ion Personal Genome Machine™ (PGM™) sequencer (life technologies) for sequencing analysis. Final sequencing data was then analysed using NextGENe® software (Softgenetics®) with insertion/deletion (INDEL) mutations discounted from analysis as the Ion Torrent™ is prone to generating these mutations during sequencing.

5.3 Results

The results in chapter 4 demonstrate that cell growth was reduced as a result of expression of both TOP1mt/FLAG and TOP1mt^{Y559A}/FLAG with knockdown of TDP1. However, the levels of mtDNA encoded proteins and mtDNA copy number were not

affected; therefore it was decided to perform deep sequencing to determine whether there was an increase mtDNA mutation load with this treatment. As a control to determine the error rate of the sequencing procedure mouse mtDNA was used. This had been cloned into pAM1 and originally used to sequence the mitochondrial genome of the house mouse (*Mus musculus*), and therefore the resulting data should have been exactly the same as the reference sequence available on GenBank (accession number J01420.1) that had been published from this paper (Bibb et al., 1981a). Using this as a control would help to distinguish errors made as a result of the sequencing procedure, and those resulting from a natural mtDNA mutation load that would have occurred when the HEK293/*TOP1mt/FLAG* and HEK293/*TOP1mt*^{Y559A}*/FLAG* cells were being cultured in normal conditions. The reference sequence used for human mtDNA was provided by Andrews *et al* (accession number NC 012920) (Andrews et al., 1999). Completion of this sequencing was anticipated to aid in determining whether mtBER was dependent on TDP1.

5.3.1 *Sequence data from expression/knockdown experiments*

As described in chapter 4 the expression/knockdown experiments had provided little data on the molecular level that could help to provide information of the exact role of TDP1 in mtDNA repair. Deep sequencing data is provided for the expression/knockdown experiments, which to remind included expression of TOP1mt/FLAG and TOP1mt^{Y559A}/FLAG for six days (results shown in table 5.2), siRNA knockdown of TDP1 in Flp-In^{TM} T-Rex^{TM} HEK293 cells for six days (results shown in table 5.3), and expression of TOP1mt/FLAG and TOP1mt^{Y559A}/FLAG with siRNA knockdown of TDP1 for six days (results shown in table 5.4). Insertion/deletion (INDELs) mutations were discounted from the analysis as the Ion PGM^{TM} sequencer

(life technologies) is prone to introducing these mutations. Explanations for headings in the tables are as follows:

- **Sample** = DNA sample from each of the expression/knockdown experiments
- **Number of matched bases** = Number of bases from sequencing data that were aligned to the reference sequence
- **Number of unmatched bases** = Number of bases that were considered mutations by the NextGENe® software (Softgenetics)
- **Ratio matched bases: unmatched bases** = Ratio of number of matched bases to number of mutations detected
- **Reference length (bp)** = Length of the reference sequence in base pairs
- **Number of bases covered from reference (bp)** = Number of bases from the reference sequence that were read during sequencing (slightly less for the control mouse mtDNA due to the availability of primers that did not include any of the pAM1 vector DNA).

Table 5.4. Deep sequencing data of the control mouse mtDNA in pAM1 and human DNA samples following expression of TOP1mt/FLAG and TOP1mt^{Y559A}/FLAG for six days as in chapter 4.

Sample	Number of matched bases	Number of unmatched bases (mutations)	Ratio bases read: unmatched bases (x10^{-3})	Reference length (bp)	Number of bases covered from reference (bp)
Mouse mtDNA	3115820	11520	3.697261	16295	16023
WT -	4094734	24478	5.977922	16569	16569
WT +	3563289	21643	6.073883	16569	16569
MUT -	4065604	24109	5.929992	16569	16569
MUT +	3034723	20325	6.697481	16569	16569

*Sequencing was carried out as described in 5.2.1 with sample labelling's as follows:
Mouse mtDNA = mouse mtDNA cloned into pAM1 (control)
WT - = HEK293/*TOP1mt/FLAG* cells without expression of TOP1mt/FLAG
WT + = HEK293/*TOP1mt/FLAG* cells with expression of TOP1mt/FLAG
MUT - = HEK293/*TOP1mt^{Y559A}/FLAG* cells without expression of TOP1mt^{Y559A}/FLAG
MUT + = HEK293/*TOP1mt^{Y559A}/FLAG* cells with expression of TOP1mt^{Y559A}/FLAG

Table 5.5. Deep sequencing data of human DNA samples following siRNA knockdown of TDP1 for six days as in chapter 4.

Sample	Number of matched bases	Number of unmatched bases (mutations)	Ratio bases read: unmatched bases (x10^{-3})	Reference length (bp)	Number of bases covered from reference (bp)
UT	5245914	28766	5.483506	16569	16569
NT	3964357	23429	5.909912	16569	16569
C	4713751	27560	5.846724	16569	16569

*Sequencing was carried out as described in 5.2.1 with sample labelling's as follows:
UT = untransfected
NT = non-targeted siRNA
C = siRNA construct

Table 5.6. Deep sequencing data of human DNA samples following siRNA knockdown of TDP1 and expression of TOP1mt/FLAG and TOP1mt^{Y559A}/FLAG for six days as in chapter 4.

Sample	Number of matched bases	Number of unmatched bases (mutations)	Ratio bases read: unmatched bases (x10^{-3})	Reference length (bp)	Number of bases covered from reference (bp)
WT-UT	4572540	25401	5.555118	16569	16569
WT-NT	5145911	30055	5.84056	16569	16569
WT-C	6623268	34649	5.231405	16569	16569
MUT-UT	5209559	29125	5.590684	16569	16569
MUT-NT	4753097	25922	5.453707	16569	16569
MUT-C	4798886	26657	5.554831	16569	16569

*Sequencing was carried out as described in 5.2.1 with sample labelling's as follows:
WT-UT = Expression of TOP1mt/FLAG without any siRNA transfection
WT-NT = Expression of TOP1mt/FLAG with transfection using non-targeted siRNA
WT-C = Expression of TOP1mt/FLAG siRNA with transfection using construct C
MUT-UT = Expression of TOP1mt^{Y559A}/FLAG without any siRNA transfection
MUT-NT = Expression of TOP1mt^{Y559A}/FLAG with transfection using non-targeted siRNA
MUT-C = Expression of TOP1mt^{Y559A}/FLAG with transfection using siRNA construct C

The data in tables 5.4, 5.5, and 5.6 do not appear to indicate a higher mutation load with any of the treatments in the cell lines used for these experiments as described earlier. Even in cells that displayed reduced cell growth with knockdown of TDP1 and expression of TOP1mt/FLAG and TOP1mt^{Y559A}/FLAG for six days there was no indication of a significant increase in mtDNA mutation load in comparison to controls. One observation to note in table 5.4 is that the overall mutation ratio (ratio bases read: unmatched bases) is lower for the control mouse mtDNA than the controls from the human cell lines when compared to the reference sequence. Although there is a difference in the levels of mutations between the control mouse mtDNA and the other samples the difference is not so high and raises questions as to the sensitivity of using this sequencing technology for our purposes, which is reviewed in the discussion of this chapter.

5.4 Discussion and conclusions

The data outlined in this chapter does not appear to show an increased mtDNA mutation load with the expression/knockdown experiments described in chapter 4. This information has aided in the attempt to determine:

- The exact role of TDP1 in mtDNA repair.

Although the data indicates that there are no significant changes in mtDNA mutation load from cells that had shown decreased growth with knockdown of TDP1 and expression of TOP1mt it is possible to make assertions as to the exact function of this enzyme in mtDNA repair. However, a critical discussion of the techniques used to assess mtDNA mutation load must first be carried out before any definitive conclusions about the role of TDP1 in mtDNA repair will be made.

Next generation sequencing to assess *de novo* mtDNA mutations

The decision to use next generation sequencing to assess mtDNA mutations was taken as the experiments in chapter 4 suggested a negative impact on cell growth with TDP1 knockdown and expression of TOP1mt, but western blot analysis and qRT-PCR did not suggest a severe impact in these cells with this treatment. It was anticipated that using Ion Torrent^{TM} technology (life technologies) would provide a more sensitive mechanism to determine the exact effect of this treatment as increased mtDNA mutation load would potentially be detected. However, before samples could be sequenced they firstly underwent a preparation phase. This began with a LR-PCR step to amplify two ≈8kb regions so that full coverage of the mitochondrial genome was achieved. There were two additional PCR steps in this protocol when fragmented DNA with ligated adapters is amplified, and when these products are then clonally amplified onto beads before being loaded onto a chip for sequencing. These PCR steps all have the potential

to introduce mutations into DNA that may then be recorded as mutations that had occurred due to knockdown of TDP1 and expression of TOP1mt/FLAG TOP1mt^{Y559A}/FLAG. Despite this all samples were treated with the same library preparation protocol and so any mutations arising from this preparation would have occurred in a similar amount in all samples and would have been taken into account in the analysis of final mutation numbers.

Ultra-deep sequencing of the mtDNA mutator mouse using the SOLiD^{TM} sequencing platform (life technologies) indicated that there were significant increases in mtDNA mutations in the homozygous PolgA^{mut}/PolgA^{mut} in comparison to heterozygous and wild type controls (a total of 10 samples were loaded onto the chip for sequencing in this instance) (Ameur et al., 2011). Although this may have been expected for the homozygous mutant, the heterozygous mice also displayed a higher ratio of mutations despite being phenotypically similar to wild type mice (Ameur et al., 2011, Trifunovic et al., 2004). This suggests that even under circumstances where a strong phenotype is not seen mutation levels are increased and detectable using deep sequencing technology (Ameur et al., 2011). This relates to our own studies as the deep sequencing of mtDNA from cells that showed a decreased growth rate would surely have produced detectable levels of mtDNA mutations using Ion Torrent^{TM} technology. However, this was not the case and there did not appear to be any notable differences in mutation levels in mtDNA from the cells used in the expression/knockdown experiments. It could be argued that the error rate generated from the library preparation and sequencing using the Ion Torrent^{TM} was too high to detect any mutations arising in mtDNA as a result of TDP1 knockdown and expression of TOP1mt/FLAG and TOP1mt^{Y559A}/FLAG. Although the mutation rate is lower in the control mtDNA ($\approx 3.7 \times 10^{-3}$) than in the samples from expression/knockdown experiments ($\approx 5.2\text{-}6.7^{-3}$) these differences are not significant

enough to suggest that they are a result of a natural mutation rate occurring in the cells as part of culturing; a frequency that is argued to be between $1x10^{-4}$ and $1x10^{-9}$ (Larsson, 2010, Vermulst et al., 2007, Vermulst et al., 2008). This suggests that Ion Torrent™ technology and/or the NextGENe® may not be capable of detecting high levels of random mtDNA mutations that may have occurred as a result of the expression/knockdown experiments. Mutations in the $PolgA^{mut}/PolgA^{mut}$ mutator mouse were reported to be $\approx 1.1\text{-}1.3x10^{-3}$ using SOLiD™ sequencing platform, mentioned earlier, which adds to the argument that the Ion Torrent™ was not sensitive enough for our purposes (Ameur et al., 2011). These mice accumulate a greater number of mtDNA mutations due to their proof-reading deficient form of PolgA (Trifunovic et al., 2004). In our experiments even the control mtDNA sample had a mutation rate higher than that of the mutator mouse suggesting a very high error rate of the Ion Torrent™ sequencing platform (Ameur et al., 2011). Despite this, the data provided in previous chapters offers the potential for further discussion of the role of TDP1 in mtDNA repair.

Although the data presented in this chapter does not provide any conclusive data the results in chapter 4 suggest it would be fair to conclude that mtBER is not dependent on TDP1 as Das et al (Das et al., 2010) suggested for the following reasons:

- *Tdp1* -/- mice did not show signs of mtDNA damage despite various treatments to induce this.
- There were no signs of severe mtDNA damage with knockdown of TDP1 in human cells.
- There are a wide variety of DNA lesions that can occur within the mitochondrial genome that TDP1 is not capable of repairing (e.g. 5' adenine monophosphate repaired by APTX).

Therefore, what role does TDP1 have in mtDNA repair? The observation in chapter 4 that there was no decrease in mtDNA copy number or levels of mtDNA encoded

proteins with TDP1 knockdown and expression of TOP1mt/FLAG and TOP1mt^{Y559A}/FLAG may suggest that either TDP1 is not involved in mtDNA to a great degree or that there are mechanisms present that can compensate for this loss. The reduction in cell growth with TDP1 knockdown and expression of TOP1mt/FLAG and TOP1mt^{Y559A}/FLAG would imply that there is some negative impact in mitochondria in these cells such as reduced levels of mitochondrial mRNA transcripts that could then affect ATP production from OXPHOS resulting in reduced cell growth. Another possibility could be that this treatment stalled mtDNA replication that then affected cell growth also, but which was not accompanied by mtDNA depletion in 6 days of this treatment as our results demonstrated in chapter 4. However, these theories are purely speculative at this point and it is necessary to discuss further how this treatment may have been detrimental in cells on the molecular level and whether there are other means of repairing any damage caused by this treatment.

The first inference that other repair mechanisms existed to compensate for the loss of TDP1 was made in *S. cerevisiae* where RAD1 and MUS81 were able to repair DNA-TOP1 lesions in the nucleus in the absence of TDP1 (Liu et al., 2002). It was proposed that these enzymes excised a section of DNA surrounding the CPT generated DNA-TOP1 lesion, which acted as a compensatory mechanism for repairing this type of damage without the preferred TDP1 (Liu et al., 2002). Another study that involved our collaborators identified tyrosyl-DNA-phosphodiesterase 2 (TDP2) to be involved in repairing DNA-TOP1 lesions in the absence of TDP1 (Zeng et al., 2012). Despite the main function of TDP2 being repair of lesions involving double strand breaks where topoisomerase 2 (TOP2) is covalently bound to the 5' end of DNA at this lesion it can still function to repair TOP1 mediated damage (Cortes Ledesma et al., 2009, Zeng et al., 2012). The data presented in this thesis suggests that there is some detrimental impact with loss of TDP1 and expression of TOP1mt/FLAG or TOP1mt^{Y559A}/FLAG shown by

a reduction in cell growth. However, mtDNA depletion and a reduction in the levels of mtDNA encoded proteins may have been prevented with compensatory repair of these lesions by TDP2. Although TOP2 and TDP2 have yet to be identified in mitochondria this evidence demonstrates that there are alternative mechanisms that could exist to repair mtDNA-TOPMT lesions when TDP1 is not present. This could explain why the impact of losing TDP1 in mice and in human cells is not so severe on the molecular level as claimed previously (Das et al., 2010).

This leads to the conclusion that mtBER is not dependent on TDP1 as proposed by Das et al using H_2O_2 treatment and a questionable semi-quantitative PCR based assay, and that this enzyme is predominantly responsible in repairing lesions involving TOP1MT bound to mtDNA in mitochondria (Das et al., 2010). The potential for this enzyme to be involved in other repair pathways as with TDP2 cannot be determined based on the data presented in this thesis, but it can be concluded that TDP1 is not essential for mtDNA repair based on our observations. Although TDP1 may not be essential to mtDNA repair it may be possible that the DNA repair machinery in mitochondria is more intricate than we think. This then leads us to ask whether there are more proteins involved in DNA repair in mitochondria, and what associations do current proteins involved in this subject have with each other and how are these associations mediated? The latter question is reviewed in the next chapter with reference to TDP1 and the mitochondrial DNA ligase.

Chapter 6. Does phosphorylation of amino acid 81 in TDP1 promote association with mitochondrial DNA ligase IIIα?

6.1 Introduction

The data previously described within this thesis has identified TDP1 as a novel DNA repair enzyme in mitochondria. Whilst investigating the exact role of TDP1 in mtDNA repair it was also decided to explore some other factors that may influence TDP1 function in mitochondria, and/or provide a greater comprehension of how the mtDNA repair network operates to protect against mtDNA damage. More specifically, the association between TDP1 and another protein involved in mtDNA repair, namely DNA ligase IIIα (LIG3α), would be scrutinised to determine whether these two proteins have a direct link with each other in mitochondria, and if so the exact mechanism that facilitates their association.

Our collaborators reported that the association between TDP1 and LIG3α in the nucleus was mediated by phosphorylation of amino acid 81 in TDP1 using both yeast (*Saccharomyces cerevisiae*) and MEFs. Phosphorylation of this amino acid (serine, S81) was shown to promote the association between TDP1 and LIG3α in A549 cells by using expression of a mutant form of TDP1 with a change in amino acid 81 from serine to alanine. This change prevented phosphorylation at this site, which inhibited the interaction between TDP1 and LIG3α. This inhibition of interaction between the two proteins reduces the stability of TDP1 which could be as a result of either a conformational change in TDP1 that affects its tertiary structure rendering it unstable, or more simply, a need for LIG3α association for stability and function. Subsequently cell survival was reduced when DNA-TOP1 lesions were induced using camptothecin

(CPT), which suggests the interaction of TDP1 with LIG3α is important to repair of these specific lesions in the nucleus. This data provides an intriguing example of the intricacies underlying post-translational modifications in relation to DNA repair in the nucleus, and based on this it was decided to try and find whether a similar association existed in mitochondria (Chiang et al., 2010).

In consideration of this and given that TDP1 had been identified in having a role in mtDNA repair, this strand of the project was set about to determine whether:

Phosphorylation of amino acid 81 in TDP1 promotes the association with mitochondrial DNA ligase IIIα.

This was accomplished by using protein complex immunoprecipitation (Co-IP) with two mitochondrially targeted variants of TDP1; a phosphomimetic version (mtTDP1^{S81E}/FLAG) and a non-phosphorylatable form (mtTDP1^{S81A}/FLAG). If this association was found it would open many possibilities as to the depth of the mtDNA repair network in terms of post-translational modifications and protein-protein interactions.

6.2 Methods

6.2.1 *Detecting expression of mtTDP1^{S81E}/FLAG and mtTDP1^{S81A}/FLAG*

Once stable transformation of Flp-In^{TM} T-Rex^{TM} HEK293 cells with both HEK293/*mtTDP1^{S81E}/FLAG* and HEK293/*mtTDP1^{S81A}/FLAG* had been completed (as described in 2.2.2 (vii) it was necessary to determine whether clones for each cell line

that resisted the antibiotics blasticidin S and hygromycin B expressed either mtTDP1^{S81E}/FLAG or mtTDP1^{S81A}/FLAG upon induction. This was carried out by seeding 5x10^5 cells for each cell line in 2ml supplemented DMEM in 2 wells of a 6-well plate for each clone. Tetracycline was then added at 1µg/ml final concentration in 1 well for each clone and all cells were incubated as described in 2.2.2 (i) for 18 hours before being harvested with 0.5ml PBS/1mM EDTA, neutralised in 0.5ml supplemented DMEM, and centrifuged for 4 mins at 200xg. Cytoplasmic protein was then isolated as described in 2.2.3 (i) to allow analysis by SDS-PAGE as in 2.2.3 (vii) and western blotting as in 2.2.3 (viii) to determine which clones for each cell line expressed their respective protein.

6.2.2 *Protein complex immunoprecipitation (Co-IP) using of mtTDP1^{S81E}/FLAG and mtTDP1^{S81A}/FLAG*

To assess the association between the mitochondrial DNA ligase (LIG3α) and TDP1 a Co-IP was carried out following expression of a phosphomimetic form of TDP1 (mtTDP1^{S81E}/FLAG) and a non-phosphorylatable form (mtTDP1^{S81A}/FLAG), as well as a control for the Flp-In^{TM} T-Rex^{TM} expression system (life technologies); a mitochondrially targeted FLAG-tagged luciferase (mtLUC/FLAG). This mtLUC/FLAG should not associate with LIG3α and would act as a control by helping to rule out any artefacts that may have been observed when using this Flp-In^{TM} T-Rex^{TM} expression system in HEK293 cells. The resulting samples would then analysed by mass spectrometry to determine whether phosphorylation of amino acid 81 of TDP1 was responsible for its association with LIG3α in the mitochondrion similar to that observed in the nucleus (Chiang et al., 2010).

The cell lines HEK293/*mtLUC/FLAG*, HEK293/*mtTDP1*^{S81E}*/FLAG*, and HEK293/*mtTDP1*^{S81A}*/FLAG* were grown in 3x 300cm^2 flasks each with 50ml supplemented DMEM. Expression of each protein was induced with addition of 1µg/ml tetracycline and cells were incubated as described in 2.2.2 (i) for 48 hours. Cells were harvested using 20ml PBS/1mM EDTA and neutralised in 20ml supplemented DMEM before being centrifuged at 200xg for 4 mins followed by mitochondrial isolation and purified as in 2.2.3 (ii) and 2.2.3 (iv), respectively. Mitochondrial protein was quantified by Bradford analysis and up to 5mg mitochondrial protein from each cell line was resuspended in 500µl lysis buffer in separate 1.5ml reaction tubes. Each sample was incubated at 4^{o}C while being rotated for 30 mins before samples were centrifuged at 12000xg for 10 mins at 4^{o}C. The supernatant from each sample was then transferred to new 1.5ml reaction tubes and protein quantified by Bradford analysis as in 2.2.3 (vi).

Then up to 3mg of each sample was transferred to separate 1.5ml hydrophobic reaction tubes with 40µl ANTI-FLAG M2 affinity gel that had already been washed 3x in 1x washing buffer, and samples were then incubated with rotation at 4^{o}C for 3 hours. Each sample was then centrifuged at 5000xg for 30 secs before the supernatant was removed and discarded. Each sample was washed 3x using 1ml 1x washing buffer and centrifuging at 5000xg for 30 secs for each wash. Once the supernatant had been discarded following the final wash step 5µl of 3xFLAG peptide (5µg/µl) was added with 100µl 1x washing buffer and added to the ANTI-FLAG M2 affinity gel now encompassing bound protein from each sample. Samples were then incubated at 4^{o}C for 45 mins with rotation. Once incubation was complete the supernatant from each sample was carefully removed and transferred to fresh 1.5ml reaction tubes for analysis of protein associations by silver staining and mass-spectrometry. The beads were also retained for further analysis by silver staining.

Lysis buffer
50mM Tris HCl, pH 7.4,
150mM NaCl
1mM EDTA
10mM $MgCl_2$
1mM PMSF
60U SUPERase•In™ (life technologies)
1% Triton X-100

10x washing buffer
0.5M Tris HCl, pH 7.4
1.5M NaCl
10mM $MgCl_2$
1mM PMSF
10U SUPERase•In™ (life technologies)
1 protease inhibitor tablet* (Roche)

*Added at the time of dilution of 1ml 10x washing buffer with 9ml DEPC treated H_2O

6.2.3 *Silver staining*

Silver staining was carried out in order to confirm presence of mtLUC/FLAG, mtTDP1^{S81E}/FLAG, and mtTDP1^{S81A}/FLAG following Co-IP and to provide some preliminary data as to the association of TDP1 with LIG3 and/or any other proteins in the mitochondrion. This was performed by first mixing 5µl of each elution sample with 5µl 2x dissociation buffer, and 2µl each beads sample with 2µl 2x dissociation buffer. Each sample was then denatured at 95^{o}C for 3 mins before being run on a 10% SDS-PAGE as described in 2.2.3 (vii). Once molecular weight marker 40kDa subunit had reached the bottom of the gel the gel was carefully removed and washed for 1 hour in 50% NaOH. Both TDP1 (≈70kDa) and LIG3α (≈113kDa) should still be in the gel at this point so any association should be seen, and any other proteins would be identified on mass-spec analysis. During this time the silver stain was prepared. After 1 hour the 50% NaOH was discarded and the gel was stained with the silver stain solution with rocking for 15mins. The silver stain was then discarded and the gel was washed 3x for 5 mins in H_2O before being developed with 50ml developer solution with agitation until protein bands could be seen (≈ 3 mins). The gel was then fixed in fixing solution overnight before being washed for 10 mins in 30% EtOH followed by washing for 10 mins in H_2O and an image taken.

2x dissociation buffer (200ml)	**Silver stain (100ml)**	**Developer solution**
0.125M tris-HCl, pH 6.8	21ml 0.36% NaOH	1ml 1% citric acid
4% SDS	1.4ml NH_4OH	300µl 37% formaldehyde
0.15M DTT	77.6ml H_2O	198.7ml H_2O
15% glycerol	0.8g $AgNO_3$ in 4ml H_2O*	
0.01% bromophenol blue		
0.01% benzonase		

*Added last in a drop by drop manner with agitation until liquid becomes slightly darker

6.2.4 *Preparation of samples for mass-spectrometry analysis*

In order for Co-IP samples to be analysed by mass-spectrometry the samples needed to be prepared by SDS-PAGE. For this 80µl of each sample from the Co-IPs of mtLUC/FLAG, mtTDP1^{S81E}/FLAG and mtTDP1^{S81A}/FLAG as described in 6.2.2 were mixed with 20µl 4x dissociation buffer. Each sample was denatured at 95^{o}C for 3 mins and samples were separated on a 12% SDS-PAGE as described in 2.2.3 (vii) at 60V until ≈1cm into the resolving gel. The gel was then removed and each lane for each sample was cut out and transferred to separate 1.5ml reaction tubes before 1ml acetonitrile was added in each tube and incubated for 30 mins at room temperature. The acetonitrile was removed and a small hole was created in the lid of each reaction tube before the lid was closed and samples incubated overnight at room temperature to allow the acetonitrile to evaporate. Each sample was then sent for mass-spectrometry analysis at:

Nijmegen Proteomics Facility/Nijmegen Centre for Mitochondrial Disorders
Department of Laboratory Medicine
Radboud University Nijmegen Medical Centre

4X Dissociation buffer
0.25M tris-HCl, pH 6.8
8% SDS
0.3M DTT
30% glycerol
0.02% bromophenol blue
0.01% benzonase

6.3 Results

6.3.1 *Expression mtTDP1^{S81E}/FLAG and mtTDP1^{S81A}/FLAG following stable transfection*

Following stable transfection of *mtTDP1^{S81E}/FLAG* and *mtTDP1^{S81A}/FLAG* into Flp-In^{TM} T-Rex^{TM} HEK293 cells as described in 2.2.2 (vii) and the expression experiments as in 6.2.1 had been completed, it was necessary to confirm that both mtTDP1^{S81E}/FLAG and mtTDP1^{S81A}/FLAG were being expressed in their cell lines. Figure 6.1 illustrates the results from expression of each protein.

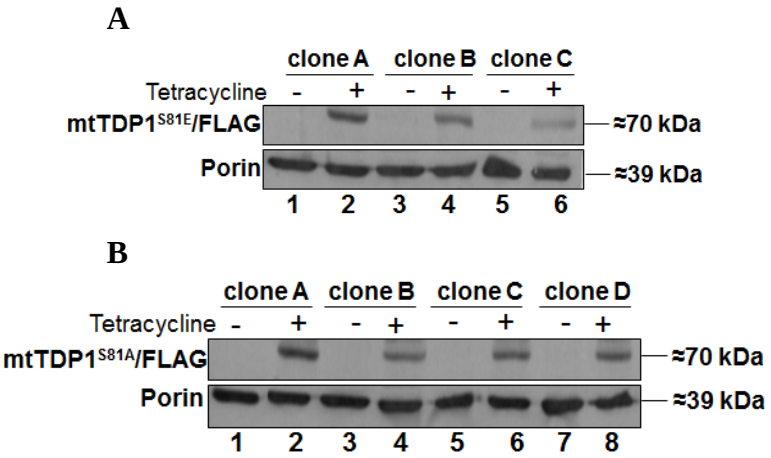

Figure 6.1. *Analysis of mtTDP1^{S81E}/FLAG and mtTDP1^{S81A}/FLAG expression*. Western blot analysis as described 2.2.3 (viii) using 20µg cytoplasmic protein isolated as described in 2.2.3 (i) to determine expression of desired protein following stable transfection of Flp-In^{TM} T-Rex^{TM} HEK293 cells as described in 2.2.2 (vii). Expression of each protein was induced with addition of 1µg/ml (final concentration) tetracycline from 5x10^5 cells in 2ml supplemented DMEM in 6-well plates, followed by incubation for 18 hours in conditions outlined in 2.2.2 (i). A separate well containing 5x10^5 cells for each clone in 2ml supplemented DMEM was left without tetracycline as controls **(A)** Analysis of 3 clones following transfection of *mtTDP1^{S81E}/FLAG*. **(B)** Analysis of 4 clones following transfection of *mtTDP1^{S81A}/FLAG*.

The results in figure 6.1 show that both mtTDP1^{S81E}/FLAG and mtTDP1^{S81A}/FLAG were successfully expressed in each of the clones that had survived treatment with the antibiotics blasticidin S and hygromycin B. In **A** expression of mtTDP1^{S81E}/FLAG can be seen in three different clones of HEK293/*mtTDP1^{S81E}/FLAG* in lanes 2, 4, and 6

whereas the uninduced samples in lanes 1, 3, and 5 show no expression. Similarly in **B** successful expression of mtTDP1^{S81A}/FLAG can be seen from four different clones of HEK293/*mtTDP1^{S81A}/FLAG* in lanes 2, 4, 6, and 8 whereas in induced samples there is no expression seen in lanes 1, 3, 5, or 7. Equal loading of the western blot was proven using the α-porin antibody. For further experiments clone A for both HEK293/*mtTDP1^{S81E}/FLAG* and HEK293/*mtTDP1^{S81A}/FLAG* would be used as they appeared to show the strongest signal on western blotting, which at the time was thought to be the best criterion for selection.

6.3.2 *Mitochondrial localisation of mtTDP1^{S81E}/FLAG and mtTDP1^{S81A}/FLAG*

In order to confirm that mtTDP1^{S81E}/FLAG and mtTDP1^{S81A}/FLAG were localised to mitochondria upon expression in respective clones A a Proteinase K (life technologies) protection assay was performed. This assay, described in 2.2.3 (v), had already been used to show localisation of TOP1mt/FLAG and TOP1mt^{Y559A}/FLAG to mitochondria in chapter 4 (figure 4.6) and so this procedure had been optimised from earlier experiments; i.e. 2µg Proteinase K (life technologies) was required to show protection of internalised protein. Figure 6.2 demonstrates this result.

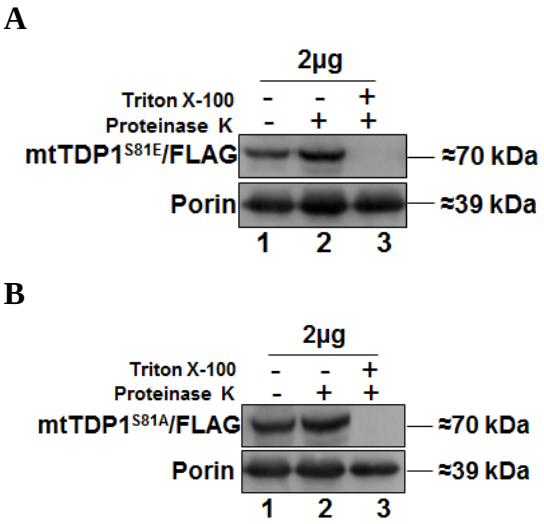

Figure 6.2. *Analysis of mtTDP1^{S81E}/FLAG and mtTDP1^{S81A}/FLAG mitochondrial localisation*. Western blot analysis as described 2.2.3 (viii) using 10µg mitochondrial protein isolated as described in 2.2.3 (iii) to determine mitochondrial localisation of both mtTDP1^{S81E}/FLAG and mtTDP1^{S81A}/FLAG following stable transfection of Flp-In^{TM} T-Rex^{TM} HEK293 cells as described in 2.2.2 (vii). Expression of each protein was induced in each cell line with addition of 1µg/ml (final concentration) tetracycline followed by incubation for 18 hours in conditions outlined in 2.2.2 (i). Localisation of both proteins was assessed by addition of 2µg Proteinase K (life technologies) with or without Triton X-100 as described in 2.2.3 (v) and optimised from chapter 4 (figure 4.6) **(A)** Analysis of mtTDP1^{S81E}/FLAG clone A **(B)** Analysis of mtTDP1^{S81A}/FLAG clone A.

The results presented here show that with 2µg Proteinase K (life technologies) in the presence on Triton X-100 was sufficient to degrade each expressed protein (lane 3 in both **A** and **B**). Lane 2 of **A** and **B** illustrates that both mtTDP1^{S81E}/FLAG and mtTDP1^{S81A}/FLAG were protected by the outer mitochondrial membrane despite addition of 2µg Proteinase K (life technologies), similar to the untreated control in lane 1 of **A** and **B**. This suggests that mtTDP1^{S81E}/FLAG and mtTDP1^{S81A}/FLAG are in fact imported to mitochondria in their respective cell lines.

6.3.3 *Co-IP using FLAG-tagged expressers*

Once the Co-IP of mtLUC/FLAG, mtTDP1^{S81E}/FLAG, and mtTDP1^{S81A}/FLAG was complete as described in 6.2.2, analysis of the binding affinities of each protein could

then be assessed. This was carried out to determine whether phosphorylation of amino acid residue 81 in TDP1 is responsible for its association with LIG3α in mitochondria, providing this association exists. Two methods for assessing this association were performed and the results from these are outlined as follows.

i) Silver staining

This was carried out in order to verify that each of the proteins mtLUC/FLAG, mtTDP1^{S81E}/FLAG, and mtTDP1^{S81A}/FLAG were expressed and present following the Co-IP, but in the main to provide preliminary data as to whether LIG3α was associated with any of these proteins. Results from silver staining as outlined in 6.2.3 are shown in figure 6.3.

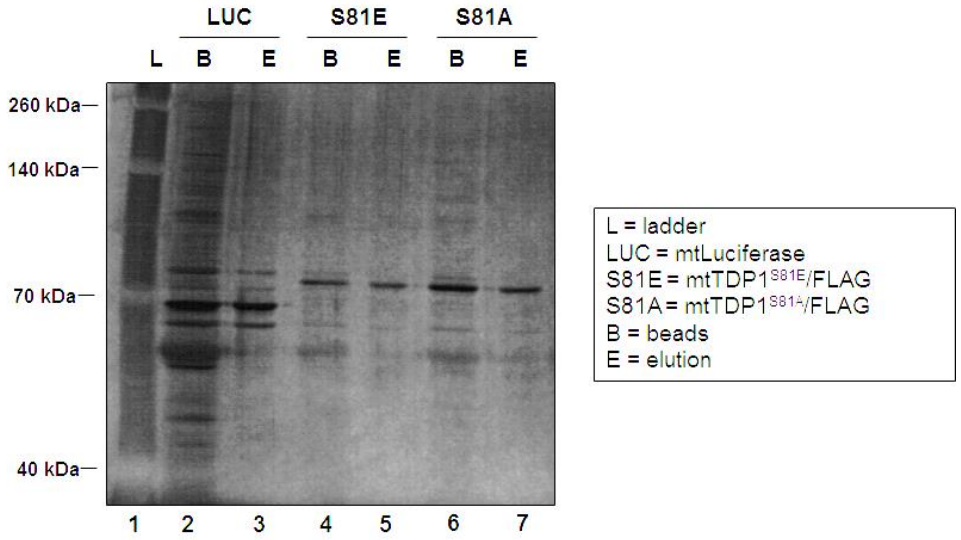

Figure 6.3. *Silver staining analysis to detect protein associations of mtTDP1^{S81E}/FLAG and mtTDP1^{S81A}/FLAG.* Silver staining as described in 6.2.3 following Co-IP as described in 6.2.2 to detect expression of mtLUC/FLAG, mtTDP1^{S81E}/FLAG, and mtTDP1^{S81A}/FLAG with associated proteins from beads (**B**) and elution (**E**) from the Co-IP. Of each sample 10µl was separated by SDS-PAGE as described in 2.2.3 (vii) before silver staining was carried out. Lane 1 (also L) represents the molecular weight marker used for the gel.

The image produced from silver staining showed that mtLUC/FLAG, mtTDP1^{S81E}/FLAG, and mtTDP1^{S81A}/FLAG were present following the Co-IP by strong

bands being present at a the correct molecular weight for each protein (≈70kDa, lanes 2-7), but that there was no obvious presence of LIG3α (expected size ≈113kDa).

ii) Mass spectrometry data

Following the data provided in figure 6.3 that shows no obvious sign that a protein of the molecular weight of LIG3α (≈113kDa) was present, samples were prepared as described in 6.2.4 and sent for mass-spectrometry analysis. Table 6.1 lists the proteins that were associated with mtTDP1^{S81E}/FLAG from the Co-IP that were different to the proteins associated with the control mtLUC/FLAG. Table 6.2 lists the proteins associated with mtTDP1^{S81A}/FLAG that were different to the control also.

Table 6.1. Mass spectrometry data of proteins identified following Co-IP (described in 6.2.2) after expression of the phosphomimetic mtTDP1^{S81E}/FLAG.

Protein GI	Protein	Gene	emPAI
83715985	3-hydroxyacyl-CoA dehydrogenase type-2 isoform 2	*HSD17B10*	0.318256739
32483377	thioredoxin-dependent peroxide reductase, mitochondrial isoform b	*PRDX3*	0.258925412
4504897	importin subunit alpha-2	*KPNA2*	0.637893707
4507231	single-stranded DNA-binding protein, mitochondrial precursor	*SSBP1*	0.165914401

*****The proteins identified are those that were found to be different to those from the control expression and Co-IP using mtLUC/FLAG. For full table including those for mtLUC/FLAG see appendix.

Table 6.2. Mass spectrometry data of proteins identified following Co-IP (described in 6.2.2) after expression of the phosphomimetic mtTDP1^{S81A}/FLAG.

Protein GI	Protein	Gene	emPAI
83715985	3-hydroxyacyl-CoA dehydrogenase type-2 isoform 2	*HSD17B10*	0.737800829
91199540	dihydrolipoyl dehydrogenase, mitochondrial precursor	*DLD*	0.333521432
32483377	thioredoxin-dependent peroxide reductase, mitochondrial isoform b	*PRDX3*	0.258925412
4504897	importin subunit alpha-2	*KPNA2*	0.245197085
15277342	estradiol 17-beta-dehydrogenase 8	*HSD17B8*	0.232846739
8923421	seryl-tRNA synthetase, mitochondrial isoform b precursor	*SARS2*	0.193776642
188528628	Polyribonucleotide nucleotidyltransferase 1, mitochondrial precursor	*PNPT1*	0.14504757
81295407	acyl-coenzyme A thioesterase 9, mitochondrial isoform a precursor	*ACOT9*	0.113042193
193082993	tRNA modification GTPase GTPBP3, mitochondrial isoform III	*GTPBP3*	0.068000433
4503943	glutaryl-CoA dehydrogenase, mitochondrial isoform a precursor	*GCDH*	0.064209244

*****The proteins characterised in this table are those that were found to be different to those from expression of mtLUC/FLAG as a control. For full table including those for mtLUC/FLAG see appendix.

The data in table 6.2 demonstrates that there is no association between mtTDP1^{S81A}/FLAG and LIG3α; however this is also the case for mtTDP1^{S81E}/FLAG which can be seen in table 6.1. Full data including all associated proteins from the Co-IP of mtLUC/FLAG, mtTDP1^{S81E}/FLAG, and mtTDP1^{S81A}/FLAG can be seen in the appendix, but this also confirms that LIG3α is not associated with mtLUC/FLAG and subsequently does not explain the absence of LIG3α from either table 6.1 or 6.2. This data suggests that phosphorylation of amino acid 81 of TDP1does not affect its association with LIG3α in the mitochondrion, and also raises the possibility that these two proteins are not directly associated in mitochondria as is discussed in 6.4.

6.4 Discussion and conclusions

The data presented in this chapter was performed in order to try and determine whether the association of TDP1 and LIG3α was present in mitochondria, and if so whether:

Phosphorylation of amino acid 81 in TDP1 promotes the association with LIG3α

Although the data provided here does not demonstrate that there is an association between TDP1 and LIG3α, it is still relevant to discuss the details underlying this kind of association in mitochondria, some of the potential reasons for our own observations, and consideration of some future perspectives regarding our results.

Phosphorylation in mitochondria

Phosphorylation of proteins is one form of post-translational modification that can affect the activity of enzymes in a regulatory manner, with other examples including modifications that incorporate nitric oxide (nitrosylation) and/or introduce acetyl groups (acetylation) into proteins to alter their function (O'Rourke et al., 2011). These examples are just a small group of a huge collection of post-translation modifications that have been reported to modify the function of an enzyme in regulated cellular processes, and conversely, as for oxidative damage, affect the ability of enzymes to fulfil their requirements (O'Rourke et al., 2011). Although post-translation modifications have a wide variety of purposes in cells it is important to discuss how these modifications impact on DNA repair to remain focussed on the theme of this thesis.

Phosphorylation of proteins by kinases is a relatively undefined in mitochondria when compared with the knowledge accrued for nuclear kinases and their role in DNA repair. Therefore, findings of nuclear mechanisms for DNA damage responses provided a basis for the experiments outlined in this chapter of my thesis (Chiang et al., 2010, Shiloh, 2006). As discussed earlier, our collaborators previously reported that phosphorylation of TDP1 at serine 81 mediated its association with LIG3α in the nucleus; thus demonstrating that factors other than the actual enzyme activity of TDP1 affected the DNA damage response (Chiang et al., 2010). This discovery resulted from previous reports that the checkpoint kinases Ataxia Telangiectasia-mutated (ATM) and ATM-Rad3-related (ATR) that phosphorylate proteins at serine-threonine-glutamine (S/TQ) sites, phosphorylate TDP1, and that TDP1 contains five S/TQ sites also (Zhou et al., 2005, Mu et al., 2007). There has recently been 77 phosphoproteins identified in mitochondria from human skeletal muscle by mass spectrometry, and ATM was also shown to have a role in phosphorylation of some of these (Zhao et al., 2011, O'Rourke et al., 2011). Although TDP1 was not included in these findings the method for interpreting mitochondrial and non-mitochondrial proteins was based on the known mitochondrial proteins at the time of the publication (Zhao et al., 2011). At that time TDP1 had not been reported to be present in mitochondria and would not have been considered in the investigations of this group (Zhao et al., 2011). Therefore, our own aim to study the interaction between TDP1 and LIG3α was valid as work is on-going to identify more mitochondrial proteins that have various functions in the organelle.

Phosphorylation of amino acid 81 in TDP1 did not promote the association with LIG3α

The data presented in table 6.1 demonstrates that despite the phosphomimetic amino acid at position 81 in TDP1, there is no observable association with LIG3α using this system. With this in mind the potential reasons for this result will be explored to try and determine whether there is no association between TDP1 and LIG3α in the mitochondrion, or whether the system and methods used to detect this association were not adequate for this purpose.

The majority of support for conducting the experiments outlined in this chapter came from published work performed by our collaborators. However, in this publication the phosphomimetic TDP1^{S81E} form of TDP1 was not used to demonstrate that LIG3α still associated with this enzyme containing this amino acid substitution (Chiang et al., 2010). This amino acid substitution to glutamic acid mimics the structure of phosphorylated serine and should form normal associations with other proteins similar to the wild type. But with our collaborators not using this form of TDP1 in their work the question was raised as to whether the association with LIG3α was ever likely to occur in mitochondria with the change in amino acid 81. Although the phosphomimetic form of TDP1 was not used in our collaborators study, previous work using this tool to assess phosphorylation has been carried out with success which would suggest that it was an acceptable method for our own purposes (Farah et al., 2012, Pepio and Sossin, 2001).

Another possibility in failing to detect the association between TDP1 and LIG3α in this case may have been the expression system used for the experiments, namely the Flp-

In^{TM} T-Rex^{TM} system. Expressing a mitochondrially targeted form of TDP1 in HEK239 cells using this system is not exactly equivalent to the levels of expression normally observed *in vivo*, which may have caused disruption of the protein complexes in mitochondria in these experiments. However, this strategy of expression in HEK293 cells has been employed in our lab with great success when expression of protein using this system matched that of the endogenous levels of the protein that was being studied (Richter et al., 2010, Rorbach et al., 2008, Temperley et al., 2010). When the experiments outlined in this thesis were carried out this was not taken into consideration when expressing TDP1 in these cells which may have saturated binding with LIG3α, thus accounting for the absence of any detectable association. Another point for consideration is that the constructs used to transform wild type Flp-In^{TM} T-Rex^{TM} HEK293 cells contained the Su9 presequence from *N. crassa*, which would likely alter the mode of transport into mitochondria than that of the TDP1 proteins without this presequence. This may have affected the association with LIG3α, but given that mtTDP1^{S81E}/FLAG and mtTDP1^{S81A}/FLAG were both successfully localised to mitochondria and were detected at the correct molecular weight (i.e. without the mitochondrial presequence that would add ≈7kDa) it is unlikely that this would have affected any potential affinity of these proteins with LIG3α once in the mitochondrion. Also, the exact mechanism of TDP1 entry into mitochondria is currently unknown and so transforming HEK293 cells with FLAG-tagged forms of TDP1 without the presequence may have prevented successful entry into the mitochondrion. Other possibilities for not detecting an association between TDP1^{S81E}/FLAG and LIG3α could be that any association between the two proteins is transient and that crosslinking may have been required before the Co-IP was performed. This could have been carried out using paraformaldehyde, however, it is likely that many other proteins that do not normally associate with TDP1 would have been found from the Co-IP and this step was

not required for previous experiments in our lab (Richter et al., 2010, Rorbach et al., 2008, Temperley et al., 2010).

Based on the data presented in this chapter and considering the limitations of some of the methods used, it has not been possible to come to a firm conclusion on whether phosphorylation of amino acid 81 of TDP1 promotes the association with LIG3α in the mitochondrion.

Notable proteins that associated with TDP1^{S81E} and TDP1^{S81A}

Although the association between TDP1 and LIG3α was not detected in these experiments it is worthwhile discussing some of the proteins that were found to be associated with TDP1 using these methods. The first protein for discussion was associated with both forms of TDP1 and was identified as 3-hydroxyacyl-CoA dehydrogenase type-2 isoform 2, which is known to be an RNase P enzyme (Holzmann et al., 2008). These enzymes are involved in the maturation of tRNAs by cleavage of nucleotides from the 5' end to form the correct sequence once processing of the 3' end has also taken place by tRNase Z (Robertson et al., 1972, Ceballos and Vioque, 2007). A mitochondrial form of human RNase P (mtRNase P) has previously been identified suggesting a role of this enzyme in the maturation of tRNAs in mitochondria (Rossmanith et al., 1995, Holzmann et al., 2008). In most cases RNase P enzymes consist of an RNA component with one or more proteins that act together to perform their desired role (Evans et al., 2006). However, it was identified that mtRNase P consisted only of protein subunits and did not require an RNA component for activity, which was the first occasion that this had been demonstrated for any RNase P (Holzmann et al., 2008). This was accomplished with tRNA maturation activity assays

that involved using reconstituted mtRNase P made with three affinity-purified proteins that established function of this enzyme without the need for an RNA subunit (Holzmann et al., 2008). The association of this protein with both forms of TDP1 may suggest that TDP1 is somehow involved in maturation of tRNA in mitochondria, but this is highly speculative as to date TDP1 has only been identified in repair of DNA.

Other proteins that were identified from the Co-IP with $TDP1^{S81A}$ that are also involved in RNA processing include polynucleotide nucleotidyltransferase 1 (PNPase) and tRNA modification GTPase (GTPBP3). PNPase was found to be involved in degradation of mRNA transcripts in the mitochondrion in cooperation with human SUV3 (hSUV3); another protein involved in mRNA degradation (Szczesny et al., 2013). Degradation by these proteins occurs in specific areas of the mitochondrial network (degradosome-foci, or D-foci) and from this it has been suggested that mRNA degradation in mitochondria by PNPase and hSUV3 is spatially organised, but further information on this has yet to be elucidated (Szczesny et al., 2013). As for GTPBP3, this protein has been found to be involved in maturation of mitochondrial tRNAs (Villarroya et al., 2008). More specifically, the protein has two isoforms in humans that have different length domains (G-domains) that are responsible for hydrolysing GTP from mRNA transcripts (Villarroya et al., 2008). Although *in vitro* assays performed by Villarroya *et al* using synthesised tRNAs and purified protein for each isoform of GTPBP3 the exact reasons for the existence of two isoforms of this protein were not found and have yet to be described (Villarroya et al., 2008). Another protein that was found from the Co-IP and is involved in maturation of tRNA is the mitochondrial seryl-tRNA synthetase (SARS2). Aminoacyl-tRNA synthetases are responsible for charging tRNAs with the correct amino acid, and in the case of SARS2 this enzyme is responsible for charging $tRNA^{Ser}$ with L-serine (Konovalova and Tyynismaa, 2013). Mutations in *SARS2* have

been linked with a disease presenting with primary pulmonary hypertension, progressive renal failure, and OXPHOS deficiency with patients dying before 14 months of life (Konovalova and Tyynismaa, 2013). This highlights the importance of correct mitochondrial RNA processing as the damaging effects caused by the loss of just one amino acid can be potentially fatal. The presence PNPase, GTPBP3, and SARS2 in mass-spec data from the Co-IP with TDP1^{S81A} similar to 3-hydroxyacyl-CoA dehydrogenase type-2 isoform 2 may further implicate TDP1 in RNA maturation processes. However, to date there have been no data described on this and PNPase, GTPBP3, and SARS2 were only found in the Co-IP with TDP1^{S81A}, which may suggest that these findings are as a result of this form of the protein being non-phosphorylatable or potentially as a result of structural changes caused by this amino acid substitution.

An interesting protein association identified from the Co-IP of both forms of TDP1 is that involving thioredoxin-dependent peroxide reductase, mitochondrial isoform b (commonly known as peroxiredoxin 3, Prx3), which is involved in the antioxidant system within mitochondria (Watabe et al., 1997). Peroxiredoxins are a group of enzymes responsible for catalysing the reduction of hydrogen peroxide (H_2O_2) to water (H_2O) with a conserved cysteine being the residue at which reduction takes place (Kil et al., 2012, Yang et al., 2002). The majority of peroxiredoxins are functional in the cytosol, however Prx3 is known to localise to mitochondria and act with its electron donors thioredoxin 2 (Trx2) and thioredoxin reductase 2 (TrxR2) to reduce H_2O_2 (Chae et al., 1999, Lee et al., 1999, Spyrou et al., 1997). On occasion incomplete reduction of oxygen (O_2) to H_2O can lead to the formation of reactive superoxide (O_2^-) anions that is converted to the less harmful H_2O_2 by superoxide dismutase (SOD) (Rhee et al., 2001). Although H_2O_2 on its own is not particularly reactive under certain circumstances it can be reduced to form the highly damaging hydroxyl radical ($^{\cdot}OH$) (Rhee et al., 2001). It is

therefore the function of peroxiredoxins to prevent this by reducing H_2O_2 to water, which will lessen the potential for damage to mtDNA in the case of Prx3 (Rhee et al., 2001). A study using siRNA was conducted and demonstrated that the loss of Prx3 led to an increase in the levels of H_2O_2 which caused a reduction in the levels of mitochondrial mRNA transcripts most probably because of an increased level of mtDNA damage (Chang et al., 2004). It was also found that apoptosis was increased in HeLa cells with Prx3 knockdown due to release of cytochrome *c* into the cytosol and an increased rate of cleavage of procaspases-3 and -9 (Chang et al., 2004). These results suggest that Prx3 is very important as an antioxidant in mitochondria, which potentially makes its association with TDP1 very meaningful. However, no obvious link between TDP1 and Prx3 exists in terms of how these enzymes might act together in DNA repair, and it was decided that this association would not be pursued scientifically with general theme of the thesis in mind.

Another protein associated with both forms of TDP1 was importin subunit alpha-2, but much of the information available on this protein suggest that it is nuclear with no link to mitochondria to date (Ito et al., 2000, Wang et al., 2011). Although this protein may function in mitochondria in some capacity it was decided not to carry on in any attempt to find a function for this protein in mitochondria. However, a protein that is known to be mitochondrial was associated with $TDP1^{S81E}$, namely the mitochondrial single stranded DNA binding protein (mtSSB). Interestingly, this protein was not found to associate with $TDP1^{S81A}$ that may suggest phosphorylation of TDP1 at amino acid 81 facilitates the interaction between these two proteins. It may also be the case that the structure of $TDP1^{S81A}$ could be altered by this amino acid change that would then prevent its interaction with mtSSB and account for some of the differences observed in tables 6.1 and 6.2. On researching mtSSB further it has been possible to find some

interesting facts about the protein and the reasons why it may interact with TDP1 *in vivo*. This protein was identified in *Xenopus laevis* oocyte mitochondria as having a high affinity for single stranded DNA in the D-loop of the mitochondrial genome (Mignotte et al., 1985). Building on this, studies using HeLa cells found that mtSSB was present in a much greater proportion than mtDNA and was proposed to act cooperatively with TFAM in maintenance of mtDNA by enveloping this genome; thus providing stability (Takamatsu et al., 2002). More recently it has been proposed that mtSSB binding of mtDNA during replication acts as a protective measure against some of the organelles own DNA repair enzymes (Wollen Steen et al., 2012). This was suggested based on activity assays that demonstrated mtDNA repair enzymes uracil-DNA glycosylase (UNG1) NEIL1, AlkB homolog 1 (ABH1), and AP endonuclease 1 (APE1) as being unable to cleave single stranded DNA substrates with engineered damage specific for each enzyme when mtSSB was present (Wollen Steen et al., 2012, Westbye et al., 2008). However, when mtSSB was not included in these assays or the assays were performed using duplex DNA substrates with specific damage for each enzyme to repair, each enzyme was able to remove the damage that had been engineered in these substrates (Wollen Steen et al., 2012). From this the authors suggested that when mtDNA was being replicated mtSSB was bound to single stranded mtDNA, which would prevent repair enzymes from compromising the integrity of mtDNA in trying to remove any damage that was present (Wollen Steen et al., 2012). This would suggest that the damaging effects created by introducing nicks in single stranded mtDNA during replication outweighs the damaging effects that are likely to occur in the presence of these forms of lesion i.e. point mutations. With regard to TDP1 these findings imply a logical association between this enzyme and mtSSB. It would appear likely that TDP1 is sequestered by mtSSB or associates with the same substrate during mtDNA replication given that TDP1 is a single strand break repair enzyme that

is involved in resolving lesions formed by TOP1mt; also very likely to be involved in initiation of mtDNA replication.

Other mitochondrial proteins that were identified in the Co-IP with TDP1^{S81A} include estradiol 17-beta-dehydrogenase 8 (HSD17B8), acyl-coenzyme A thioesterase 9 (ACOT9), and glutaryl-CoA dehydrogenase (GCDH). From these it is GCDH that has the most data published with regard to mitochondria. This protein is involved as part of the process of degradation of lysine and tryptophan in mitochondria, and more specifically it acts as a homotetramer to catalyse the oxidative decarboxylation of glutaryl-CoA (Keyser et al., 2008). Mutations in *GCDH* can cause the autosomal recessive neurometabolic disorder glutaric aciduria type 1 (GA1) with more than 150 mutations in *GCDH* known to cause this disease (Keyser et al., 2008). As for HSD17B8 this protein was identified in having a role in the synthesis of androgens and oestrogens, and controlling their activity in mammals, but was not initially thought to be mitochondrial (Pletnev and Duax, 2005). However, it was suggested that this protein may be involved in fatty acid metabolism in mitochondria based on bioinformatics that analysed the structure and substrate specificity of the enzyme (Pletnev and Duax, 2005). Despite this publication there have been no further reports of this enzyme in mitochondria and also the link between TDP1 and fatty acid metabolism is not particularly obvious. Any link between TDP1 and GCDH is also hard to establish as there is also no obvious reason why these two proteins would associate with each other based on their known function. It may simply be the case that these proteins were found to associate with TDP1^{S81A} due to the relatively high levels of expression of this protein in mitochondria during this experiment and/or the altered structure of TDP1^{S81A} due to its amino acid change. This may also be true for ACOT9 for which there is no data to

date other than it is predicted to be mitochondrial by RefSeq based on its amino acid sequence.

The data presented in this chapter has shown that from our experiments there was no evidence to show that phosphorylation of amino acid 81 in TDP1 mediates its association with LIG3α. . However, the limitations of experimental procedures discussed in this chapter cannot give us any clear conclusions on this and so the association between TDP1 and LIG3α in mitochondria cannot be ruled out. Although this association was not found the other proteins identified from the Co-IP has opened the possibility that TDP1 may be involved in processes other than the direct repair of mtDNA. This data also implies that repair of mtDNA, or even inhibition of repair, involves an intricate interplay between several proteins suggesting the mechanisms surrounding mtDNA repair are maybe more complex than considered at this point in time.

Chapter 7. Conclusions and future perspectives

The data provided in this thesis helped to delineate the role of tyrosyl-DNA-phosphodiesterase (TDP1) in mtDNA repair. This was achieved using a variety of methods from DNA repair assays to assess the activity of TDP1 in mitochondria to protein complex immunoprecipitations to ascertain the protein associations between our enzyme of interest and others in mitochondria. The main findings from the studies carried out throughout this PhD that are outlined in this thesis include:

- Identification of TDP1 presence and activity in mitochondria of human cells and in mouse brain, which provided evidence for the activity of a novel mtDNA repair enzyme at the time of this finding.
- Evidence to suggest that mtBER is not dependent on TDP1 as was concluded by Das et al., 2010.
- Repair of mtDNA by TDP1 is most probably limited to repair of mtDNA-TOP1mt lesions.
- Based on our experiments it was not possible to determine whether phosphorylation of amino acid 81 in TDP1 mediates the interaction between this enzyme and LIG3α in mitochondria.

The identification of a novel enzyme involved in mtDNA repair that is likely not to be essential to the integrity of this genome suggests that the DNA repair mechanisms in mitochondria are more intricate than thought at the time of writing this thesis. The machinery involved in mtDNA repair is far less characterised than in the nucleus, and although it is most certainly the case that the mechanisms for nDNA repair are far more complex than in mitochondria, there is still the possibility for identification of many more repair enzymes for mtDNA.

In the coming years it may be possible to determine more factors involved in mtDNA repair and to assess the impact of mtDNA damage on downstream processes such as transcription and translation of mtDNA encoded proteins as this is a subject on which little has been reported. Also, it may be possible to expand on the current knowledge of the role of epigenetic factors on mtDNA that affect processes within mitochondria.

Although the findings in this thesis may be informative in identifying relatively new DNA repair pathways in mitochondria, there are many questions that still exist in relation to this subject. Questions such as:

- What is the exact role of mtDNA damage in ageing and disease?
- Does mtDNA contribute to the ageing process or is it merely a sign of ageing?
- To what extent does mtDNA need to be damaged, with reference to mtDNA lesions, before an impact is seen in cells?

These are just a few examples of questions that remain on the subject of mtDNA repair with many more still to be answered despite the findings in this thesis and reports in the literature from the beginning of this PhD.

To sum up, the results provided in this thesis provide knowledge on just a small section of the mtDNA repair field in which there is still much to learn. By persisting in attaining information on this subject on the molecular level it will be possible to determine how mtDNA damage impacts in ageing and disease, and from this potential advances in the treatment of patients may be obtained.

Appendix

COX/SDH histochemical optimisation
Incubation times: A= 5 mins, B= 10 mins, C= 15 mins, D= 20 mins, D= 25 mins, E= 30 mins, F= 35 mins, G= 40 mins, H= 45 mins, J= 50 mins, K= 55 mins, L= 60 mins

i) Mouse brain COX

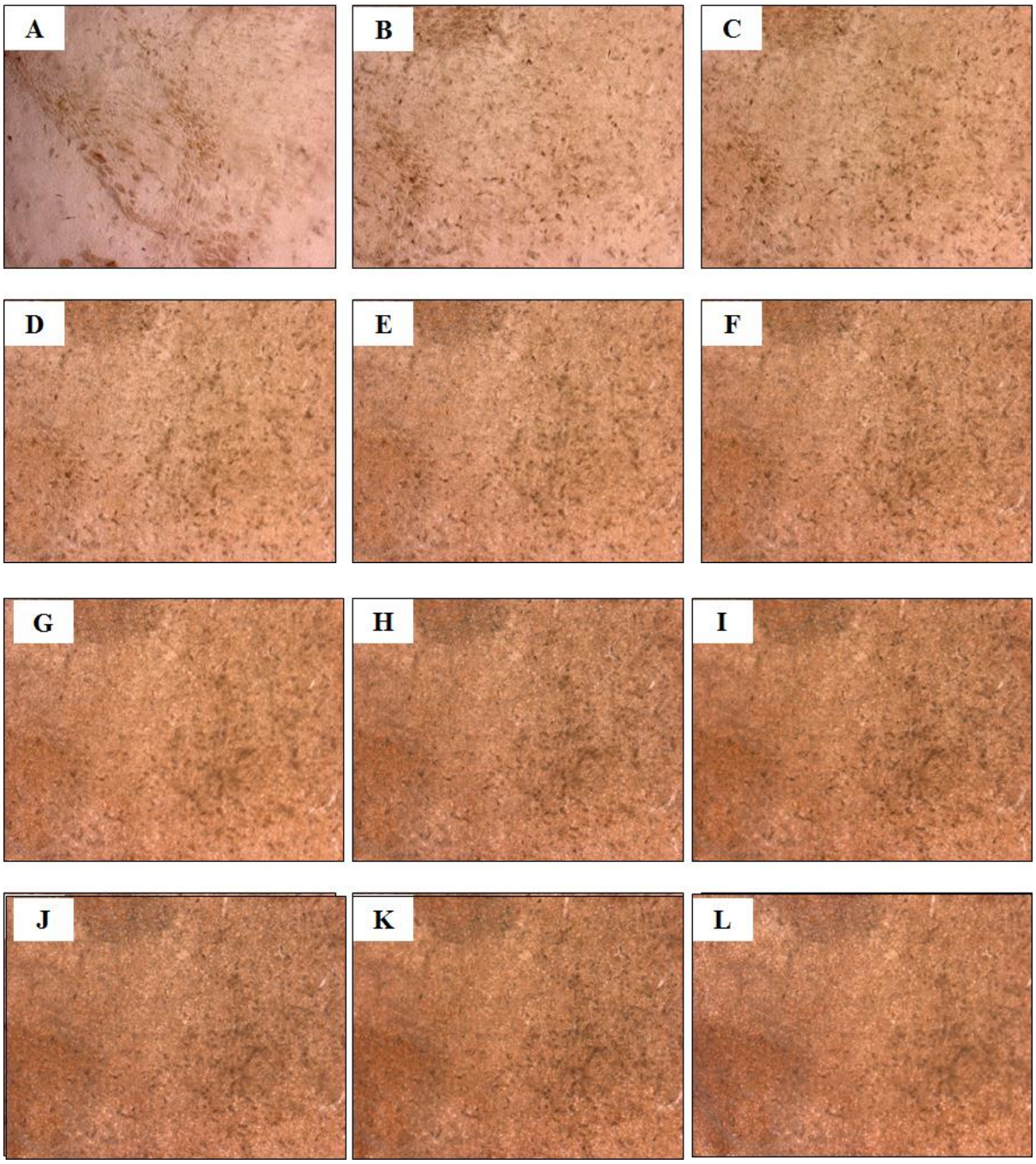

Optimal incubation time was determined by assessing the most intensely stained image before saturation occurred. In this case 35 mins (F).

Incubation times: A= 5 mins, B= 10 mins, C= 15 mins, D= 20 mins, D= 25 mins, E= 30 mins, F= 35 mins, G= 40 mins, H= 45 mins, J= 50 mins, K= 55 mins, L= 60 mins

ii) Mouse brain SDH

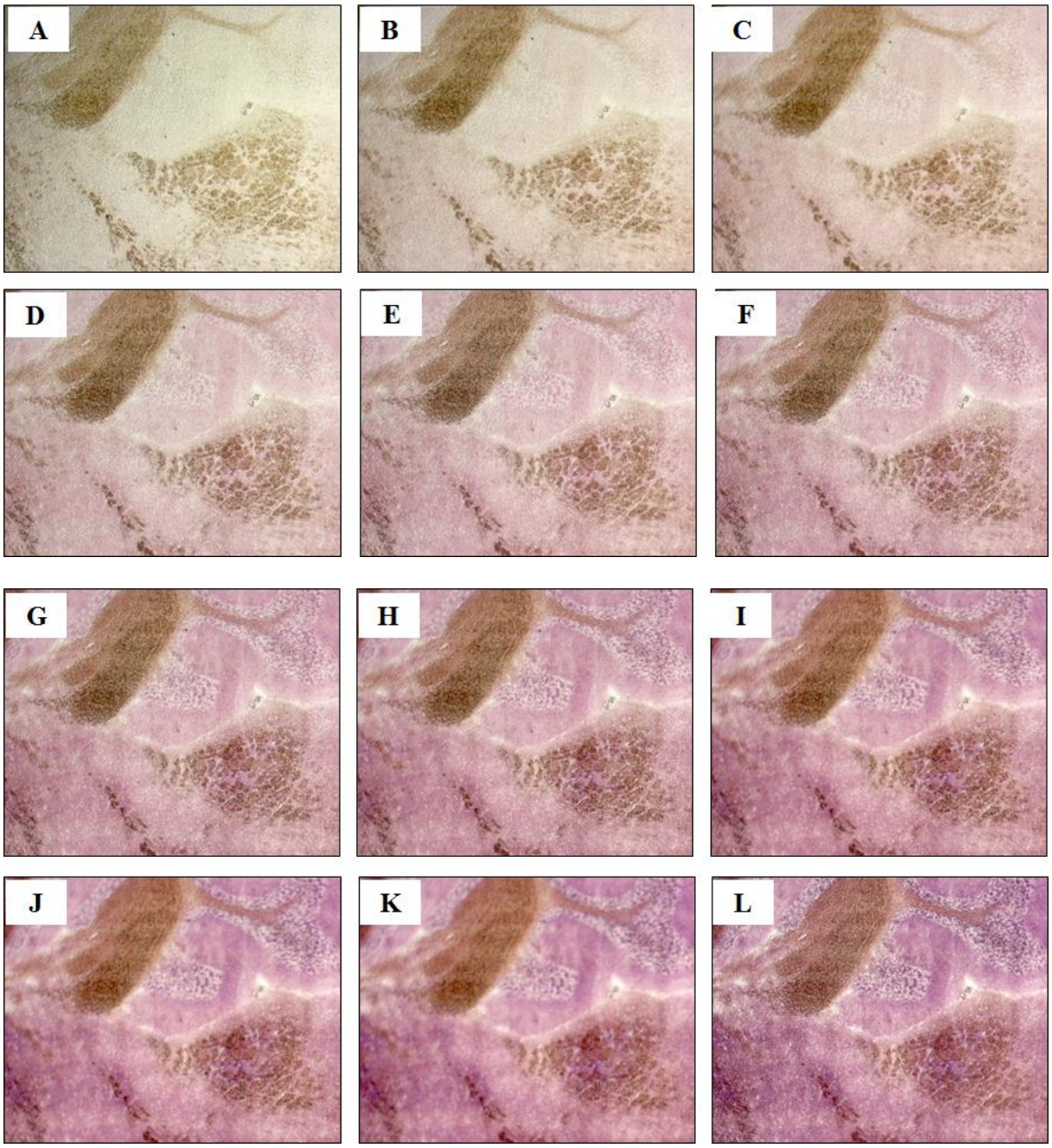

Optimal incubation time was determined by assessing the most intensely stained image before saturation occurred. In this case 40 mins (G).

Incubation times: A= 5 mins, B= 10 mins, C= 15 mins, D= 20 mins, D= 25 mins, E= 30 mins, F= 35 mins, G= 40 mins, H= 45 mins, J= 50 mins, K= 55 mins, L= 60 mins

iii) Mouse eye COX

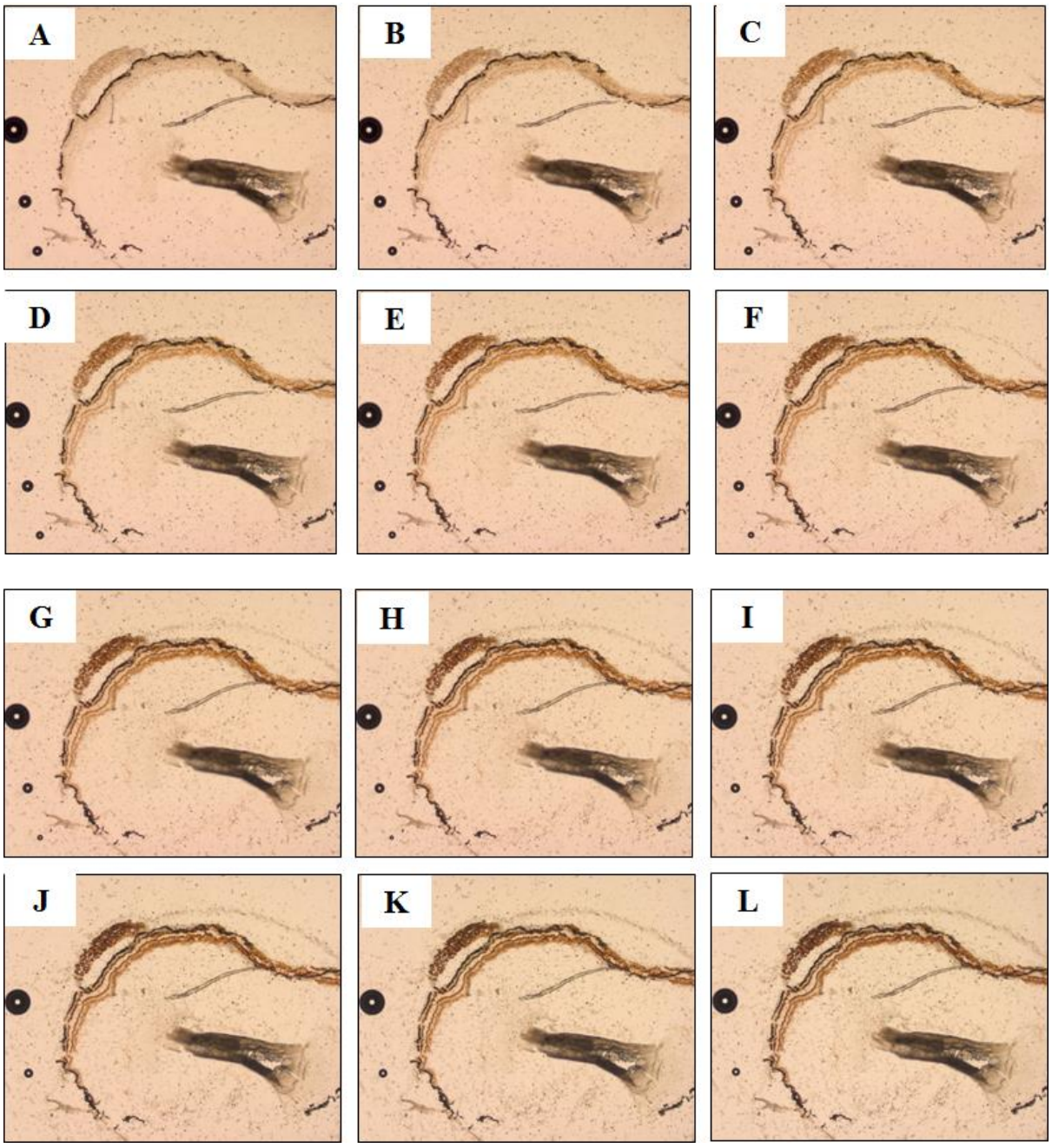

Optimal incubation time was determined by assessing the most intensely stained image before saturation occurred. In this case 30 mins (E).

Incubation times: A= 5 mins, B= 10 mins, C= 15 mins, D= 20 mins, D= 25 mins, E= 30 mins, F= 35 mins, G= 40 mins, H= 45 mins, J= 50 mins, K= 55 mins, L= 60 mins

iv) Mouse eye SDH

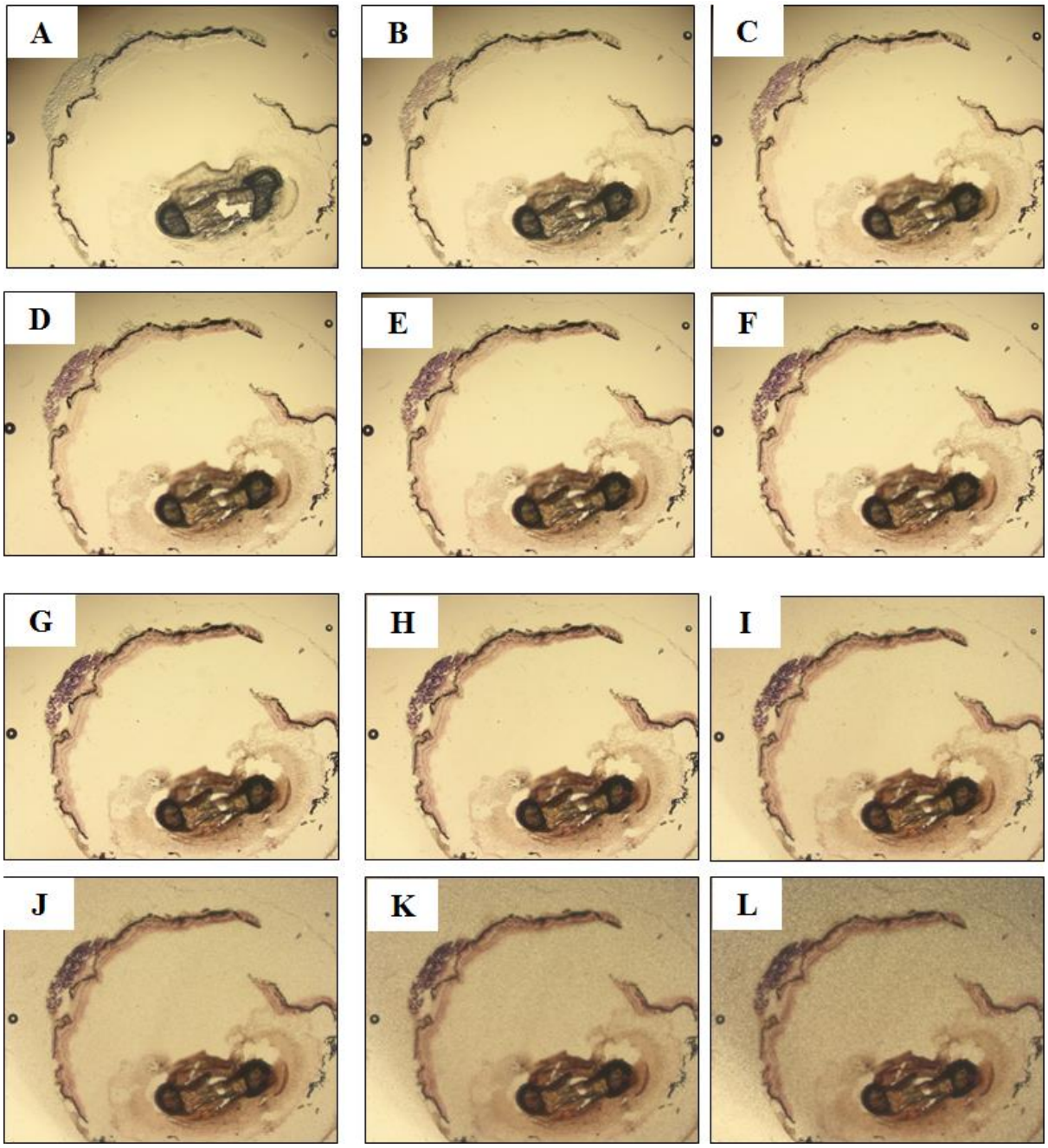

Optimal incubation time was determined by assessing the most intensely stained image before saturation occurred. In this case 35 mins (F).

v) Full data including all exponentially modified protein abundance index (emPAI) values from the Co-IP of mtLUC/FLAG, mtTDP1^{S81E}/FLAG, and mtTDP1^{S81A}/FLAG.

PROTEIN GI	PROTEIN	GENE	emPAI mtLUC/ FLAG	emPAI mtTDP1^{S81E}/ FLAG	emPAI mtTDP1^{S81A}/ FLAG
41399285	60 kDa heat shock protein, mitochondrial	HSPD1P6	50.46813857	2.025305457	1.648969288
20127586	tyrosyl-DNA phosphodiesterase 1	TDP1	0	1.94915073	1.15443469
24234688	stress-70 protein, mitochondrial precursor	HSPA9	10.15883993	1.15443469	1.077113926
83715985	3-hydroxyacyl-CoA dehydrogenase type-2 isoform 2	HSD17B10	0	0.318256739	0.737800829
50345984	ATP synthase subunit alpha, mitochondrial precursor	Atp5a1	0.865663579	0.211527659	0.467799268
91199540	dihydrolipoyl dehydrogenase, mitochondrial precursor	dld	0	0	0.333521432
156071459	ADP/ATP translocase 2	SLC25A5	0.508590709	0.279802214	0.279802214
32189394	ATP synthase subunit beta, mitochondrial precursor	ATP5B	1.187761624	0.513561248	0.258925412
32483377	thioredoxin-dependent peroxide reductase, mitochondrial isoform b	prdx3	0	0.258925412	0.258925412
295842266	3,2-trans-enoyl-CoA isomerase, mitochondrial isoform 2 precursor	ECI1	0	0	0.258925412
4504897	importin subunit alpha-2	KPNA2	0	0.637893707	0.245197085
15277342	estradiol 17-beta-dehydrogenase 8	HSD17B8	0	0	0.232846739
4501885	actin, cytoplasmic 1	ACTB	0.564748142	0.291549665	0.211527659
261862352	serine hydroxymethyltransferase, mitochondrial isoform 3	SHMT2	0.154781985	0.211527659	0.211527659
8923421	seryl-tRNA synthetase, mitochondrial isoform b precursor	SARS2	0	0	0.193776642
10337581	keratin, type I cuticular Ha3-II	KRT33B	0.052500285	0.165914401	0.165914401
188528628	polyribonucleotide nucleotidyltransferase 1, mitochondrial precursor	Pnpt1	0	0	0.14504757
189458821	protein-glutamine gamma-glutamyltransferase E precursor	TGM3	0	0	0.14280206
155722983	heat shock protein 75	Trap1	0.099248522	0.03204499	0.134473931

	kDa, mitochondrial precursor				
16507237	78 kDa glucose-regulated protein precursor	LOC400750	1.069138081	0.223824937	0.128837892
81295407	acyl-coenzyme A thioesterase 9, mitochondrial isoform a precursor	acot9	0	0	0.113042193
56549662	alpha-amylase 1 precursor	Amy1a	0	0	0.107756851
36796743	monofunctional C1-tetrahydrofolate synthase, mitochondrial precursor	MTHFD1L	0.091376715	0	0.091376715
67191208	polyubiquitin-C	UBC	0.058501208	0	0.089022962
156071462	ADP/ATP translocase 3	SLC25A6	0.44974067	0.160155302	0.077105056
70995211	delta(3,5)-Delta(2,4)-dienoyl-CoA isomerase, mitochondrial precursor	ech1	0.160155302	0	0.077105056
301897479	beta-enolase isoform 2	ENO3	0	0	0.072267222
193082993	tRNA modification GTPase GTPBP3, mitochondrial isoform III	GTPBP3	0	0	0.068000433
4503943	glutaryl-CoA dehydrogenase, mitochondrial isoform a precursor	gcdH	0	0	0.064209244
4826702	desmocollin-1 isoform Dsc1b preproprotein	DSC1	0	0	0.062467831
25777721	succinate-semialdehyde dehydrogenase, mitochondrial isoform 1 precursor	ALDH5A1	0.05776756	0.118872212	0.05776756
34147630	elongation factor Tu, mitochondrial precursor	Tufm	0.24782547	0	0.045275495
148539842	deleted in malignant brain tumors 1 protein isoform b precursor	DMBT1	0	0	0.031605178
31621305	leucine-rich PPR motif-containing protein, mitochondrial precursor	lrpprc	0.015787165	0	0.015787165
4504523	10 kDa heat shock protein, mitochondrial	HSPE1	0.232846739	0	0
24308295	grpE protein homolog 1, mitochondrial precursor	GRPEL1	0.389495494	0	0
11596859	39S ribosomal protein L17, mitochondrial precursor	MRPL17	0.136463666	0	0
6005854	prohibitin-2 isoform 2	PHB2	0.629750835	0	0
291084742	pyruvate dehydrogenase E1 component subunit alpha, somatic form, mitochondrial isoform 2	PDHA1	0.188502227	0	0

	precursor				
4757732	apoptosis-inducing factor 1, mitochondrial isoform 1 precursor	AIFM1	0.197929811	0	0
4557237	acetyl-CoA acetyltransferase, mitochondrial precursor	ACAT1	0.125335583	0	0
156564403	pyruvate dehydrogenase E1 component subunit beta, mitochondrial isoform 1 precursor	pdhB	0.417474163	0	0
4507231	single-stranded DNA-binding protein, mitochondrial precursor	SSBP1	0	0.165914401	0
13699824	kinesin-like protein KIF11	KIF11	0.065425129	0	0
4502303	ATP synthase subunit O, mitochondrial precursor	atp5o	0.232846739	0	0
4557809	ornithine aminotransferase, mitochondrial isoform 1 precursor	OAT	0.218187912	0	0
102469034	tyrosine-protein kinase JAK1	JAK1	0.110336318	0	0
193211616	protein NipSnap homolog 1	NIPSNAP1	0.100694171	0	0
31711992	dihydrolipoyllysine-residue acetyltransferase component of pyruvate dehydrogenase complex, mitochondrial precursor	dlaT	0.478465929	0	0
50345988	ATP synthase subunit gamma, mitochondrial isoform L (liver) precursor	Atp5c1	0.115883993	0	0
126635329	luciferase [Photinus pyralis] + mitochondrial targeting sequence and FLAG tag	GENE	39.23936909	0.055008148	0

References

AMEUR, A., STEWART, J. B., FREYER, C., HAGSTROM, E., INGMAN, M., LARSSON, N. G. & GYLLENSTEN, U. 2011. Ultra-deep sequencing of mouse mitochondrial DNA: mutational patterns and their origins. *PLoS Genet,* 7**,** e1002028.

ANDERSON, S., BANKIER, A. T., BARRELL, B. G., DE BRUIJN, M. H. L., COULSON, A. R., DROUIN, J., EPERON, I. C., NIERLICH, D. P., ROE, B. A., SANGER, F., SCHREIER, P. H., SMITH, A. J. H., STADEN, R. & YOUNG, I. G. 1981. Sequence and organization of the human mitochondrial genome. *Nature,* 290**,** 457-465.

ANDREWS, R. M., KUBACKA, I., CHINNERY, P. F., LIGHTOWLERS, R. N., TURNBULL, D. M. & HOWELL, N. 1999. Reanalysis and revision of the Cambridge reference sequence for human mitochondrial DNA. *Nat Genet,* 23**,** 147.

ATTARDI, G. & SCHATZ, G. 1988. Biogenesis of mitochondria. *Annu Rev Cell Biol,* 4**,** 289-333.

BACMAN, S. R., WILLIAMS, S. L. & MORAES, C. T. 2009. Intra- and inter-molecular recombination of mitochondrial DNA after in vivo induction of multiple double-strand breaks. *Nucleic Acids Res,* 37**,** 4218-26.

BAROT, M., GOKULGANDHI, M. R. & MITRA, A. K. 2011. Mitochondrial dysfunction in retinal diseases. *Curr Eye Res,* 36**,** 1069-77.

BATISTA, L. F., KAINA, B., MENEGHINI, R. & MENCK, C. F. 2009. How DNA lesions are turned into powerful killing structures: insights from UV-induced apoptosis. *Mutat Res,* 681**,** 197-208.

BECKER, T., BOTTINGER, L. & PFANNER, N. 2012. Mitochondrial protein import: from transport pathways to an integrated network. *Trends Biochem Sci,* 37**,** 85-91.

BENDER, A., KRISHNAN, K. J., MORRIS, C. M., TAYLOR, G. A., REEVE, A. K., PERRY, R. H., JAROS, E., HERSHESON, J. S., BETTS, J., KLOPSTOCK, T., TAYLOR, R. W. & TURNBULL, D. M. 2006. High levels of mitochondrial DNA deletions in substantia nigra neurons in aging and Parkinson disease. *Nat Genet,* 38**,** 515-7.

BERK, A. J. & CLAYTON, D. A. 1974. Mechanism of mitochondrial DNA replication in mouse L-cells: asynchronous replication of strands, segregation of circular daughter molecules, aspects of topology and turnover of an initiation sequence. *J Mol Biol,* 86**,** 801-24.

BIBB, M. J., VAN ETTEN, R. A., WRIGHT, C. T., WALBERG, M. W. & CLAYTON, D. A. 1981a. Sequence and gene organization of mouse mitochondrial DNA. *Cell,* 26**,** 167-180.

BIBB, M. J., VAN ETTEN, R. A., WRIGHT, C. T., WALBERG, M. W. & CLAYTON, D. A. 1981b. Sequence and gene organization of mouse mitochondrial DNA. *Cell,* 26**,** 167-80.

BOESCH, P., WEBER-LOTFI, F., IBRAHIM, N., TARASENKO, V., COSSET, A., PAULUS, F., LIGHTOWLERS, R. N. & DIETRICH, A. 2011. DNA repair in organelles: Pathways, organization, regulation, relevance in disease and aging. *Biochimica et Biophysica Acta (BBA) - Molecular Cell Research,* 1813**,** 186-200.

BOGENHAGEN, D. F. 1999. Repair of mtDNA in vertebrates. *Am J Hum Genet,* 64**,** 1276-81.

BOLENDER, N., SICKMANN, A., WAGNER, R., MEISINGER, C. & PFANNER, N. 2008. Multiple pathways for sorting mitochondrial precursor proteins. *EMBO Rep,* 9**,** 42-9.

BONAWITZ, N. D. & SHADEL, G. S. 2007. Rethinking the mitochondrial theory of aging: the role of mitochondrial gene expression in lifespan determination. *Cell Cycle,* 6**,** 1574-8.

BOWMAKER, M., YANG, M. Y., YASUKAWA, T., REYES, A., JACOBS, H. T., HUBERMAN, J. A. & HOLT, I. J. 2003. Mammalian mitochondrial DNA replicates bidirectionally from an initiation zone. *J Biol Chem,* 278**,** 50961-9.

BRAND, M. D. 2010. The sites and topology of mitochondrial superoxide production. *Exp Gerontol,* 45**,** 466-72.

BURNEY, S., CAULFIELD, J. L., NILES, J. C., WISHNOK, J. S. & TANNENBAUM, S. R. 1999. The chemistry of DNA damage from nitric oxide and peroxynitrite. *Mutat Res,* 424**,** 37-49.

CALDECOTT, K. W. 2008. Single-strand break repair and genetic disease. *Nat Rev Genet,* 9**,** 619-31.

CAPALDI, R. A. 1990. Structure and function of cytochrome c oxidase. *Annu Rev Biochem,* 59**,** 569-96.

CEBALLOS, M. & VIOQUE, A. 2007. tRNase Z. *Protein Pept Lett,* 14**,** 137-45.

CHAE, H. Z., KIM, H. J., KANG, S. W. & RHEE, S. G. 1999. Characterization of three isoforms of mammalian peroxiredoxin that reduce peroxides in the presence of thioredoxin. *Diabetes Res Clin Pract,* 45**,** 101-12.

CHANG, T. S., CHO, C. S., PARK, S., YU, S., KANG, S. W. & RHEE, S. G. 2004. Peroxiredoxin III, a mitochondrion-specific peroxidase, regulates apoptotic signaling by mitochondria. *J Biol Chem,* 279**,** 41975-84.

CHAUDIERE, J. & FERRARI-ILIOU, R. 1999. Intracellular antioxidants: from chemical to biochemical mechanisms. *Food Chem Toxicol,* 37**,** 949-62.

CHEN, H. & CHAN, D. C. 2005. Emerging functions of mammalian mitochondrial fusion and fission. *Hum Mol Genet,* 14 Spec No. 2**,** R283-9.

CHIANG, S. C., CARROLL, J. & EL-KHAMISY, S. F. 2010. TDP1 serine 81 promotes interaction with DNA ligase IIIalpha and facilitates cell survival following DNA damage. *Cell Cycle,* 9**,** 588-595.

CLAYTON, D. A., DODA, J. N. & FRIEDBERG, E. C. 1974. The absence of a pyrimidine dimer repair mechanism in mammalian mitochondria. *Proc Natl Acad Sci U S A,* 71**,** 2777-81.

CLINE, S. D. 2012. Mitochondrial DNA damage and its consequences for mitochondrial gene expression. *Biochim Biophys Acta,* 1819**,** 979-91.

COLBEAU, A., NACHBAUR, J. & VIGNAIS, P. M. 1971. Enzymic characterization and lipid composition of rat liver subcellular membranes. *Biochim Biophys Acta,* 249**,** 462-92.

CORTES LEDESMA, F., EL KHAMISY, S. F., ZUMA, M. C., OSBORN, K. & CALDECOTT, K. W. 2009. A human 5'-tyrosyl DNA phosphodiesterase that repairs topoisomerase-mediated DNA damage. *Nature,* 461**,** 674-8.

CRAMER, W. A., HASAN, S. S. & YAMASHITA, E. 2011. The Q cycle of cytochrome bc complexes: a structure perspective. *Biochim Biophys Acta,* 1807**,** 788-802.

CROSBY, A. H., PATEL, H., CHIOZA, B. A., PROUKAKIS, C., GURTZ, K., PATTON, M. A., SHARIFI, R., HARLALKA, G., SIMPSON, M. A., DICK, K., REED, J. A., AL-MEMAR, A., CHRZANOWSKA-LIGHTOWLERS, Z. M., CROSS, H. E. & LIGHTOWLERS, R. N. 2010. Defective mitochondrial mRNA maturation is associated with spastic ataxia. *Am J Hum Genet,* 87**,** 655-60.

DALLA ROSA, I., GOFFART, S., WURM, M., WIEK, C., ESSMANN, F., SOBEK, S., SCHROEDER, P., ZHANG, H., KRUTMANN, J., HANENBERG, H., SCHULZE-OSTHOFF, K., MIELKE, C., POMMIER, Y., BOEGE, F. & CHRISTENSEN, M. O. 2009. Adaptation of topoisomerase I paralogs to nuclear and mitochondrial DNA. *Nucleic Acids Res,* 37**,** 6414-28.

DAS, B. B., DEXHEIMER, T. S., MADDALI, K. & POMMIER, Y. 2010. Role of tyrosyl-DNA phosphodiesterase (TDP1) in mitochondria. *Proc Natl Acad Sci U S A,* 107**,** 19790-5.

DAVIES, D. R., INTERTHAL, H., CHAMPOUX, J. J. & HOL, W. G. 2002a. Insights into substrate binding and catalytic mechanism of human tyrosyl-DNA phosphodiesterase (Tdp1) from vanadate and tungstate-inhibited structures. *J Mol Biol,* 324**,** 917-32.

DAVIES, D. R., INTERTHAL, H., CHAMPOUX, J. J. & HOL, W. G. J. 2002b. The Crystal Structure of Human Tyrosyl-DNA Phosphodiesterase, Tdp1. *Structure (London, England : 1993),* 10**,** 237-248.

DE SOUZA-PINTO, N. C., EIDE, L., HOGUE, B. A., THYBO, T., STEVNSNER, T., SEEBERG, E., KLUNGLAND, A. & BOHR, V. A. 2001. Repair of 8-oxodeoxyguanosine lesions in mitochondrial dna depends on the oxoguanine dna glycosylase (OGG1) gene and 8-oxoguanine accumulates in the mitochondrial dna of OGG1-defective mice. *Cancer Res,* 61**,** 5378-81.

DE SOUZA-PINTO, N. C., MASON, P. A., HASHIGUCHI, K., WEISSMAN, L., TIAN, J., GUAY, D., LEBEL, M., STEVNSNER, T. V., RASMUSSEN, L. J. & BOHR, V. A. 2009. Novel DNA mismatch-repair activity involving YB-1 in human mitochondria. *DNA Repair (Amst),* 8**,** 704-19.

DEBETHUNE, L., KOHLHAGEN, G., GRANDAS, A. & POMMIER, Y. 2002. Processing of nucleopeptides mimicking the topoisomerase I-DNA covalent complex by tyrosyl-DNA phosphodiesterase. *Nucleic Acids Res,* 30**,** 1198-204.

DIZDAROGLU, M., JARUGA, P., BIRINCIOGLU, M. & RODRIGUEZ, H. 2002. Free radical-induced damage to DNA: mechanisms and measurement. *Free Radic Biol Med,* 32**,** 1102-15.

EFREMOV, R. G. & SAZANOV, L. A. 2012. The coupling mechanism of respiratory complex I - a structural and evolutionary perspective. *Biochim Biophys Acta,* 1817**,** 1785-95.

EL-KHAMISY, S. F., KATYAL, S., PATEL, P., JU, L., MCKINNON, P. J. & CALDECOTT, K. W. 2009. Synergistic decrease of DNA single-strand break repair rates in mouse neural cells lacking both Tdp1 and aprataxin. *DNA Repair (Amst),* 8**,** 760-6.

EL-KHAMISY, S. F., SAIFI, G. M., WEINFELD, M., JOHANSSON, F., HELLEDAY, T., LUPSKI, J. R. & CALDECOTT, K. W. 2005. Defective DNA single-strand break repair in spinocerebellar ataxia with axonal neuropathy-1. *Nature,* 434**,** 108-113.

ESTERBAUER, H., SCHAUR, R. J. & ZOLLNER, H. 1991. Chemistry and biochemistry of 4-hydroxynonenal, malonaldehyde and related aldehydes. *Free Radic Biol Med,* 11**,** 81-128.

EVANS, D., MARQUEZ, S. M. & PACE, N. R. 2006. RNase P: interface of the RNA and protein worlds. *Trends Biochem Sci,* 31**,** 333-41.

EVANS, M. D., DIZDAROGLU, M. & COOKE, M. S. 2004. Oxidative DNA damage and disease: induction, repair and significance. *Mutat Res,* 567**,** 1-61.

FAIRFIELD, F. R., BAUER, W. R. & SIMPSON, M. V. 1979. Mitochondria contain a distinct DNA topoisomerase. *J Biol Chem,* 254**,** 9352-4.

FALKENBERG, M., GASPARI, M., RANTANEN, A., TRIFUNOVIC, A., LARSSON, N. G. & GUSTAFSSON, C. M. 2002. Mitochondrial transcription factors B1 and B2 activate transcription of human mtDNA. *Nat Genet,* 31**,** 289-94.

FALKENBERG, M., LARSSON, N. G. & GUSTAFSSON, C. M. 2007. DNA replication and transcription in mammalian mitochondria. *Annu Rev Biochem,* 76**,** 679-99.

FARAH, C. A., LINDEMAN, A. A., SIU, V., GUPTA, M. D. & SOSSIN, W. S. 2012. Autophosphorylation of the c2 domain inhibits translocation of the novel protein kinase c (npkc) apl ii. *J Neurochem.*

FOYER, C. H. & NOCTOR, G. 2009. Redox regulation in photosynthetic organisms: signaling, acclimation, and practical implications. *Antioxid Redox Signal,* 11**,** 861-905.

FUKUI, H. & MORAES, C. T. 2009. Mechanisms of formation and accumulation of mitochondrial DNA deletions in aging neurons. *Hum Mol Genet,* 18**,** 1028-36.

GAO, Y., KATYAL, S., LEE, Y., ZHAO, J., REHG, J. E., RUSSELL, H. R. & MCKINNON, P. J. 2011. DNA ligase III is critical for mtDNA integrity but not Xrcc1-mediated nuclear DNA repair. *Nature,* 471**,** 240-4.

GEGG, M. E. & SCHAPIRA, A. H. 2011. PINK1-parkin-dependent mitophagy involves ubiquitination of mitofusins 1 and 2: Implications for Parkinson disease pathogenesis. *Autophagy,* 7**,** 243-5.

GERMAIN, M., MATHAI, J. P., MCBRIDE, H. M. & SHORE, G. C. 2005. Endoplasmic reticulum BIK initiates DRP1-regulated remodelling of mitochondrial cristae during apoptosis. *EMBO J,* 24**,** 1546-56.

GRAY, M. W., BURGER, G. & LANG, B. F. 1999. Mitochondrial evolution. *Science,* 283**,** 1476-81.

HACKENBROCK, C. R. 1966. Ultrastructural bases for metabolically linked mechanical activity in mitochondria. I. Reversible ultrastructural changes with change in metabolic steady state in isolated liver mitochondria. *J Cell Biol,* 30**,** 269-97.

HAGERHALL, C. 1997. Succinate: quinone oxidoreductases. Variations on a conserved theme. *Biochim Biophys Acta,* 1320**,** 107-41.

HALLBERG, B. M. & LARSSON, N. G. 2011. TFAM forces mtDNA to make a U-turn. *Nat Struct Mol Biol,* 18**,** 1179-81.

HALLIWELL, B. & GUTTERIDGE, J. M. 1984. Free radicals, lipid peroxidation, and cell damage. *Lancet,* 2**,** 1095.

HARMAN, D. 1956. Aging: a theory based on free radical and radiation chemistry. *J Gerontol,* 11**,** 298-300.

HEGDE, M. L., MANTHA, A. K., HAZRA, T. K., BHAKAT, K. K., MITRA, S. & SZCZESNY, B. 2012. Oxidative genome damage and its repair: implications in aging and neurodegenerative diseases. *Mech Ageing Dev,* 133**,** 157-68.

HEIDE, H., BLEIER, L., STEGER, M., ACKERMANN, J., DROSE, S., SCHWAMB, B., ZORNIG, M., REICHERT, A. S., KOCH, I., WITTIG, I. & BRANDT, U. 2012. Complexome profiling identifies TMEM126B as a component of the mitochondrial complex I assembly complex. *Cell Metab,* 16**,** 538-49.

HENZE, K. & MARTIN, W. 2003. Evolutionary biology: essence of mitochondria. *Nature,* 426**,** 127-8.

HIRANO, T. 2008. Repair system of 7, 8-dihydro-8-oxoguanine as a defense line against carcinogenesis. *J Radiat Res,* 49**,** 329-40.

HIRST, J. 2005. Energy transduction by respiratory complex I--an evaluation of current knowledge. *Biochem Soc Trans,* 33**,** 525-9.

HOFHAUS, G., WEISS, H. & LEONARD, K. 1991. Electron microscopic analysis of the peripheral and membrane parts of mitochondrial NADH dehydrogenase (complex I). *J Mol Biol,* 221**,** 1027-43.

HOLT, I. J., LORIMER, H. E. & JACOBS, H. T. 2000. Coupled leading- and lagging-strand synthesis of mammalian mitochondrial DNA. *Cell,* 100**,** 515-24.

HOLZMANN, J., FRANK, P., LOFFLER, E., BENNETT, K. L., GERNER, C. & ROSSMANITH, W. 2008. RNase P without RNA: identification and functional reconstitution of the human mitochondrial tRNA processing enzyme. *Cell,* 135**,** 462-74.

HOPPINS, S., LACKNER, L. & NUNNARI, J. 2007. The machines that divide and fuse mitochondria. *Annu Rev Biochem,* 76**,** 751-80.

HOWELL, N., ELSON, J. L., CHINNERY, P. F. & TURNBULL, D. M. 2005. mtDNA mutations and common neurodegenerative disorders. *Trends Genet,* 21**,** 583-6.

HSIEH, P. & YAMANE, K. 2008. DNA mismatch repair: molecular mechanism, cancer, and ageing. *Mech Ageing Dev,* 129**,** 391-407.

INAMDAR, K. V., POULIOT, J. J., ZHOU, T., LEES-MILLER, S. P., RASOULI-NIA, A. & POVIRK, L. F. 2002. Conversion of phosphoglycolate to phosphate termini on 3' overhangs of DNA double strand breaks by the human tyrosyl-DNA phosphodiesterase hTdp1. *J Biol Chem,* 277**,** 27162-8.

INTERTHAL, H., CHEN, H. J. & CHAMPOUX, J. J. 2005. Human Tdp1 cleaves a broad spectrum of substrates, including phosphoamide linkages. *J Biol Chem,* 280**,** 36518-28.

INTERTHAL, H., POULIOT, J. J. & CHAMPOUX, J. J. 2001. The tyrosyl-DNA phosphodiesterase Tdp1 is a member of the phospholipase D superfamily. *Proc Natl Acad Sci U S A,* 98**,** 12009-14.

ITO, S., IKEDA, M., KATO, N., MATSUMOTO, A., ISHIKAWA, Y., KUMAKUBO, S. & YANAGI, K. 2000. Epstein-barr virus nuclear antigen-1 binds to nuclear transporter karyopherin alpha1/NPI-1 in addition to karyopherin alpha2/Rch1. *Virology,* 266**,** 110-9.

JANG, Y. C. & REMMEN, V. H. 2009. The mitochondrial theory of aging: insight from transgenic and knockout mouse models. *Exp Gerontol,* 44**,** 256-60.

KAMIYA, H. & KASAI, H. 1995. Formation of 2-hydroxydeoxyadenosine triphosphate, an oxidatively damaged nucleotide, and its incorporation by DNA polymerases. Steady-state kinetics of the incorporation. *J Biol Chem,* 270**,** 19446-50.

KANG, D., NISHIDA, J., IYAMA, A., NAKABEPPU, Y., FURUICHI, M., FUJIWARA, T., SEKIGUCHI, M. & TAKESHIGE, K. 1995. Intracellular localization of 8-oxo-dGTPase in human cells, with special reference to the role of the enzyme in mitochondria. *J Biol Chem,* 270**,** 14659-65.

KARAHALIL, B., DE SOUZA-PINTO, N. C., PARSONS, J. L., ELDER, R. H. & BOHR, V. A. 2003. Compromised incision of oxidized pyrimidines in liver mitochondria of mice deficient in NTH1 and OGG1 glycosylases. *J Biol Chem,* 278**,** 33701-7.

KASAMATSU, H., ROBBERSON, D. L. & VINOGRAD, J. 1971. A novel closed-circular mitochondrial DNA with properties of a replicating intermediate. *Proc Natl Acad Sci U S A,* 68**,** 2252-7.

KATYAL, S., EL-KHAMISY, S. F., RUSSELL, H. R., LI, Y., JU, L., CALDECOTT, K. W. & MCKINNON, P. J. 2007. TDP1 facilitates chromosomal single-strand break repair in neurons and is neuroprotective in vivo. *EMBO J,* 26**,** 4720-4731.

KEYSER, B., MUHLHAUSEN, C., DICKMANNS, A., CHRISTENSEN, E., MUSCHOL, N., ULLRICH, K. & BRAULKE, T. 2008. Disease-causing missense mutations affect enzymatic activity, stability and oligomerization of glutaryl-CoA dehydrogenase (GCDH). *Hum Mol Genet,* 17**,** 3854-63.

KIL, I. S., LEE, S. K., RYU, K. W., WOO, H. A., HU, M. C., BAE, S. H. & RHEE, S. G. 2012. Feedback control of adrenal steroidogenesis via H2O2-dependent, reversible inactivation of peroxiredoxin III in mitochondria. *Mol Cell,* 46**,** 584-94.

KINOSITA, K., JR. 2012. F(1)-ATPase: a prototypical rotary molecular motor. *Adv Exp Med Biol,* 726**,** 5-16.

KONOVALOVA, S. & TYYNISMAA, H. 2013. Mitochondrial aminoacyl-tRNA synthetases in human disease. *Mol Genet Metab,* 108**,** 206-11.

KOSTER, D. A., CROQUETTE, V., DEKKER, C., SHUMAN, S. & DEKKER, N. H. 2005. Friction and torque govern the relaxation of DNA supercoils by eukaryotic topoisomerase IB. *Nature,* 434**,** 671-4.

KRISHNAN, K. J., GREAVES, L. C., REEVE, A. K. & TURNBULL, D. 2007. The ageing mitochondrial genome. *Nucleic Acids Res,* 35**,** 7399-405.

KRUSE, B., NARASIMHAN, N. & ATTARDI, G. 1989. Termination of transcription in human mitochondria: identification and purification of a DNA binding protein factor that promotes termination. *Cell,* 58**,** 391-7.

KUKAT, C., WURM, C. A., SPAHR, H., FALKENBERG, M., LARSSON, N. G. & JAKOBS, S. 2011. Super-resolution microscopy reveals that mammalian mitochondrial nucleoids have a uniform size and frequently contain a single copy of mtDNA. *Proc Natl Acad Sci U S A,* 108**,** 13534-9.

LAKSHMIPATHY, U. & CAMPBELL, C. 1999a. Double strand break rejoining by mammalian mitochondrial extracts. *Nucleic Acids Res,* 27**,** 1198-204.

LAKSHMIPATHY, U. & CAMPBELL, C. 1999b. The human DNA ligase III gene encodes nuclear and mitochondrial proteins. *Mol Cell Biol,* 19**,** 3869-76.

LARSSON, N. G. 2010. Somatic mitochondrial DNA mutations in mammalian aging. *Annu Rev Biochem,* 79**,** 683-706.

LAX, N. Z., HEPPLEWHITE, P. D., REEVE, A. K., NESBITT, V., MCFARLAND, R., JAROS, E., TAYLOR, R. W. & TURNBULL, D. M. 2012. Cerebellar ataxia in patients with mitochondrial DNA disease: a molecular clinicopathological study. *J Neuropathol Exp Neurol,* 71**,** 148-61.

LEE, S. R., KIM, J. R., KWON, K. S., YOON, H. W., LEVINE, R. L., GINSBURG, A. & RHEE, S. G. 1999. Molecular cloning and characterization of a mitochondrial selenocysteine-containing thioredoxin reductase from rat liver. *J Biol Chem,* 274**,** 4722-34.

LEMARIE, A. & GRIMM, S. 2011. Mitochondrial respiratory chain complexes: apoptosis sensors mutated in cancer? *Oncogene,* 30**,** 3985-4003.

LI, M. X., WANG, D., ZHONG, Z. Y., XIANG, D. B., LI, Z. P., XIE, J. Y., YANG, Z. Z., JIN, F. & QING, Y. 2008. Targeting truncated APE1 in mitochondria enhances cell survival after oxidative stress. *Free Radic Biol Med,* 45**,** 592-601.

LIU, C., POULIOT, J. J. & NASH, H. A. 2002. Repair of topoisomerase I covalent complexes in the absence of the tyrosyl-DNA phosphodiesterase Tdp1. *Proc Natl Acad Sci U S A,* 99**,** 14970-5.

LIU, L., LI, Y., LI, S., HU, N., HE, Y., PONG, R., LIN, D., LU, L. & LAW, M. 2012. Comparison of next-generation sequencing systems. *J Biomed Biotechnol,* 2012**,** 251364.

LIU, L. F., LIU, C. C. & ALBERTS, B. M. 1980. Type II DNA topoisomerases: enzymes that can unknot a topologically knotted DNA molecule via a reversible double-strand break. *Cell,* 19**,** 697-707.

LIU, P. & DEMPLE, B. 2010. DNA repair in mammalian mitochondria: Much more than we thought? *Environ Mol Mutagen,* 51**,** 417-26.

LIU, P., QIAN, L., SUNG, J. S., DE SOUZA-PINTO, N. C., ZHENG, L., BOGENHAGEN, D. F., BOHR, V. A., WILSON, D. M., 3RD, SHEN, B. & DEMPLE, B. 2008. Removal of oxidative DNA damage via FEN1-dependent long-patch base excision repair in human cell mitochondria. *Mol Cell Biol,* 28**,** 4975-87.

MANNELLA, C. A., PFEIFFER, D. R., BRADSHAW, P. C., MORARU, II, SLEPCHENKO, B., LOEW, L. M., HSIEH, C. E., BUTTLE, K. & MARKO, M. 2001. Topology of the mitochondrial inner membrane: dynamics and bioenergetic implications. *IUBMB Life,* 52**,** 93-100.

MARGULIS, L. 1996. Archaeal-eubacterial mergers in the origin of Eukarya: phylogenetic classification of life. *Proc Natl Acad Sci U S A,* 93**,** 1071-6.

MARTIN, L. J. 2012. Biology of mitochondria in neurodegenerative diseases. *Prog Mol Biol Transl Sci,* 107**,** 355-415.

MASON, P. A. & LIGHTOWLERS, R. N. 2003. Why do mammalian mitochondria possess a mismatch repair activity? *FEBS Lett,* 554**,** 6-9.

MASON, P. A., MATHESON, E. C., HALL, A. G. & LIGHTOWLERS, R. N. 2003. Mismatch repair activity in mammalian mitochondria. *Nucleic Acids Res,* 31**,** 1052-8.

MCCULLOCH, V., SEIDEL-ROGOL, B. L. & SHADEL, G. S. 2002. A human mitochondrial transcription factor is related to RNA adenine methyltransferases and binds S-adenosylmethionine. *Mol Cell Biol,* 22**,** 1116-25.

MIGNOTTE, B., BARAT, M. & MOUNOLOU, J. C. 1985. Characterization of a mitochondrial protein binding to single-stranded DNA. *Nucleic Acids Res,* 13**,** 1703-16.

MITCHELL, P. 1975. Protonmotive redox mechanism of the cytochrome b-c1 complex in the respiratory chain: protonmotive ubiquinone cycle. *FEBS Lett,* 56**,** 1-6.

MITCHELL, P. 1976. Possible molecular mechanisms of the protonmotive function of cytochrome systems. *J Theor Biol,* 62**,** 327-67.

MITRA, S., IZUMI, T., BOLDOGH, I., BHAKAT, K. K., CHATTOPADHYAY, R. & SZCZESNY, B. 2007. Intracellular trafficking and regulation of mammalian AP-endonuclease 1 (APE1), an essential DNA repair protein. *DNA Repair (Amst),* 6**,** 461-9.

MONTOYA, J., OJALA, D. & ATTARDI, G. 1981. Distinctive features of the 5'-terminal sequences of the human mitochondrial mRNAs. *Nature,* 290**,** 465-70.

MU, J. J., WANG, Y., LUO, H., LENG, M., ZHANG, J., YANG, T., BESUSSO, D., JUNG, S. Y. & QIN, J. 2007. A proteomic analysis of ataxia telangiectasia-mutated (ATM)/ATM-Rad3-related (ATR) substrates identifies the ubiquitin-proteasome system as a regulator for DNA damage checkpoints. *J Biol Chem,* 282**,** 17330-4.

MULKIDJANIAN, A. Y. 2010. Activated Q-cycle as a common mechanism for cytochrome bc1 and cytochrome b6f complexes. *Biochim Biophys Acta,* 1797**,** 1858-68.

MYERS, K. A., SAFFHILL, R. & O'CONNOR, P. J. 1988. Repair of alkylated purines in the hepatic DNA of mitochondria and nuclei in the rat. *Carcinogenesis,* 9**,** 285-92.

NAKABEPPU, Y. 2001a. Molecular genetics and structural biology of human MutT homolog, MTH1. *Mutat Res,* 477**,** 59-70.

NAKABEPPU, Y. 2001b. Regulation of intracellular localization of human MTH1, OGG1, and MYH proteins for repair of oxidative DNA damage. *Prog Nucleic Acid Res Mol Biol,* 68**,** 75-94.

NILSEN, H., OTTERLEI, M., HAUG, T., SOLUM, K., NAGELHUS, T. A., SKORPEN, F. & KROKAN, H. E. 1997. Nuclear and mitochondrial uracil-DNA glycosylases are generated by alternative splicing and transcription from different positions in the UNG gene. *Nucleic Acids Res,* 25**,** 750-5.

NOJI, H., YASUDA, R., YOSHIDA, M. & KINOSITA, K., JR. 1997. Direct observation of the rotation of F1-ATPase. *Nature,* 386**,** 299-302.

O'ROURKE, B., VAN EYK, J. E. & FOSTER, D. B. 2011. Mitochondrial protein phosphorylation as a regulatory modality: implications for mitochondrial dysfunction in heart failure. *Congest Heart Fail,* 17**,** 269-82.

OHNO, M., OKA, S. & NAKABEPPU, Y. 2009. Quantitative analysis of oxidized guanine, 8-oxoguanine, in mitochondrial DNA by immunofluorescence method. *Methods Mol Biol,* 554**,** 199-212.

OJALA, D., MONTOYA, J. & ATTARDI, G. 1981. tRNA punctuation model of RNA processing in human mitochondria. *Nature,* 290**,** 470-4.

OLD, S. L. & JOHNSON, M. A. 1989. Methods of microphotometric assay of succinate dehydrogenase and cytochrome c oxidase activities for use on human skeletal muscle. *Histochem J,* 21**,** 545-55.

OTTERLEI, M., HAUG, T., NAGELHUS, T. A., SLUPPHAUG, G., LINDMO, T. & KROKAN, H. E. 1998. Nuclear and mitochondrial splice forms of human uracil-DNA glycosylase contain a complex nuclear localisation signal and a strong classical mitochondrial localisation signal, respectively. *Nucleic Acids Res,* 26**,** 4611-7.

PALADE, G. E. 1952. The fine structure of mitochondria. *Anat Rec,* 114**,** 427-51.

PALADE, G. E. 1953. An electron microscope study of the mitochondrial structure. *J Histochem Cytochem,* 1**,** 188-211.

PALMER, C. S., OSELLAME, L. D., STOJANOVSKI, D. & RYAN, M. T. 2011. The regulation of mitochondrial morphology: intricate mechanisms and dynamic machinery. *Cell Signal,* 23**,** 1534-45.

PAPA, S., MARTINO, P. L., CAPITANIO, G., GABALLO, A., DE RASMO, D., SIGNORILE, A. & PETRUZZELLA, V. 2012. The oxidative phosphorylation system in mammalian mitochondria. *Adv Exp Med Biol,* 942**,** 3-37.

PARK, C. B. & LARSSON, N. G. 2011. Mitochondrial DNA mutations in disease and aging. *J Cell Biol,* 193**,** 809-18.

PEPIO, A. M. & SOSSIN, W. S. 2001. Membrane translocation of novel protein kinase Cs is regulated by phosphorylation of the C2 domain. *J Biol Chem,* 276**,** 3846-55.

PLETNEV, V. Z. & DUAX, W. L. 2005. Rational proteomics IV: modeling the primary function of the mammalian 17beta-hydroxysteroid dehydrogenase type 8. *J Steroid Biochem Mol Biol,* 94**,** 327-35.

PLO, I., LIAO, Z. Y., BARCELO, J. M., KOHLHAGEN, G., CALDECOTT, K. W., WEINFELD, M. & POMMIER, Y. 2003. Association of XRCC1 and tyrosyl DNA phosphodiesterase (Tdp1) for the repair of topoisomerase I-mediated DNA lesions. *DNA Repair (Amst),* 2**,** 1087-100.

RABINOWITZ, M., SINCLAIR, J., DESALLE, L., HASELKORN, R. & SWIFT, H. H. 1965. Isolation of deoxyribonucleic acid from mitochondria of chick embryo heart and liver. *Proc Natl Acad Sci U S A,* 53**,** 1126-33.

RAYMOND, A. C., RIDEOUT, M. C., STAKER, B., HJERRILD, K. & BURGIN, A. B., JR. 2004. Analysis of human tyrosyl-DNA phosphodiesterase I catalytic residues. *J Mol Biol,* 338**,** 895-906.

REDINBO, M. R., STEWART, L., KUHN, P., CHAMPOUX, J. J. & HOL, W. G. 1998. Crystal structures of human topoisomerase I in covalent and noncovalent complexes with DNA. *Science,* 279**,** 1504-13.

RHEE, S. G., KANG, S. W., CHANG, T. S., JEONG, W. & KIM, K. 2001. Peroxiredoxin, a novel family of peroxidases. *IUBMB Life,* 52**,** 35-41.

RICHTER, R., RORBACH, J., PAJAK, A., SMITH, P. M., WESSELS, H. J., HUYNEN, M. A., SMEITINK, J. A., LIGHTOWLERS, R. N. & CHRZANOWSKA-

LIGHTOWLERS, Z. M. 2010. A functional peptidyl-tRNA hydrolase, ICT1, has been recruited into the human mitochondrial ribosome. *EMBO J,* 29**,** 1116-25.

ROBBERSON, D. L., KASAMATSU, H. & VINOGRAD, J. 1972. Replication of mitochondrial DNA. Circular replicative intermediates in mouse L cells. *Proc Natl Acad Sci U S A,* 69**,** 737-41.

ROBERTSON, H. D., ALTMAN, S. & SMITH, J. D. 1972. Purification and properties of a specific Escherichia coli ribonuclease which cleaves a tyrosine transfer ribonucleic acid presursor. *J Biol Chem,* 247**,** 5243-51.

ROEDE, J. R. & JONES, D. P. 2010. Reactive species and mitochondrial dysfunction: mechanistic significance of 4-hydroxynonenal. *Environ Mol Mutagen,* 51**,** 380-90.

RORBACH, J., RICHTER, R., WESSELS, H. J., WYDRO, M., PEKALSKI, M., FARHOUD, M., KUHL, I., GAISNE, M., BONNEFOY, N., SMEITINK, J. A., LIGHTOWLERS, R. N. & CHRZANOWSKA-LIGHTOWLERS, Z. M. 2008. The human mitochondrial ribosome recycling factor is essential for cell viability. *Nucleic Acids Res,* 36**,** 5787-99.

ROSSMANITH, W., TULLO, A., POTUSCHAK, T., KARWAN, R. & SBISA, E. 1995. Human mitochondrial tRNA processing. *J Biol Chem,* 270**,** 12885-91.

ROTHBERG, J. M., HINZ, W., REARICK, T. M., SCHULTZ, J., MILESKI, W., DAVEY, M., LEAMON, J. H., JOHNSON, K., MILGREW, M. J., EDWARDS, M., HOON, J., SIMONS, J. F., MARRAN, D., MYERS, J. W., DAVIDSON, J. F., BRANTING, A., NOBILE, J. R., PUC, B. P., LIGHT, D., CLARK, T. A., HUBER, M., BRANCIFORTE, J. T., STONER, I. B., CAWLEY, S. E., LYONS, M., FU, Y., HOMER, N., SEDOVA, M., MIAO, X., REED, B., SABINA, J., FEIERSTEIN, E., SCHORN, M., ALANJARY, M., DIMALANTA, E., DRESSMAN, D., KASINSKAS, R., SOKOLSKY, T., FIDANZA, J. A., NAMSARAEV, E., MCKERNAN, K. J., WILLIAMS, A., ROTH, G. T. & BUSTILLO, J. 2011. An integrated semiconductor device enabling non-optical genome sequencing. *Nature,* 475**,** 348-52.

RUTTER, J., WINGE, D. R. & SCHIFFMAN, J. D. 2010. Succinate dehydrogenase - Assembly, regulation and role in human disease. *Mitochondrion,* 10**,** 393-401.

SANGER, F., NICKLEN, S. & COULSON, A. R. 1977. DNA sequencing with chain-terminating inhibitors. *Proc Natl Acad Sci U S A,* 74**,** 5463-7.

SCALETTAR, B. A., ABNEY, J. R. & HACKENBROCK, C. R. 1991. Dynamics, structure, and function are coupled in the mitochondrial matrix. *Proc Natl Acad Sci U S A,* 88**,** 8057-61.

SCHAPIRA, A. H. 2012. Mitochondrial diseases. *Lancet,* 379**,** 1825-34.

SCHLAME, M., REN, M., XU, Y., GREENBERG, M. L. & HALLER, I. 2005. Molecular symmetry in mitochondrial cardiolipins. *Chem Phys Lipids,* 138**,** 38-49.

SHADEL, G. S. & CLAYTON, D. A. 1997. Mitochondrial DNA maintenance in vertebrates. *Annu Rev Biochem,* 66**,** 409-35.

SHARMA, M. R., KOC, E. C., DATTA, P. P., BOOTH, T. M., SPREMULLI, L. L. & AGRAWAL, R. K. 2003. Structure of the mammalian mitochondrial ribosome reveals an expanded functional role for its component proteins. *Cell,* 115**,** 97-108.

SHEFTEL, A., STEHLING, O. & LILL, R. 2010. Iron-sulfur proteins in health and disease. *Trends Endocrinol Metab,* 21**,** 302-14.

SHIFLETT, A. M. & JOHNSON, P. J. 2010. Mitochondrion-related organelles in eukaryotic protists. *Annu Rev Microbiol,* 64**,** 409-29.

SHILOH, Y. 2006. The ATM-mediated DNA-damage response: taking shape. *Trends Biochem Sci,* 31**,** 402-10.

SIMSEK, D., FURDA, A., GAO, Y., ARTUS, J., BRUNET, E., HADJANTONAKIS, A. K., VAN HOUTEN, B., SHUMAN, S., MCKINNON, P. J. & JASIN, M. 2011. Crucial role for DNA ligase III in mitochondria but not in Xrcc1-dependent repair. *Nature,* 471**,** 245-8.

SJOSTRAND, F. S. 1953. Electron microscopy of mitochondria and cytoplasmic double membranes. *Nature,* 171**,** 30-2.

SLED, V. D., RUDNITZKY, N. I., HATEFI, Y. & OHNISHI, T. 1994. Thermodynamic analysis of flavin in mitochondrial NADH:ubiquinone oxidoreductase (complex I). *Biochemistry,* 33**,** 10069-75.

SLESAREV, A. I., STETTER, K. O., LAKE, J. A., GELLERT, M., KRAH, R. & KOZYAVKIN, S. A. 1993. DNA topoisomerase V is a relative of eukaryotic topoisomerase I from a hyperthermophilic prokaryote. *Nature,* 364**,** 735-7.

SMIRNOVA, E., GRIPARIC, L., SHURLAND, D. L. & VAN DER BLIEK, A. M. 2001. Dynamin-related protein Drp1 is required for mitochondrial division in mammalian cells. *Mol Biol Cell,* 12**,** 2245-56.

SPELBRINK, J. N. 2010. Functional organization of mammalian mitochondrial DNA in nucleoids: history, recent developments, and future challenges. *IUBMB Life,* 62**,** 19-32.

SPYROU, G., ENMARK, E., MIRANDA-VIZUETE, A. & GUSTAFSSON, J. 1997. Cloning and expression of a novel mammalian thioredoxin. *J Biol Chem,* 272**,** 2936-41.

ST-PIERRE, J., BUCKINGHAM, J. A., ROEBUCK, S. J. & BRAND, M. D. 2002. Topology of superoxide production from different sites in the mitochondrial electron transport chain. *J Biol Chem,* 277**,** 44784-90.

STIERUM, R. H., DIANOV, G. L. & BOHR, V. A. 1999. Single-nucleotide patch base excision repair of uracil in DNA by mitochondrial protein extracts. *Nucleic Acids Res,* 27**,** 3712-9.

STUMPF, J. D. & COPELAND, W. C. 2011. Mitochondrial DNA replication and disease: insights from DNA polymerase gamma mutations. *Cell Mol Life Sci,* 68**,** 219-33.

SYKORA, P., CROTEAU, D. L., BOHR, V. A. & WILSON, D. M., 3RD 2011. Aprataxin localizes to mitochondria and preserves mitochondrial function. *Proc Natl Acad Sci U S A,* 108**,** 7437-42.

SZCZESNY, R. J., WOJCIK, M. A., BOROWSKI, L. S., SZEWCZYK, M. J., SKROK, M. M., GOLIK, P. & STEPIEN, P. P. 2013. Yeast and human mitochondrial helicases. *Biochim Biophys Acta*.

TAKAMATSU, C., UMEDA, S., OHSATO, T., OHNO, T., ABE, Y., FUKUOH, A., SHINAGAWA, H., HAMASAKI, N. & KANG, D. 2002. Regulation of mitochondrial D-loops by transcription factor A and single-stranded DNA-binding protein. *EMBO Rep,* 3**,** 451-6.

TAKASHIMA, H., BOERKOEL, C. F., JOHN, J., SAIFI, G. M., SALIH, M. A. M., ARMSTRONG, D., MAO, Y., QUIOCHO, F. A., ROA, B. B., NAKAGAWA, M., STOCKTON, D. W. & LUPSKI, J. R. 2002. Mutation of TDP1, encoding a topoisomerase I-dependent DNA damage repair enzyme, in spinocerebellar ataxia with axonal neuropathy. *Nat Genet,* 32**,** 267-272.

TEMPERLEY, R., RICHTER, R., DENNERLEIN, S., LIGHTOWLERS, R. N. & CHRZANOWSKA-LIGHTOWLERS, Z. M. 2010. Hungry codons promote frameshifting in human mitochondrial ribosomes. *Science,* 327**,** 301.

THYAGARAJAN, B., PADUA, R. A. & CAMPBELL, C. 1996. Mammalian mitochondria possess homologous DNA recombination activity. *J Biol Chem,* 271**,** 27536-43.

TOVAR, J., LEON-AVILA, G., SANCHEZ, L. B., SUTAK, R., TACHEZY, J., VAN DER GIEZEN, M., HERNANDEZ, M., MULLER, M. & LUCOCQ, J. M. 2003. Mitochondrial remnant organelles of Giardia function in iron-sulphur protein maturation. *Nature,* 426**,** 172-6.

TRIFUNOVIC, A., HANSSON, A., WREDENBERG, A., ROVIO, A. T., DUFOUR, E., KHVOROSTOV, I., SPELBRINK, J. N., WIBOM, R., JACOBS, H. T. & LARSSON, N. G. 2005. Somatic mtDNA mutations cause aging phenotypes without affecting reactive oxygen species production. *Proc Natl Acad Sci U S A,* 102**,** 17993-8.

TRIFUNOVIC, A., WREDENBERG, A., FALKENBERG, M., SPELBRINK, J. N., ROVIO, A. T., BRUDER, C. E., BOHLOOLY, Y. M., GIDLOF, S., OLDFORS, A., WIBOM, R., TORNELL, J., JACOBS, H. T. & LARSSON, N. G. 2004. Premature ageing in mice expressing defective mitochondrial DNA polymerase. *Nature,* 429**,** 417-23.

TSE, Y. C., KIRKEGAARD, K. & WANG, J. C. 1980. Covalent bonds between protein and DNA. Formation of phosphotyrosine linkage between certain DNA topoisomerases and DNA. *J Biol Chem,* 255**,** 5560-5.

TURRENS, J. F. 2003. Mitochondrial formation of reactive oxygen species. *J Physiol,* 552**,** 335-44.

VERMULST, M., BIELAS, J. H., KUJOTH, G. C., LADIGES, W. C., RABINOVITCH, P. S., PROLLA, T. A. & LOEB, L. A. 2007. Mitochondrial point mutations do not limit the natural lifespan of mice. *Nat Genet,* 39**,** 540-3.

VERMULST, M., BIELAS, J. H. & LOEB, L. A. 2008. Quantification of random mutations in the mitochondrial genome. *Methods,* 46**,** 263-8.

VILLARROYA, M., PRADO, S., ESTEVE, J. M., SORIANO, M. A., AGUADO, C., PEREZ-MARTINEZ, D., MARTINEZ-FERRANDIS, J. I., YIM, L., VICTOR, V. M., CEBOLLA, E., MONTANER, A., KNECHT, E. & ARMENGOD, M. E. 2008. Characterization of human GTPBP3, a GTP-binding protein involved in mitochondrial tRNA modification. *Mol Cell Biol,* 28**,** 7514-31.

VONGSAMPHANH, R., FORTIER, P. K. & RAMOTAR, D. 2001. Pir1p mediates translocation of the yeast Apn1p endonuclease into the mitochondria to maintain genomic stability. *Mol Cell Biol,* 21**,** 1647-55.

VOS, S. M., TRETTER, E. M., SCHMIDT, B. H. & BERGER, J. M. 2011. All tangled up: how cells direct, manage and exploit topoisomerase function. *Nat Rev Mol Cell Biol,* 12**,** 827-41.

VOULGARIDOU, G. P., ANESTOPOULOS, I., FRANCO, R., PANAYIOTIDIS, M. I. & PAPPA, A. 2011. DNA damage induced by endogenous aldehydes: current state of knowledge. *Mutat Res,* 711**,** 13-27.

WANG, C. I., WANG, C. L., WANG, C. W., CHEN, C. D., WU, C. C., LIANG, Y., TSAI, Y. H., CHANG, Y. S., YU, J. S. & YU, C. J. 2011. Importin subunit alpha-2 is identified as a potential biomarker for non-small cell lung cancer by integration of the cancer cell secretome and tissue transcriptome. *Int J Cancer,* 128**,** 2364-72.

WANG, J. C. 1971. Interaction between DNA and an Escherichia coli protein omega. *J Mol Biol,* 55**,** 523-33.

WATABE, S., HIROI, T., YAMAMOTO, Y., FUJIOKA, Y., HASEGAWA, H., YAGO, N. & TAKAHASHI, S. Y. 1997. SP-22 is a thioredoxin-dependent peroxide reductase in mitochondria. *Eur J Biochem,* 249**,** 52-60.

WESTBYE, M. P., FEYZI, E., AAS, P. A., VAGBO, C. B., TALSTAD, V. A., KAVLI, B., HAGEN, L., SUNDHEIM, O., AKBARI, M., LIABAKK, N. B., SLUPPHAUG, G., OTTERLEI, M. & KROKAN, H. E. 2008. Human AlkB homolog 1 is a mitochondrial protein that demethylates 3-methylcytosine in DNA and RNA. *J Biol Chem,* 283**,** 25046-56.

WOLLEN STEEN, K., DOSETH, B., M, P. W., AKBARI, M., KANG, D., FALKENBERG, M. & SLUPPHAUG, G. 2012. mtSSB may sequester UNG1 at mitochondrial ssDNA and delay uracil processing until the dsDNA conformation is restored. *DNA Repair (Amst),* 11**,** 82-91.

WYATT, M. D. & PITTMAN, D. L. 2006. Methylating agents and DNA repair responses: Methylated bases and sources of strand breaks. *Chem Res Toxicol,* 19**,** 1580-94.

XIAO, W. & SAMSON, L. 1993. In vivo evidence for endogenous DNA alkylation damage as a source of spontaneous mutation in eukaryotic cells. *Proc Natl Acad Sci U S A,* 90**,** 2117-21.

YAKES, F. M. & VAN HOUTEN, B. 1997. Mitochondrial DNA damage is more extensive and persists longer than nuclear DNA damage in human cells following oxidative stress. *Proc Natl Acad Sci U S A,* 94**,** 514-9.

YANG, D., OYAIZU, Y., OYAIZU, H., OLSEN, G. J. & WOESE, C. R. 1985. Mitochondrial origins. *Proc Natl Acad Sci U S A,* 82**,** 4443-7.

YANG, K. S., KANG, S. W., WOO, H. A., HWANG, S. C., CHAE, H. Z., KIM, K. & RHEE, S. G. 2002. Inactivation of human peroxiredoxin I during catalysis as the result of the oxidation of the catalytic site cysteine to cysteine-sulfinic acid. *J Biol Chem,* 277**,** 38029-36.

YANG, S. W., BURGIN, A. B., JR., HUIZENGA, B. N., ROBERTSON, C. A., YAO, K. C. & NASH, H. A. 1996. A eukaryotic enzyme that can disjoin dead-end covalent complexes between DNA and type I topoisomerases. *Proc Natl Acad Sci U S A,* 93**,** 11534-9.

YASUKAWA, T., REYES, A., CLUETT, T. J., YANG, M. Y., BOWMAKER, M., JACOBS, H. T. & HOLT, I. J. 2006. Replication of vertebrate mitochondrial DNA entails transient ribonucleotide incorporation throughout the lagging strand. *EMBO J,* 25**,** 5358-71.

YOSHIKAWA, S., MURAMOTO, K. & SHINZAWA-ITOH, K. 2012. Reaction mechanism of mammalian mitochondrial cytochrome c oxidase. *Adv Exp Med Biol,* 748**,** 215-36.

YOULE, R. J. & VAN DER BLIEK, A. M. 2012. Mitochondrial fission, fusion, and stress. *Science,* 337**,** 1062-5.

ZENG, Z., SHARMA, A., JU, L., MURAI, J., UMANS, L., VERMEIRE, L., POMMIER, Y., TAKEDA, S., HUYLEBROECK, D., CALDECOTT, K. W. & EL-KHAMISY, S. F. 2012. TDP2 promotes repair of topoisomerase I-mediated DNA damage in the absence of TDP1. *Nucleic Acids Res*.

ZHANG, H., BARCELO, J. M., LEE, B., KOHLHAGEN, G., ZIMONJIC, D. B., POPESCU, N. C. & POMMIER, Y. 2001. Human mitochondrial topoisomerase I. *Proc Natl Acad Sci U S A,* 98**,** 10608-13.

ZHANG, H., MENG, L. H. & POMMIER, Y. 2007. Mitochondrial topoisomerases and alternative splicing of the human TOP1mt gene. *Biochimie,* 89**,** 474-81.

ZHANG, H. & POMMIER, Y. 2008. Mitochondrial topoisomerase I sites in the regulatory D-loop region of mitochondrial DNA. *Biochemistry,* 47**,** 11196-203.

ZHAO, X., LEON, I. R., BAK, S., MOGENSEN, M., WRZESINSKI, K., HOJLUND, K. & JENSEN, O. N. 2011. Phosphoproteome analysis of functional mitochondria isolated from resting human muscle reveals extensive phosphorylation of inner membrane protein complexes and enzymes. *Mol Cell Proteomics,* 10**,** M110 000299.

ZHOU, T., LEE, J. W., TATAVARTHI, H., LUPSKI, J. R., VALERIE, K. & POVIRK, L. F. 2005. Deficiency in 3'-phosphoglycolate processing in human cells with a hereditary mutation in tyrosyl-DNA phosphodiesterase (TDP1). *Nucleic Acids Res,* 33**,** 289-97.